Stefan Fürtinger

Comparison Of Cardiovascular Control Mechanisms Under Orthostatic Stress

Diplomarbeit

zur Erlangung des Mag. rer. nat.
an der Naturwissenschaftlichen Fakultät
der Karl-Franzens Universität Graz

Betreuer:

Em.Univ-Prof. Dr. Franz Kappel

Zweitbetreuer:

Dr. Jerry Batzel

Institut für Mathematik und
wissenschaftliches Rechnen

Graz, im August 2009

Danksagung

Ich möchte mich herzlich bei Herrn Prof. Franz Kappel für seine fortwährende Unterstützung im Lauf der Entstehung dieser Arbeit bedanken. Seine hilfreichen Ratschläge machten deren Realisierung erst möglich. Viele Konzepte sind aus der langen Zusammenarbeit mit Herrn Dr. Jerry Batzel entstanden bei dem ich mich an dieser Stelle für unzählige Stunden der Diskussion, zahllose Email Konversationen und seinen meist unverwüstlichen Humor bedanken will.
Nicht zuletzt gilt ein großer Dank meiner Mutter. Ihre jahrelange Unterstützung, ihr großes Verständnis und ihre bedingungslose Hilfsbereitschaft brachten mich durch alle Hochs und Tiefs des Studiums und machten mir es erst möglich diese Diplomarbeit zu verfassen. Ich danke ihr von ganzem Herzen und möchte ihr auch diese Arbeit widmen.

Graz, im August 2009 Stefan Fürtinger

Contents

Introduction

Mathematical modelling plays a key role in modern medicine and the life sciences. In medicine many processes are not observable via non invasive measurements. Thus mathematical modelling is often the only way to assess underlying mechanisms of complex systems such as the human cardiovascular system. A wide variation of models is used nowadays to study physiological phenomena that are very difficult to measure even in experimentally controllable situations.

Of main interest here is the influence of orthostatic stress on the cardiovascular system. Studying effects of gravitationally induced hypovolemia on the human body is a wide and active field of research. Hypovolemia provokes a drop in venous return which leads to a decrease in arterial blood pressure. This is counteracted by a number of interdependent control mechanisms which act to stabilize cardiovascular function and recover blood pressure. Many clinically relevant conditions arise from impaired control responses, e.g. orthostatic intolerance or postural orthostatic tachycardia syndrome.

A number of different deterministic mathematical models have been proposed to simulate such effects, all having in common that the short term control response induced by hypovolemia has to be quantified in some way. The lack of detailed physiological knowledge concerning the exact modes of operation of the controls lead to a wide variety in design of control loops.

In this thesis three control formulations representing popular techniques currently used in physiological modeling are presented: a straightforward differential equation using the arc tangent simulating basic correlations, a differential set point equation modelling not only saturation but also time decays, and an optimal control approach based on considerations coming from cybernetics. The first two are explicit controls requiring the detailed design of a control gain. The latter is obtained as solution of a minimization problem.

The basic physiological concepts needed in the context of this thesis together with a description of the most common clinical tests to study the cardiovascular system under orthostatic stress are presented in Chapter 1. Chapter 2 describes the derivation of a system of nonlinear ordinary differential constituting the mathematical model. In addition the design of the presented explicit controls is explained and motivated using concepts introduced in Chapter 1. Finally the background needed to establish the optimal control strategy is given and applied to the introduced model. Chapter 3 is concerned with numerical simulations of the model employing each control formulation. The presented results give a qualitative overview of the three controls under orthostatic stress. The final discussion investigates benefits and drawbacks when employing these (or similar) controls in comparable lumped compartmental models. Necessary auxiliary equations, a comprehensive list of all used parameter (and their values) and a detailed explanation of the steady state computation of the model (needed for the optimal control approach) is found in the Appendix.

1 Physiological Background

We will give a brief overview of the basic physiological principles regarding the human cardiovascular system needed in the context of this thesis. The description given here is based on [26, 6] and [17] but the topics covered can be found in any physiology text book as well. Following physiological conventions, volumes are given in liters [ℓ], flows in liters per minute [ℓ/min] and pressures in millimeters of mercury [mmHg]. The latter is a non SI unit using a predefined density of mercury at 0° Celsius and a fixed value of gravitational acceleration and is thus of limited precision (see for instance [21]).

1.1 Heart and Circulatory System

Every cell in the human body needs a constant supply of oxygen and nutrients and a way to remove metabolic byproducts (such as carbon dioxide) to ensure proper activity. It is not possible for a single cell to accomplish this task on its own. Thus a mechanism is necessary which ensures constant delivery of nutrients and removal of waste products. In the human body this is done by a complex circulatory system of blood vessels which makes the exchange of fluids, gases and various metabolic substrates between cells and the external environment possible. This system is called the *cardiovascular system* (CVS) and consists of the heart, blood, and blood vessels. It can be separated into two series-connected circuits: the *systemic circuit* and the *pulmonary circuit*. The systemic circuit connects the heart to organs and peripheral tissue regions, while the pulmonary circuit perfuses the lungs. The heart connects both circuits and serves as a pump.

1.1.1 Blood Circulation

A sketch of the circulatory system is depicted in Figure 1.1. The human heart consists of two pumps in series which we refer to as the *left heart* and the *right heart*. The left heart pumps oxygenated blood into the *aorta*, the largest artery in the body. The aorta bifurcates into smaller arteries conducting the blood from the heart to different regions of the body. The arteries arborize into smaller and smaller branches called *arterioles* which finally fork into the smallest vessels, the *capillaries*. The vessel walls of the capillaries are thin enough to allow exchange by simple diffusion of nutrients, electrolytes and molecules between blood and extracellular fluid, the so-called *interstitium*. This tissue fluid surrounds the cells and transports materials to and from them. Deoxygenated blood flows from the capillaries into the *venules* which conjoin to larger and larger veins. Finally the largest vein in the human body, the *vena cava*, brings the blood back to the right heart. From there it is pumped into the pulmonary circuit which shows essentially the same structure as the systemic circuit. However, there is one big difference: the pulmonary arteries carry *deoxygenated* blood from the right heart to the capillary network in the lungs. Here oxygen and carbon dioxide are exchanged via breathing air and oxygenated blood leaves the capillaries to flow through the pulmonary venules and veins back to the left heart which completes the loop. The pressure in the arterial part of the systemic circuit is much higher compared to its venous

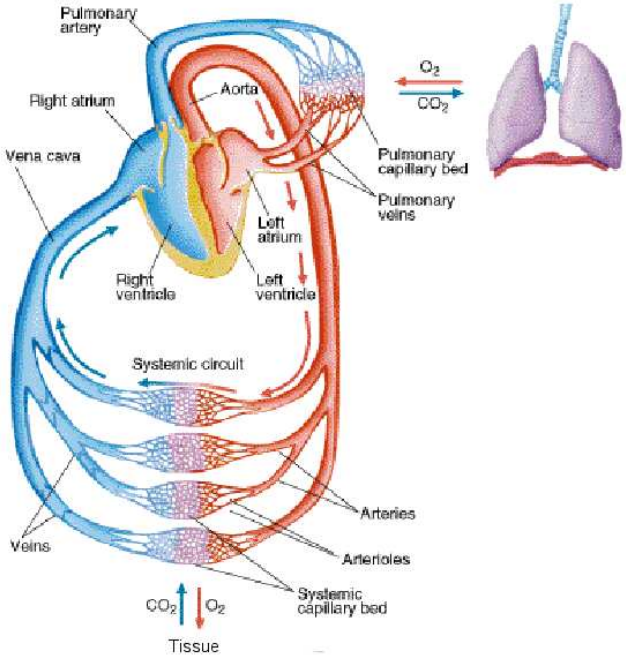

Figure 1.1: Sketch of the CVS. Taken from [2].

part and the whole pulmonary circuit. Thus it is also common to divide the CVS into a *high-* and a *low-pressure system*.

1.1.2 Vasculature

Blood vessels are often characterized by their interaction with the blood flow. Of main interest here are *compliance vessels* (sometimes also called *Windkessel-vessels*) and *resistance vessels*. The first type of vessels includes the arteries close to the heart which are elastic to ensure a continuous blood flow despite the pulsating ejection of blood by the heart. If, for instance, the aorta would have the properties of a steel pipe, the blood stream would stand still after completion of each heart beat. Instead, the vessel walls are able to expand and contract helping the pulse wave to evolve smoothly. This is called Windkessel-function (referring to reservoirs connected to piston pumps). Similar mechanisms make it possible to shift blood from the venous system (65% of the total blood volume are located in veins and venules) to other vascular regions. The so-called *unstressed volume* plays a key role in such blood transfers. The unstressed volume of a vessel is the volume which fills the blood vessel without stressing its walls. Accordingly the *stressed volume* refers to the volume which when added to the unstressed volume expands the vessel wall. Thus the total volume of a blood vessel is given by its unstressed volume plus the stressed volume. The structure of the venous vasculature makes it possible to decrease unstressed volume and transfer it to stressed volume if needed. Furthermore, larger veins are able to push blood to the heart by activation of muscle cells surrounding their vessel walls. Additionally small eversions inside the veins, the so-called *venous valves*, prevent blood from pooling back into the capillaries.

The second type of vasculature include arterioles and venules which exhibit quite other properties. These are resistance vessels which are able to change their diameter via contraction or relaxation of muscle fibers located in their walls. A decrease in the diameter of arterioles called *vasoconstriction* increases local resistance to blood flow whereas an increase (referred to as *vasodilation*) decreases local resistance. This makes it possible to regulate perfusion of body regions. The total resistance presented to the blood flow in the CVS is called *systemic* or *total peripheral resistance* (sometimes also *vascular resistance*).

1.1.3 The Heart as a Pump

As mentioned above the human heart consists of the left and the right heart which act as two pumps in series. The right heart sucks in deoxygenated blood from the systemic veins and pumps it into the pulmonary arteries. From there blood flows to the left heart which pushes it into the aorta. Each of the two pumps consists of an *atrium* and a *ventricle*. The atria aid in loading blood into the ventricles which pump it into the systemic and pulmonary circuit, respectively. The pumping is realized by a sudden contraction of the heart (called *systole*) which ejects blood out of the ventricles. The heart of a healthy adult beats around 70 times per minute which gives a *heart rate* of 70 beats per minute [bpm]. The volume which is ejected at each heart beat by both left and right ventricles is called *stroke volume* (about 70-80 milliliters for healthy adults). Heart rate times stroke volume gives the *cardiac output* which lies for a resting healthy individual at about 5 liters per minute.

1.1.3.1 The Cardiac Cycle

At the beginning of the systole the inflow valves to the ventricles (*tricuspid valve* for the left and *mitral valve* for the right ventricle) close and ventricular pressures increase until they reach arterial pressures (about 80 mmHg in the aorta and ca. 10 mmHg in the pulmonary artery). This phase is called *isovolumetric contraction* since until now the ventricular volumes have not changed. As soon as ventricular pressures equal arterial pressures the ventricular outflow valves (the *aortic valve* and the *pulmonary valve*, respectively) open and blood is ejected. This is the beginning of the *ejection phase* in which ventricular pressures keep increasing (up to a value of about 120 mmHg in the left and 15 mmHg in the right ventricle). The end of the ejection phase is also the end of the systole and the heart relaxes. Thus ventricular pressures decrease and the aortic and pulmonary valve respectively close as soon as ventricular pressures are lower than arterial pressures.
This marks the beginning of the relaxation phase, the so-called *diastole*: the pressures in the ventricles decrease down to the pressures in the atria which causes tricuspid and mitral valve to open. Ventricular volumes were constant until the valves opened thus this phase is called *isovolumetric relaxation*. Since the heart muscle continues relaxing after opening of the inflow valves blood pours from the atria into the ventricles. As soon as the heart starts contracting again the diastole ends and a new systole begins. A graphical representation of ventricular pressure and volume during one cardiac cycle is given in Fig. 1.2.

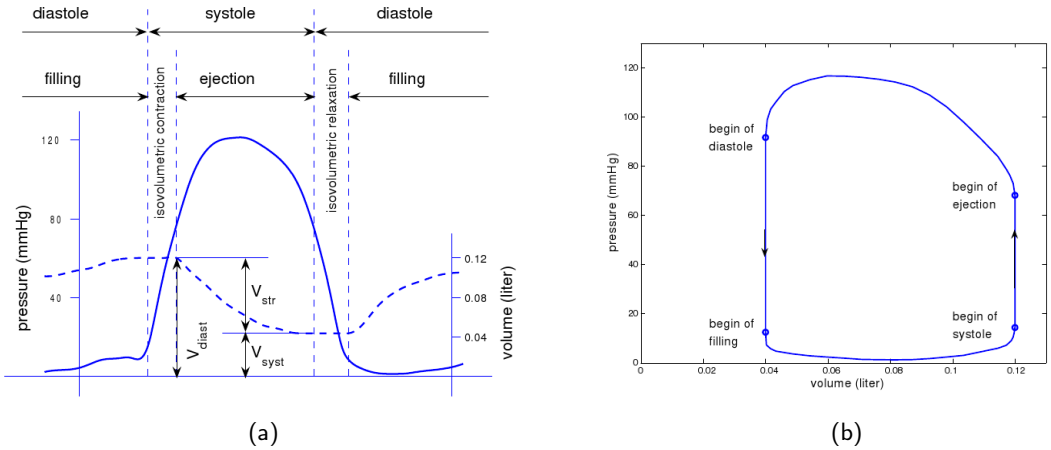

Figure 1.2: Panel (a) shows variations in pressure (solid) and volume (dashed) during one cardiac cycle. Panel (b) illustrates the pressure-volume relationship further. Both graphs present typical volumes and pressures of the left ventricle. Taken from [6].

1.1.3.2 Regulation of Heart Rate and Contraction

The cardiac muscle is able to modulate both *contractility* (i.e. the heart's ability to contract) and stroke volume within certain bounds. For instance a rise in the amount of systemic venous blood flowing to the heart (the so-called *venous return*) increases ventricular filling and *preload* (i.e. the end-diastolic filling pressure in the left ventricle). This causes a stretching of the cardiac muscle which results in a higher contractile force and thus a larger stroke volume. This effect is called the *Frank–Starling law*. On the other hand a suddenly increased *afterload* (i.e. the end-diastolic aortic pressure) may cause a slight increase in contractility as well. This mechanism is called *Anrep effect*, and its exact mode of operation needs to be clarified. Additionally a higher heart rate makes contractility grow as well (known as *Bowditch effect*).
However, besides the heart's intrinsic regulative mechanisms *sympathetic* and *parasympathetic nervous systems* (both part of the *autonomic nervous system*) play a major role in controlling the heart as well. Sympathetic influence generally increases cardiac activity, whereas parasympathetic action decreases it. At rest parasympathetic regulation dominates though sympathetic modulation is active as well. Parasympathetic influence on the heart is mediated via the *vagal nerve* which is of major importance in cardiac adaption to short-term stresses. In case of withdrawal of parasympathetic inhibition heart rate and contractility grow rapidly and can be increased further by the sympathetic nervous system.

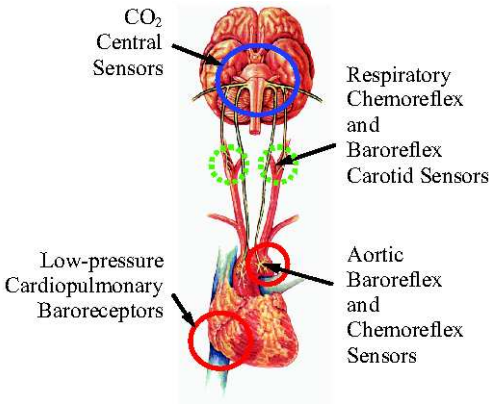

Figure 1.3: Location of baro- and chemoreceptors. Taken from [6].

1.2 Blood Pressure Regulation

If we talk about blood pressure we always refer to *arterial* blood pressure unless otherwise stated. In medicine blood pressure is usually given as *systolic pressure* P_{sys} (the maximal pressure in the vessels during the systole) to *diastolic pressure* P_{dia} (minimal pressure during the diastole; used as measure for the permanent load of the vessels). We will later on use mean pressures P_{mean} from which systolic and diastolic pressures can be obtained by using the empirical formula (see for instance [17])

$$P_{\text{mean}} = 2/3 \cdot P_{\text{dia}} + 1/3 \cdot P_{\text{sys}}.$$

It should be noted that systolic and diastolic pressures may change without any visible alteration of mean arterial pressure. However, variations in P_{sys} and P_{dia} are a relevant input to several blood pressure regulation mechanisms. Thus by using mean pressures some information about the current state of the system is lost (this issue and a possible remedy is discussed in [10]).
It is of greatest importance that blood pressure stays within appropriate bounds. Severely elevated values of pressure harm the heart, brain and the kidneys. If blood pressure is too low oxygen supply of organs is deteriorated which (in case of a shock) ultimately leads to multiple organ failure. On the other hand blood pressure has to be adapted to various stresses such as physical exercise. Thus blood pressure regulation is a complex composite of mechanisms which differ greatly in effect and functionality. Moreover, these controls act on different time scales which motivates the classification into *short-* (responding within seconds or minutes), *mid-* (minutes to hours) and *long-term regulation* (hours and longer). The main focus here lies on the short term regulation. However, the human body is a closed system thus all mechanisms are to some extent influencing each other so they should not be seen as completely separate.

1.2.1 Short-Term Regulation

The most prominent short-term control is the so-called *baroreflex-loop* which depends on stretch receptors sensitive to distensions of vessel walls caused by pressure deviations. These sensors signal blood pressure changes to the brain, namely the medulla oblongata, which stimulates the autonomic nervous system. A combination of sympathetic and

parasympathetic responses alters systemic resistance, cardiac contractility, venous tone and unstressed volume.
The pressure receptors can be divided into two groups: the *arterial baroreceptors* found in the high-pressure system, namely in the aorta and the carotid sinuses, sense arterial blood pressure. Low-pressure sensors, the *cardio-pulmonary baroreceptors*, are found in the atria, the ventricles, the pulmonary arteries and veins and most important the veno-atrial junction with the vena cava. Figure 1.3 provides an overview of receptor locations. If *central venous pressure* (measured at the entrance to the right atrium) decreases, total peripheral resistance and venous tone are altered to minimize any perturbation of arterial blood pressure. Thus the cardio-pulmonary sensors monitor cardiac input conditions whereas the arterial baroreceptors observe the heart's output. It should be noted that the interaction and interference of low- and high-pressure sensors is a topic of research.
Another important control loop is the respiratory system. Besides some rather obvious connections between the CVS and the respiratory system (e.g. the association between pulmonary perfusion rate, ventilation and blood gas transport) blood pressure regulation links both systems as well. Chemoreceptors in the carotid and aortic bodies are sensitive to changes in levels of oxygen and carbon dioxide in the blood. Variations in these blood gases activate the receptors which alters systemic resistance and heart rate. However, it should be noted that the chemoreceptors are primarily important when the baroreceptors become insensitive to pressure changes. This is the case if blood pressure is extremely low and thus blood gas levels are heavily altered. Finally hydrostatic effects can move interstitial fluid into the blood circulation to increase blood volume and thus maintain blood pressure.

1.2.2 Mid-Term Regulation

The main control in mid-term blood pressure regulation is the so-called *renin-angiotensin-aldosterone system* (RAAS) which is active if the perfusion of the kidneys decreases. Via a chain of various hormones, angiotensin II is released which induces vasoconstriction. Note that this loop acts in concordance with the baroreflex.

1.2.3 Long-Term Regulation

Blood pressure regulation on longer time scales is realized by blood volume changes via the kidney. High levels of blood pressure provoke an increase in excretion of fluid by the kidneys, called *pressure diuresis*. This is achieved by several hormonal circuits acting on renal tissue of which the most important are the decrease in secretion of *anti-diuretic hormone* (ADH) in the brain (namely in the hypothalamus), inhibition of the RAAS and release of *atrial natriuretic factor* (ANF) in the atria.

1.3 Orthostatic Stress

In supine position the impact of gravity is perpendicular to the body and therefore does not significantly influence CVS function. Upon standing a hydrostatic force is induced causing blood to pool in the lower limbs due to gravitational effects. The impact of these gravitational effects on the CVS is called *orthostatic stress*. The postural change from lying to standing up may sound like a trivial challenge, however, the amount of blood pooling in the lower extremities is about 0.5 liters. This provokes a severe decrease in arterial blood pressure if not compensated by short-term blood pressure regulation

(a) (b)

Figure 1.4: HUT-table (a) and LBNP-chamber (b). Taken from [8].

mechanisms. Thus the body tries to compensate for the imposed stress before CVS function is impaired: the baroreflex reacts and provokes an increase in systemic resistance, heart rate and contractility and probably a decrease in venous compliance and unstressed volume. However, people suffering from orthostatic intolerance or postural orthostatic tachycardia syndrome (POTS) show only insufficient control responses to orthostatic stress resulting in a drop in arterial and hence cerebral blood pressure which provokes dizziness or even syncope and may cause injuries. Thus studying reactions to orthostatic stress is of clinical relevance and still a field of active research.
A number of clinical tests have been developed to investigate the CVS under orthostatic stress. These are mainly the sit-to-stand-test, the *head-up-tilt* (HUT) test and the *lower-body-negative-pressure* (LBNP) test. The last two of which are most common since they provide better experimental controllability. Via non invasive methods at least heart rate and arterial blood pressure (or more cardiovascular variables) are measured. In the HUT test a subject lies flat on a tilt-table until a resting steady state is reached. Then the table is smoothly (within a few seconds) tilted to an angle of 70 degrees or more, see Fig. 1.4 (a).
In this thesis we focus on the LBNP-test. The subject is placed in supine position on a table which is partially covered by a tube-like chamber, depicted in Fig. 1.4 (b). This chamber encloses the subject's lower body and induces a partial vacuum by exhausting air. Thus vessels subject to LBNP dilate which provokes a local volume increase and hence reduces venous return. This leads to a decrease in arterial blood pressure and results in control responses similar to those seen under stress imposed by gravitational effects. The impact of LBNP on CVS function depends of course on the magnitude of applied sucking pressure but also on how much of the subject's body is exposed to the stress. There exist two standard protocols: either the LBNP chamber is sealed at the iliac crest (from now on referred to as *'hips'*-case) or the splanchnic region is subject to LBNP as well (the *'ribs'*-case). Some researchers combine LBNP and HUT to provoke severe *hypovolemia* (i.e. a reduction in circulating blood volume) even in healthy subjects. It should be noted that LBNP and HUT are not completely equivalent: HUT applies stress to the CVS by gravitational forces whereas LBNP creates an artificial negative pressure that sucks on vascular walls. Thus the observed blood shifts are the same but *transmural pressures* (i.e. the pressure across

the vessel wall) in the lower limbs differ. This is due to the squeezing of the weight of upper blood cells on lower cells in upright position. This means that, strictly speaking, LBNP stress is by definition not a form of orthostatic stress since no gravitational effects are observed. However, both tests induce a temporary hypovolemia which has a comparable impact on CVS function. Thus it is common to refer to LBNP stress as orthostatic stress as well. Moreover, LBNP provides a highly controllable experimental environment which has been widely and successfully used when studying the impact of weightlessness on the CVS.

2 The Mathematical Model

The human CVS is modeled using a system of ordinary differential equations (ODEs). The model is mainly composed of three parts: the heart model (developed in [16]), the vascular components (similar to [12]) and the controls for heart rate, unstressed volume and systemic resistance. What follows is a short description of the model's components and an explanation of the fundamental assumptions that have been made (a very detailed presentation of central suppositions and techniques in modeling the human CVS can be found in [6] or [13]).
We use the model to study the behavior of different control strategies when simulating short-term orthostatic stress. For simplicity baroreflex regulation and local vasoconstriction are considered to be the only control circuits in the body. This means the model lacks a respiratory control, interstitial volume exchange effects, and any mid- or long-term controls (such as volume regulation via the kidneys, the RAAS, ADH- or ANF-release as described in Sec. 1.2). Heart rate, unstressed volume, and systemic resistance are controlled depending on arterial systemic or central venous pressure. Three different control-approaches will be discussed in this chapter: two explicit formulations using either first order differential set point equations or arc tangents and an optimal control strategy.
The heart model that is used is non-pulsatile, that means it computes a mean cardiac output using mean values of heart rate and stroke volume. Contractility of the left and right ventricle, respectively (subject to heart rate) is governed by two second order ODEs simulating the Bowditch–effect.
Blood vessels in the arterial and venous parts of the pulmonary and systemic circuits are lumped together into compartments. We consider a compartment to be a vessel presenting no resistance to blood flow. This means the vessel has the ability to dilate and increase its volume which is quantified by the vessel's *compliance*, accordingly we assume these vessels to be compliance vessels. The volume in the compartment is therefore only determined by the applied transmural pressure (inside minus outside pressure).
Arterial and venous parts are connected by arterioles and venules, which are also lumped together into vessels that are considered to be pure resistances to blood flow. Thus these vessels are only characterized by the flow through them and are therefore supposed to be resistance vessels.
The arterial and venous vasculature is modeled using ten compartments: arterial systemic (as), peripheral (per), upper (up), renal (ren), splanchnic (spl), legs (leg), vena cava (vc), abdominal vena cava (avc), arterial pulmonary (ap) and venous pulmonary (vp) compartment. An organizational diagram is depicted in Figure 2.1. The pulmonary circuit is split into two components (the venous and the arterial pulmonary compartments), whereas the systemic circuit is separated into eight sections. The arterial systemic compartment represents basically the aortic root and the aortic branch. Skin and body surface tissue of the thorax is lumped into the peripheral compartment. The upper compartment contains the upper limbs. Note that the complex autoregulative effects which govern the brain's blood supply are not considered in this model. The kidneys are located in the renal compartment, the gastrointestinal system in the splanchnic compartment, and lower body and

legs in the legs compartment. These are connected in parallel to the first section of the venous part of the systemic circuit, the abdominal vena cava compartment, representing large abdominal veins and the vena cava inferior. The last systemic component, the vena cava compartment, holds the vena cava superior. The pulmonary and systemic circuit are connected via the heart where the left atrium is assumed to be part of the pulmonary venous system and the right atrium is supposed to be located in the abdominal vena cava compartment (see Fig. 2.1).

2.1 Derivation of the model

In this section the basic elements of the model will be deduced from general physical and special physiological considerations. A very detailed description using a similar approach can be found in [6, 13], a related model from the viewpoint of electrical circuits is presented in [12]. A list of all used parameters and their meaning is given in Appendix A.3.

2.1.1 Modelling hemodynamics

As explained above, the volume in a compartment is characterized by its unstressed volume and the applied transmural pressure, thus we start by formulating a basic pressure volume relationship. Let V denote the total compartmental volume, c its compliance, $\tilde{P}$ the transmural pressure and V_{u} its unstressed volume. For simplification we use a linear relation of the form

$$V = c\tilde{P} + V_{\mathrm{u}}. \tag{2.1}$$

We assume a constant compliance c, however, in reality the compliance depends on the pressure $\tilde{P}$, i.e. $c = c(\tilde{P})$ and the general pressure volume relation is nonlinear (see for instance [6, p. 7], [9] or [15]). If $\tilde{P} = 0$ then $V = V_{\mathrm{u}}$ thus $c\tilde{P}$ represents the compartment's stressed volume. Let P be the pressure within the compartment and P_{bias} be the external (atmospheric or LBNP) pressure. Then the transmural pressure $\tilde{P}$ can be written as $\tilde{P} = P - P_{\mathrm{bias}}$, thus eq. (2.1) reads

$$V = c(P - P_{\mathrm{bias}}) + V_{\mathrm{u}}. \tag{2.2}$$

The flow in the resistance vessels between compartments is depending on the pressures in the adjacent compartments and on the resistance to blood flow. Applying Ohm's law gives

$$F = \frac{P_{\mathrm{in}} - P_{\mathrm{out}}}{R}, \tag{2.3}$$

where F denotes the flow, P_{in} the inflow-, P_{out} the outflow-pressure and R the Ohmic resistance.
The hemodynamics of the system are obtained by looking at the change of compartmental volumes over time. Mass balance considerations imply

$$\frac{d}{dt}V = F_{\mathrm{in}} - F_{\mathrm{out}}, \tag{2.4}$$

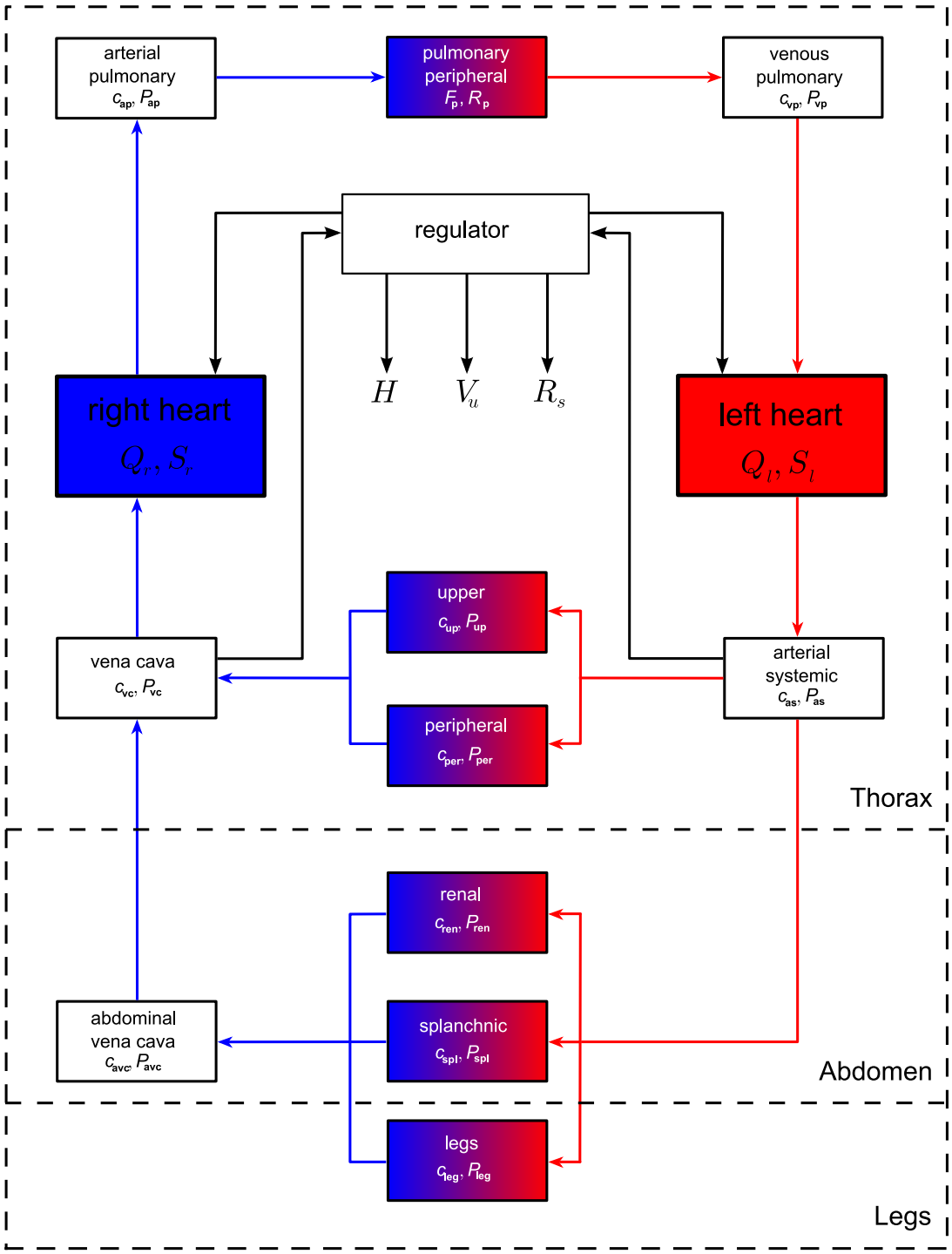

Figure 2.1: Architecture of the CVS-model. Arrows indicate blood flow (red symbolizes oxygenated, blue deoxygenated blood respectively).

where F_{in} denotes the flow into and F_{out} the flow out of the compartment. Assuming that the following quantities are time dependent (whereby state dependencies are ignored)

$$\begin{aligned} P &= P(t), \\ P_{\text{bias}} &= P_{\text{bias}}(t), \\ V_{\text{u}} &= V_{\text{u}}(t), \end{aligned}$$

combining relations (2.2) and (2.4) yields

$$c\left(\frac{d}{dt}P - \frac{d}{dt}P_{\text{bias}}\right) + \frac{d}{dt}V_{\text{u}} = F_{\text{in}} - F_{\text{out}},$$

or equivalently

$$\dot{P} = \frac{1}{c}(F_{\text{in}} - F_{\text{out}} + c\dot{P}_{\text{bias}} - \dot{V}_{\text{u}}), \tag{2.5}$$

which is the general equation used to describe hemodynamic changes in a compartment.

2.1.2 A non pulsatile heart model

By looking at the filling process and the ejection phase in the ventricles of the heart, a model for cardiac output can be derived (see [6, Sec. 1.1.2] or [16] for details). The inflow into the ventricle can be obtained using a similar approach as with inter-compartmental flows (see Sec. 2.1.1): looking at the time course of the ventricle's volume $V(t)$ (see Fig. 1.2), we introduce the end-diastolic volume V_{diast} and assume that the end-systolic volume V_{syst} of the current heart beat is the same as of the previous heart beat, thus $V(0) = V_{\text{syst}}$. Let P_{v} be the venous inflow pressure which is assumed to be constant during the diastole, $P(t)$ the pressure in the ventricle and R the ventricle's total resistance to the inflow. Then the flow into the ventricle (i.e. the change of the ventricular volume over time) is governed by laws of mass balance, thus we obtain the initial value problem

$$\begin{cases} \dot{V} &= \frac{1}{R}(P_{\text{v}} - P(t)), \\ V(0) &= V_{\text{syst}}. \end{cases} \tag{2.6}$$

Assuming that the compliance c of the relaxed ventricle is constant during the diastole and the external pressure applied to the ventricle is zero, the pressure volume relationship (2.2) can be used to model the relaxed ventricle's volume:

$$V(t) = cP(t) + V_0, \tag{2.7}$$

where V_0 denotes the ventricle's unstressed volume. Using relation (2.7) in eq. (2.6) and integrating gives

$$V(t) = V_{\text{syst}}e^{-(cR)^{-1}t} + (cP_{\text{v}} + V_0)(1 - e^{-(cR)^{-1}t}). \tag{2.8}$$

Bazett's formula (see [6, p. 10]) is used to compute the duration of the systole $t_s(H)$, where H denotes the heart rate: let $\kappa \in [0.0387, 0.0516]$ then

$$t_s(H) = \frac{\kappa}{\sqrt{H}}.$$

With $t_d(H)$ denoting the duration of the diastole it has to hold that $t_d + t_s = 1/H$, thus

$$t_d(H) = \frac{1}{\sqrt{H}}(\frac{1}{\sqrt{H}} - \kappa). \tag{2.9}$$

And we have using (2.8) at $t = t_d$

$$V_{\text{diast}} = V(t_d) = k(H)V_{\text{syst}} + (cP_{\text{v}} + V_0)a(H), \tag{2.10}$$

with

$$k(H) = e^{-(cR)^{-1}t_d(H)} \quad \text{and} \quad a(H) = 1 - k(H). \tag{2.11}$$

The Frank–Starling mechanism (the higher the end-diastolic volume, the higher the contractility in the systole) can be modeled by the formula

$$V_{\text{str}} = \frac{S(V_{\text{diast}} - V_0)}{P_{\text{a}}}, \tag{2.12}$$

where V_{str} denotes the stroke volume, S the ventricle's contractility and P_{a} the after-load. Furthermore, the stroke volume obeys

$$V_{\text{str}} = V_{\text{diast}} - V_{\text{syst}}. \tag{2.13}$$

Equations (2.10), (2.12) and (2.13) together form a linear equation system for V_{diast}, V_{syst} and V_{str}. Solving for the volumes yields

$$V_{\text{str}} = \frac{ca(H)P_{\text{v}}S}{a(H)P_{\text{a}} + k(H)S}, \tag{2.14}$$

$$\begin{aligned} V_{\text{diast}} &= cP_{\text{v}} + V_0 - \frac{ck(H)P_{\text{v}}S}{a(H)P_{\text{a}} + k(H)S}, \\ V_{\text{syst}} &= cP_{\text{v}} + V_0 - \frac{cP_{\text{v}}S}{a(H)P_{\text{a}} + k(H)S}. \end{aligned} \tag{2.15}$$

From now on we assume $V_0 = 0$. For ensuring that

$$V_{\text{syst}} \leq V_{\text{diast}}$$

or equivalently (using (2.14) and (2.15))

$$cP_{\text{v}}a(H)S \leq a(H)P_{\text{a}}cP_{\text{v}} \quad \text{or} \quad S \leq P_{\text{a}},$$

we introduce the minimum function $\min(S, P)$ in (2.14) which yields

$$V_{\text{str}} = \frac{cP_{\text{v}}a(H)\min(S, P_{\text{a}})}{a(H)P_{\text{a}} + k(H)\min(S, P_{\text{a}})}, \quad S \geq 0.$$

Let the subscripts 'ℓ' and 'r' denote the left and right ventricle respectively. Furthermore let $a_\ell(H)$, $k_\ell(H)$ and $a_{\text{r}}(H)$, $k_{\text{r}}(H)$ be the variables introduced in (2.11) with $c = c_\ell$, $R = R_\ell$ and $c = c_{\text{r}}$, $R = R_{\text{r}}$. The pre-load P_{v} to the left and right ventricle, respectively is the venous pulmonary pressure P_{vp} and the vena cava pressure P_{vc}, respectively. The

after-load P_{a} is given by the arterial systemic pressure P_{as} and the arterial pulmonary pressure P_{ap} (see Fig. 2.1). Thus we obtain the stroke volumes

$$\begin{aligned} V_{\mathrm{str},\ell} =& \frac{c_\ell P_{\mathrm{vp}} a_\ell(H) \min(S_\ell, P_{\mathrm{as}})}{a_\ell(H) P_{\mathrm{as}} + k_\ell(H) \min(S_\ell, P_{\mathrm{as}})}, \\ V_{\mathrm{str,r}} =& \frac{c_{\mathrm{r}} P_{\mathrm{vc}} a_{\mathrm{r}}(H) \min(S_{\mathrm{r}}, P_{\mathrm{ap}})}{a_{\mathrm{r}}(H) P_{\mathrm{ap}} + k_{\mathrm{r}}(H) \min(S_{\mathrm{r}}, P_{\mathrm{ap}})}. \end{aligned} \tag{2.16}$$

The cardiac output Q_ℓ of the left heart and Q_{r} of the right heart is given by heart rate times stroke volume. Thus

$$\begin{aligned} Q_\ell &= H \frac{c_\ell P_{\mathrm{vp}} a_\ell(H) \min(S_\ell, P_{\mathrm{as}})}{a_\ell(H) P_{\mathrm{as}} + k_\ell(H) \min(S_\ell, P_{\mathrm{as}})}, \\ Q_{\mathrm{r}} &= H \frac{c_{\mathrm{r}} P_{\mathrm{vc}} a_{\mathrm{r}}(H) \min(S_{\mathrm{r}}, P_{\mathrm{ap}})}{a_{\mathrm{r}}(H) P_{\mathrm{ap}} + k_{\mathrm{r}}(H) \min(S_{\mathrm{r}}, P_{\mathrm{ap}})}. \end{aligned} \tag{2.17}$$

Finally a ventricle's contractile forces have to be determined to calculate cardiac output. In general, the contractility of a ventricle is influenced by the autonomic nervous system via baroreflex responses and by the heart rate H (compare Sec. 1.1.3.2). For simplification we only consider the dependency on H, i.e. the Bowditch effect, since a control for H will be used to simulate the action of the baroreflex. The influence of H on S_ℓ and S_{r} is modeled using the following second order ODEs

$$\begin{aligned} \ddot{S}_\ell + \gamma_\ell \dot{S}_\ell + \alpha_\ell S_\ell =& \beta_\ell H, \\ \ddot{S}_{\mathrm{r}} + \gamma_{\mathrm{r}} \dot{S}_{\mathrm{r}} + \alpha_{\mathrm{r}} S_{\mathrm{r}} =& \beta_{\mathrm{r}} H, \end{aligned} \tag{2.18}$$

with positive constants α_ℓ, α_{r}, β_ℓ, β_{r}, γ_ℓ and γ_{r}. It can be shown that solutions of (2.18) are asymptotically stable for constant values of H and in steady state changes in H provoke aligned changes in S_ℓ and S_{r} (see also [6, p. 13]).

2.1.3 Incorporating controls

In order to obtain a complete model, the impact of the controls for heart rate H, unstressed volume V_{u}, and systemic resistance R_{s} on the system has to be quantified. The relation of heart rate and contractility was explained in the previous section, thus here only the effects of V_{u} and R_{s} are considered.
Under orthostatic stress sympathetically induced vasoconstriction is one of the counter measures the body takes to prevent a drop in arterial pressure (see Sec. 1.3). However, local control mechanisms may react to global increases in resistance by vasodilation according to metabolic demands in the tissue (see for instance [6, Sec. 3.1.1]). This can be seen as maximal tolerable increase in local resistance (a similar approach was taken in [11]). Let $R^{\mathrm{in}}_{\mathrm{comp}}$ be the inflow resistance to the compartment 'comp', where 'comp' stands for the systemic sections 'per', 'up', 'ren', 'spl' and 'leg'. Furthermore let R_{aux} be an auxiliary variable which to some extent quantifies sympathetic net activation, R^0_{comp} the initial compartmental inflow resistance and K_{comp} determine the maximal sustainable local resistance increase which is assumed to be constant. We define

$$R^{\mathrm{in}}_{\mathrm{comp}} = \min(R^0_{\mathrm{comp}} + \kappa_{\mathrm{comp}} R_{\mathrm{aux}}, K_{\mathrm{comp}} R^0_{\mathrm{comp}}), \tag{2.19}$$

where κ_{comp} regulates the distribution of the net increase in resistance over the compartments. The inflows to the compartments 'per', 'up', 'ren', 'spl' and 'leg' are given by

$$F_{\text{comp}}^{\text{in}} = \frac{P_{\text{in}} - P_{\text{out}}}{R_{\text{comp}}^{\text{in}}}. \tag{2.20}$$

Flows out of a compartment are computed according to (2.3) with the addition that the effect of venous valves is included using a maximum formulation

$$F_{\text{comp}}^{\text{out}} = \max(0, \frac{P_{\text{in}} - P_{\text{out}}}{R_{\text{comp}}^{\text{out}}}), \tag{2.21}$$

where $R_{\text{comp}}^{\text{out}}$ denotes the outflow resistance (which is in contrast to the inflow resistance assumed to be a constant parameter) of compartment 'comp', where 'comp' stands for 'per', 'up', 'ren', 'spl', 'leg' and 'avc'. The pulmonary flow is assumed to be neither altered by sympathetic vasoconstriction nor by effects of venous valves thus

$$F_{\text{p}} = \frac{P_{\text{ap}} - P_{\text{vp}}}{R_{\text{p}}}. \tag{2.22}$$

For a full list of all flows and resistances, see Appendix A.1. Another volume shift is present by the change in unstressed volume V_{u}, which is included in a compartment's general hemodynamical equation (2.5). However, since unstressed volume is mainly recruited from the abdominal region (see for instance [6, p. 145]) we assume a constant unstressed volume, i.e. $\dot{V}_{\text{u}} = 0$ in all compartments except for 'ren' and 'spl'.

2.1.4 Setting up the complete model

For connecting the introduced parts to obtain a single model we have to transfer the second order ODE-model for the Bowditch effect (2.18) into first order ODEs introducing two new variables σ_ℓ and σ_r such that

$$\begin{aligned} \sigma_\ell =& \dot{S}_\ell, \quad \dot{\sigma}_\ell = -\alpha_\ell S_\ell - \gamma_\ell \sigma_\ell + \beta_\ell H, \\ \sigma_\mathrm{r} =& \dot{S}_\mathrm{r}, \quad \dot{\sigma}_\mathrm{r} = -\alpha_\mathrm{r} S_\mathrm{r} - \gamma_\mathrm{r} \sigma_\mathrm{r} + \beta_\mathrm{r} H. \end{aligned} \tag{2.23}$$

Using (2.5), (2.17), (2.20), (2.21), (2.22) and (2.23) the full model is given by the following system of ODEs

$$\begin{aligned} \dot{P}_\mathrm{as} =& \frac{1}{c_\mathrm{as}}(Q_\ell - (F_\mathrm{per}^\mathrm{in} + F_\mathrm{up}^\mathrm{in} + F_\mathrm{ren}^\mathrm{in} + F_\mathrm{spl}^\mathrm{in} + F_\mathrm{leg}^\mathrm{in}) + c_\mathrm{as}\dot{P}_\mathrm{as}^\mathrm{bias}), \\ \dot{P}_\mathrm{per} =& \frac{1}{c_\mathrm{per}}(F_\mathrm{per}^\mathrm{in} - F_\mathrm{per}^\mathrm{out} + c_\mathrm{per}\dot{P}_\mathrm{per}^\mathrm{bias}), \\ \dot{P}_\mathrm{up} =& \frac{1}{c_\mathrm{up}}(F_\mathrm{up}^\mathrm{in} - F_\mathrm{up}^\mathrm{out} + c_\mathrm{up}\dot{P}_\mathrm{up}^\mathrm{bias}), \\ \dot{P}_\mathrm{ren} =& \frac{1}{c_\mathrm{ren}}(F_\mathrm{ren}^\mathrm{in} - F_\mathrm{ren}^\mathrm{out} + c_\mathrm{ren}\dot{P}_\mathrm{ren}^\mathrm{bias} - k_\mathrm{ren}\dot{V}_\mathrm{u}), \\ \dot{P}_\mathrm{spl} =& \frac{1}{c_\mathrm{spl}}(F_\mathrm{spl}^\mathrm{in} - F_\mathrm{spl}^\mathrm{out} + c_\mathrm{spl}\dot{P}_\mathrm{spl}^\mathrm{bias} - k_\mathrm{spl}\dot{V}_\mathrm{u}), \\ \dot{P}_\mathrm{leg} =& \frac{1}{c_\mathrm{leg}}(F_\mathrm{leg}^\mathrm{in} - F_\mathrm{leg}^\mathrm{out} + c_\mathrm{leg}\dot{P}_\mathrm{leg}^\mathrm{bias}), \\ \dot{P}_\mathrm{vc} =& \frac{1}{c_\mathrm{vc}}(F_\mathrm{avc} + F_\mathrm{per}^\mathrm{out} + F_\mathrm{up}^\mathrm{out} - Q_\mathrm{r} + c_\mathrm{vc}\dot{P}_\mathrm{vc}^\mathrm{bias}), \\ \dot{P}_\mathrm{vp} =& \frac{1}{c_\mathrm{vp}}(F_\mathrm{p} - Q_\ell + c_\mathrm{vp}\dot{P}_\mathrm{vp}^\mathrm{bias}), \\ \dot{P}_\mathrm{avc} =& \frac{1}{c_\mathrm{avc}}(F_\mathrm{ren}^\mathrm{out} + F_\mathrm{spl}^\mathrm{out} + F_\mathrm{leg}^\mathrm{out} - F_\mathrm{avc} + c_\mathrm{avc}\dot{P}_\mathrm{avc}^\mathrm{bias}), \\ \dot{S}_\ell =& \sigma_\ell, \\ \dot{\sigma}_\ell =& -\alpha_\ell S_\ell - \gamma_\ell \sigma_\ell + \beta_\ell H, \\ \dot{S}_\mathrm{r} =& \sigma_\mathrm{r}, \\ \dot{\sigma}_\mathrm{r} =& -\alpha_\mathrm{r} S_\mathrm{r} - \gamma_\mathrm{r} \sigma_\mathrm{r} + \beta_\mathrm{r} H, \\ \dot{V}_\mathrm{u} =& u_1, \\ \dot{R}_\mathrm{aux} =& u_2, \\ \dot{H} =& u_3, \end{aligned} \tag{2.24}$$

where k_ren and k_spl regulate the sequestration of unstressed volume and u_i, $i = 1, 2, 3$ are the control responses. Note that there is no equation for P_ap. This is due to the following fact: the initial assumption was that there is no exchange of liquid between vessels and intercellular space, thus the total blood volume V_tot is given by

$$\begin{aligned} V_\mathrm{tot} = & c_\mathrm{as}(P_\mathrm{as} - P_\mathrm{as}^\mathrm{bias}) + c_\mathrm{per}(P_\mathrm{per} - P_\mathrm{per}^\mathrm{bias}) + c_\mathrm{up}(P_\mathrm{up} - P_\mathrm{up}^\mathrm{bias}) \\ & + c_\mathrm{ren}(P_\mathrm{ren} - P_\mathrm{ren}^\mathrm{bias}) + c_\mathrm{spl}(P_\mathrm{spl} - P_\mathrm{spl}^\mathrm{bias}) + c_\mathrm{leg}(P_\mathrm{leg} - P_\mathrm{leg}^\mathrm{bias}) \\ & + c_\mathrm{vc}(P_\mathrm{vc} - P_\mathrm{vc}^\mathrm{bias}) + c_\mathrm{vp}(P_\mathrm{vp} - P_\mathrm{vp}^\mathrm{bias}) + c_\mathrm{avc}(P_\mathrm{avc} - P_\mathrm{avc}^\mathrm{bias}) \\ & + c_\mathrm{ap}(P_\mathrm{ap} - P_\mathrm{ap}^\mathrm{bias}) + V_\mathrm{u}, \end{aligned} \tag{2.25}$$

which can be used to get an explicit formula for P_{ap}:

$$\begin{aligned} P_{\mathrm{ap}} =& \frac{1}{c_{\mathrm{ap}}} \Big(V_{\mathrm{tot}} - V_{\mathrm{u}} - c_{\mathrm{as}}(P_{\mathrm{as}} - P_{\mathrm{as}}^{\mathrm{bias}}) \\ & - c_{\mathrm{per}}(P_{\mathrm{per}} - P_{\mathrm{per}}^{\mathrm{bias}}) - c_{\mathrm{up}}(P_{\mathrm{up}} - P_{\mathrm{up}}^{\mathrm{bias}}) - c_{\mathrm{ren}}(P_{\mathrm{ren}} - P_{\mathrm{ren}}^{\mathrm{bias}}) \\ & - c_{\mathrm{spl}}(P_{\mathrm{spl}} - P_{\mathrm{spl}}^{\mathrm{bias}}) - c_{\mathrm{leg}}(P_{\mathrm{leg}} - P_{\mathrm{leg}}^{\mathrm{bias}}) - c_{\mathrm{vc}}(P_{\mathrm{vc}} - P_{\mathrm{vc}}^{\mathrm{bias}}) \\ & - c_{\mathrm{vp}}(P_{\mathrm{vp}} - P_{\mathrm{vp}}^{\mathrm{bias}}) - c_{\mathrm{avc}}(P_{\mathrm{avc}} - P_{\mathrm{avc}}^{\mathrm{bias}}) \Big) + P_{\mathrm{ap}}^{\mathrm{bias}}. \end{aligned} \tag{2.26}$$

Now let $u(t) = (u_1(t), u_2(t), u_3(t))^\top$ and

$$x = (P_{\mathrm{as}}, P_{\mathrm{per}}, P_{\mathrm{up}}, P_{\mathrm{ren}}, P_{\mathrm{spl}}, P_{\mathrm{leg}}, P_{\mathrm{vc}}, P_{\mathrm{vp}}, P_{\mathrm{avc}}, S_\ell, \sigma_\ell, S_{\mathrm{r}}, \sigma_{\mathrm{r}}, V_{\mathrm{u}}, R_{\mathrm{aux}}, H)^\top \in \mathbb{R}^{16}$$

be the state vector of the system. Then the model can be written compactly as

$$\begin{cases} \dot{x}(t) = \mathcal{F}(x(t), u(t), t), \\ x(t_0) = x^0, \end{cases} \tag{2.27}$$

with initial conditions x^0 at time $t = t_0$ (we will assume $t_0 = 0$) and the coordinates of $\mathcal{F}$ given by (2.24).

2.2 The controls

As mentioned above three different control formulations for V_{u}, R_{aux} and H will be incorporated into the model to test their behavior under simulated orthostatic stress. The first one is a basic arctan-approach (a related model using these controls was presented in [11]) which is easy to use and implement but is of very limited adaptivity (for details see Sec. 2.2.1). The second formulation is a differential set point equation (Sec. 2.2.2). It has the advantage over the arctan-controls that the shape of the control response can be designed in more detail due to more adjustable parameters. However, the number of parameters is also a drawback since those have to be estimated if the model is fit to data. The last approach is an optimal control formulation. Without explicitly designing a control gain we will show how a stabilizing control that simulates counteractions of the CVS under orthostatic stress can be obtained (Sec. 2.2.3). However, it is rather complicated to set up and the model has to meet some additional requirements compared to the arctan- or set point controls.

2.2.1 The arctan-controls

Corresponding to [12] we consider the inputs to the arterial and cardiopulmonary baroreflex to be P_{as} and P_{vc} respectively. We assume that the arterial baroreflex only alters systemic resistance and heart rate, whereas information from the venous receptors only influences unstressed volume recruitment. The baroreflex is a negative feedback loop thus the responses have to be designed such that low levels of P_{as} or P_{vc} provoke actions which result in an increase in those pressures and vice versa. This is realized by subtracting initial resting steady state values $P_{\mathrm{as}}^0 = P_{\mathrm{as}}(0)$ and $P_{\mathrm{vc}}^0 = P_{\mathrm{vc}}(0)$ from the current values of P_{as} and P_{vc} respectively, scaling it by positive constants c_1 and c_2 and generating control

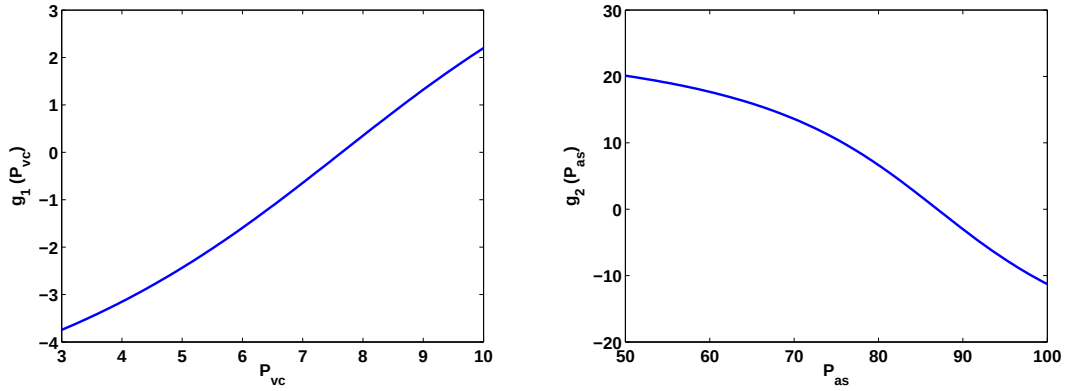

Figure 2.2: Response of $g_1(P_{\mathrm{vc}})$ (a) and $g_2(P_{\mathrm{as}})$ (b) from (2.28) with $P^0_{\mathrm{as}} = 87.7$ mmHg, $P^0_{\mathrm{vc}} = 7.5$ mmHg and $c_1 = \bar{c}_1 = 5$, $c_2 = \bar{c}_2 = 18$

responses by using the sigmoidal shaped arc tangent. Thus deviations of P_{as} and P_{vc} from P^0_{as} and P^0_{vc} respectively are counteracted:

$$\begin{aligned}
\dot{V}_{\mathrm{u}} =& \bar{c}_1 \arctan\left(\frac{P_{\mathrm{vc}} - P^0_{\mathrm{vc}}}{c_1}\right), \\
\dot{R}_{\mathrm{aux}} =& -\bar{c}_2 \arctan\left(\frac{P_{\mathrm{as}} - P^0_{\mathrm{as}}}{c_2}\right), \\
\dot{H} =& -\bar{c}_2 \arctan\left(\frac{P_{\mathrm{as}} - P^0_{\mathrm{as}}}{c_2}\right).
\end{aligned}$$

This approach as well as the values of the constants $\bar{c}_1$, $\bar{c}_2$, c_1 and c_2 were taken from [12] (however, there the arc tangents are used to generate error signals which are then further processed to compute baroreflex effects). The right hand sides

$$g_1(P_{\mathrm{vc}}) = \bar{c}_1 \arctan\left(\frac{P_{\mathrm{vc}} - P^0_{\mathrm{vc}}}{c_1}\right) \quad \text{and} \quad g_2(P_{\mathrm{as}}) = -\bar{c}_2 \arctan\left(\frac{P_{\mathrm{as}} - P^0_{\mathrm{as}}}{c_2}\right), \tag{2.28}$$

are depicted in Figure 2.2. Note that controlling V_{u} means that low levels of blood pressure are counteracted by recruiting unstressed volume to transfer it to stressed volume, i.e. decreasing V_{u}. This explains the changed signs in $g_1(P_{\mathrm{vc}})$.
However, since $g_1(P_{\mathrm{vc}})$ and $g_2(P_{\mathrm{as}})$ directly influence derivatives, i.e. rates of change of H, V_{u} and R_{aux} some maximal and minimal values have to be imposed, otherwise the controlled quantities would soon reach non physiological values. Therefore we introduce maximal and minimal heart rates $H^{\max}$ and $H^{\min}$, maximal and minimal unstressed volumes $V_{\mathrm{u}}^{\max}$ and $V_{\mathrm{u}}^{\min}$ and a maximal sympathetic vasodilational effect $R_{\mathrm{aux}}^{\min}$. A maximal vasoconstrictional effect for R_{aux} is not needed since maximal compartmental resistances are already included in the local metabolic control (2.19). For ensuring that, for instance, values of H higher than $H^{\max}$ can return into the interval $[H^{\min}, H^{\max}]$ if blood pressure increases again after an initial perturbation of orthostatic stress, the sign of the current value of $g_2(P_{\mathrm{as}})$ has to

be taken into account as well. Thus using (2.28) we define $u(t)$ from system (2.27) to be

$$
\begin{aligned}
u_1 &= \begin{cases} 0, & \text{for } g_1(P_{\mathrm{vc}}) < 0 \wedge V_{\mathrm{u}} \leq V_{\mathrm{u}}^{\max}, \\ 0, & \text{for } g_1(P_{\mathrm{vc}}) > 0 \wedge V_{\mathrm{u}} \geq V_{\mathrm{u}}^{\min}, \\ g_1(P_{\mathrm{vc}}), & \text{otherwise}, \end{cases} \\
u_2 &= \begin{cases} 0, & \text{for } g_2(P_{\mathrm{as}}) < 0 \wedge R_{\mathrm{aux}} \leq R_{\mathrm{aux}}^{\min}, \\ g_2(P_{\mathrm{as}}), & \text{otherwise}, \end{cases} \\
u_3 &= \begin{cases} 0, & \text{for } g_2(P_{\mathrm{as}}) > 0 \wedge H \geq H^{\max}, \\ 0, & \text{for } g_2(P_{\mathrm{as}}) < 0 \wedge H \leq H^{\min}, \\ g_2(P_{\mathrm{as}}), & \text{otherwise}. \end{cases}
\end{aligned} \tag{2.29}
$$

We will from now on refer to (2.29) as arctan controls.

2.2.2 The set point controls

The definition of the arctan controls (2.29) shows that imposing reasonable physiological bounds on sigmoidal functions can be problematic the more complex a control loop becomes. However, sigmoids such as the arc tangent are very well suited to model saturation effects which are often observed in biomedical applications. One way to use the advantages of sigmoids is employing differential set point equations. This approach is taken from [22] where it is used to model autonomic regulation.
Again we make use of $H^{\min}$, $H^{\max}$, $V_{\mathrm{u}}^{\min}$, $V_{\mathrm{u}}^{\max}$ and $R_{\mathrm{aux}}^{\min}$ and additionally we need $R_{\mathrm{aux}}^{\max}$ to specify maximal and minimal values of H, V_{u} and R_{aux}, respectively. As was the case for the arctan controls we assume that H and R_{aux} are regulated via changes in P_{as} and V_{u} is controlled based on variations in P_{vc}. We define sigmoidal set point functions $V_{\mathrm{u}}^{\mathrm{ctrl}}$, $R_{\mathrm{aux}}^{\mathrm{ctrl}}$ and H^{ctrl} to be

$$
\begin{aligned}
V_{\mathrm{u}}^{\mathrm{ctrl}}(P_{\mathrm{vc}}) &= (V_{\mathrm{u}}^{\max} - V_{\mathrm{u}}^{\min}) \frac{P_{\mathrm{vc}}^{k_1}}{P_{\mathrm{vc}}^{k_1} + \hat{P}_{\mathrm{vc}}^{k_1}} + V_{\mathrm{u}}^{\min}, \\
R_{\mathrm{aux}}^{\mathrm{ctrl}}(P_{\mathrm{as}}) &= (R_{\mathrm{aux}}^{\max} - R_{\mathrm{aux}}^{\min}) \frac{\hat{P}_{\mathrm{as}}{}^{k_2}}{P_{\mathrm{as}}^{k_2} + \hat{P}_{\mathrm{as}}{}^{k_2}} + R_{\mathrm{aux}}^{\min}, \\
H^{\mathrm{ctrl}}(P_{\mathrm{as}}) &= (H^{\max} - H^{\min}) \frac{\hat{P}_{\mathrm{as}}^{k_3}}{P_{\mathrm{as}}^{k_3} + \hat{P}_{\mathrm{as}}{}^{k_3}} + H^{\min},
\end{aligned} \tag{2.30}
$$

where $\hat{P}_{\mathrm{as}}$ and $\hat{P}_{\mathrm{vc}}$ are predefined steady state values of P_{as} and P_{vc}. The minimal and maximal values of V_{u}, R_{aux}, and H are chosen such that a preset steady state value $\hat{V}_{\mathrm{u}}$ is obtained at $\hat{P}_{\mathrm{vc}}$ and $\hat{R}_{\mathrm{aux}}$ and $\hat{H}$ are obtained at $\hat{P}_{\mathrm{as}}$. Thus it has to hold that

$$
\begin{aligned}
V_{\mathrm{u}}^{\mathrm{ctrl}}(\hat{P}_{\mathrm{vc}}) &= \frac{V_{\mathrm{u}}^{\max} + V_{\mathrm{u}}^{\min}}{2} = \hat{V}_{\mathrm{u}}, \\
R_{\mathrm{aux}}^{\mathrm{ctrl}}(\hat{P}_{\mathrm{as}}) &= \frac{R_{\mathrm{aux}}^{\max} + R_{\mathrm{aux}}^{\min}}{2} = \hat{R}_{\mathrm{aux}}, \\
H^{\mathrm{ctrl}}(\hat{P}_{\mathrm{as}}) &= \frac{H^{\max} + H^{\min}}{2} = \hat{H}.
\end{aligned} \tag{2.31}
$$

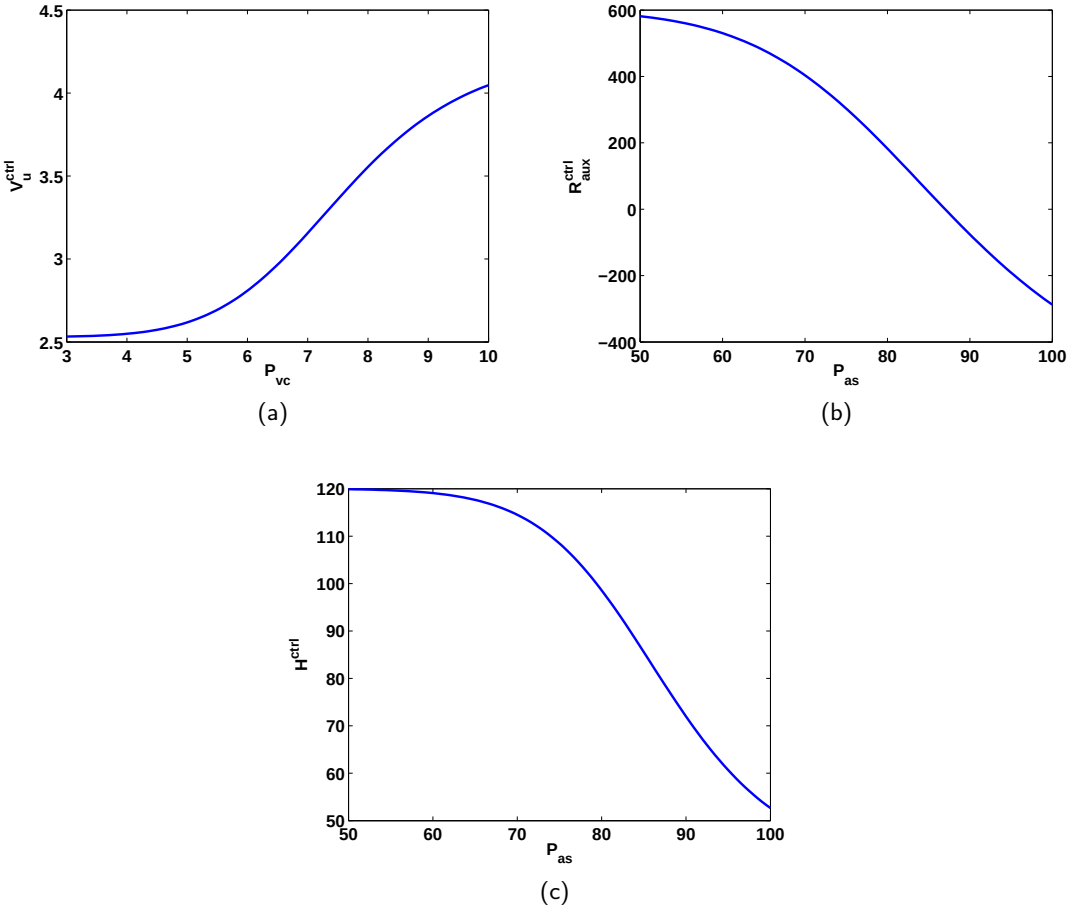

Figure 2.3: The sigmoidal functions $V_{\mathrm{u}}^{\mathrm{ctrl}}$ (a), $R_{\mathrm{aux}}^{\mathrm{ctrl}}$ (b) and H^{ctrl} (c) defined by (2.30) with $\hat{P}_{\mathrm{vc}} = 7.5$ mmHg, $\hat{P}_{\mathrm{as}} = 87.7$ mmHg and other parameters as given in Appendix A.3.

Note that the maximum and minimum values of V_{u}, R_{aux} and H are not determined uniquely by (2.31) which can make parameter identification using experimental data difficult (parameter identification with a related model using similar controls was carried out in [5]). The asymptotic values of the sigmoids are given by

$$V_{\mathrm{u}}^{\mathrm{ctrl}}(P_{\mathrm{vc}}) \to \begin{cases} (V_{\mathrm{u}}^{\max} - V_{\mathrm{u}}^{\min}) \cdot 0 + V_{\mathrm{u}}^{\min} = V_{\mathrm{u}}^{\min}, & \text{for } P_{\mathrm{vc}} \to 0, \\ (V_{\mathrm{u}}^{\max} - V_{\mathrm{u}}^{\min}) \cdot 1 + V_{\mathrm{u}}^{\min} = V_{\mathrm{u}}^{\max} & \text{for } P_{\mathrm{vc}} \to \infty, \end{cases}$$

$$R_{\mathrm{aux}}^{\mathrm{ctrl}}(P_{\mathrm{as}}) \to \begin{cases} (R_{\mathrm{aux}}^{\max} - R_{\mathrm{aux}}^{\min}) \cdot 1 + R_{\mathrm{aux}}^{\min} = R_{\mathrm{aux}}^{\max}, & \text{for } P_{\mathrm{as}} \to 0, \\ (R_{\mathrm{aux}}^{\max} - R_{\mathrm{aux}}^{\min}) \cdot 0 + R_{\mathrm{aux}}^{\min} = R_{\mathrm{aux}}^{\max}, & \text{for } P_{\mathrm{as}} \to \infty, \end{cases}$$

$$H^{\mathrm{ctrl}}(P_{\mathrm{as}}) \to \begin{cases} (H^{\max} - H^{\min}) \cdot 1 + H^{\min} = H^{\max}, & \text{for } P_{\mathrm{as}} \to 0, \\ (H^{\max} - H^{\min}) \cdot 0 + H^{\min} = H^{\min}, & \text{for } P_{\mathrm{as}} \to \infty, \end{cases}$$

thus $V_{\mathrm{u}}^{\mathrm{ctrl}}$ is an increasing, $R_{\mathrm{aux}}^{\mathrm{ctrl}}$ and H^{ctrl} are decreasing sigmoidal functions (see Fig. 2.3).

Finally the sigmoids given in (2.30) are used in the following ODEs for $u(t)$ from system (2.27)

$$\begin{aligned} u_1 =& \frac{-V_{\mathrm{u}} + V_{\mathrm{u}}^{\mathrm{ctrl}}}{\tau_1}, \\ u_2 =& \frac{-R_{\mathrm{aux}} + R_{\mathrm{aux}}^{\mathrm{ctrl}}}{\tau_2}, \\ u_3 =& \frac{-H + H^{\mathrm{ctrl}}}{\tau_3}, \end{aligned} \tag{2.32}$$

where τ_i, $i = 1, 2, 3$ are time constants influencing how long it takes until the full control response is reached (see [22]). Note that if minimal and maximal values of V_{u}, R_{aux} and H are chosen according to (2.31), in steady state, i.e. $V_{\mathrm{u}} = \hat{V}_{\mathrm{u}}$, $R_{\mathrm{aux}} = \hat{R}_{\mathrm{aux}}$ and $H = \hat{H}$, the control response is zero, $u = 0$.

2.2.3 The optimal control

For incorporating an optimal control strategy in the model (2.27) some background from control theory is required. The basic theoretical principles needed in the context of this thesis will be briefly presented (following [14, 18, 1] and [23]) to show how they are applied to the specific problem (similar to [6]).

2.2.3.1 Linearization

Instead of looking at a non linear system such as (2.27) it is often useful to find approximate solutions of an associated linear model. Let $\mathcal{F} \in C^1(\mathbb{R}^n \times \mathbb{R}^m \times [t_0, t_1], \mathbb{R}^n)$, $x \in C^1([t_0, t_1], \mathbb{R}^n)$, $u \in C([t_0, t_1], \mathbb{R}^m)$ with $m < n$ and x^0 be a vector in $\mathbb{R}^n$. Look at $x(t)$ satisfying

$$\begin{cases} \dot{x}(t) = \mathcal{F}(x(t), u(t), t), & -\infty < t_0 < t \leq t_1 < \infty, \\ x(t_0) = x^0. \end{cases} \tag{2.33}$$

Introducing "small" perturbations $\tilde{x}(t)$, $\tilde{u}(t)$ and $\tilde{x}(t_0)$ we define the neighboring solutions

$$\hat{x}(t) = x(t) + \tilde{x}(t), \qquad t_0 < t \leq t_1, \tag{2.34}$$

$$\hat{u}(t) = u(t) + \tilde{u}(t), \qquad t_0 \leq t \leq t_1, \tag{2.35}$$

$$\hat{x}(t_0) = x(t_0) + \tilde{x}(t_0). \tag{2.36}$$

Using (2.56) and (2.68) in (2.33) gives

$$\dot{\hat{x}}(t) = \dot{x}(t) + \dot{\tilde{x}}(t) = \mathcal{F}(x(t) + \tilde{x}(t), u(t) + \tilde{u}(t), t). \tag{2.37}$$

A Taylor expansion of $\mathcal{F}$ around $(x(t), u(t), t)$ yields

$$\begin{aligned} \mathcal{F}(x(t) + \tilde{x}(t), u(t) + \tilde{u}(t), t) =& \mathcal{F}(x(t), u(t), t) + \mathcal{F}_x(x(t), u(t), t)\tilde{x}(t) \\ &+ \mathcal{F}_u(x(t), u(t), t)\tilde{u}(t) + h(t), \end{aligned} \tag{2.38}$$

where $h(t) \in \mathbb{R}^n$ is the remainder term and $\mathcal{F}_x \in \mathbb{R}^{n \times n}$ denotes the Jacobian of $\mathcal{F}$ with respect to x (thus

$$(\mathcal{F}_x)_{i,j} = \frac{\partial f_i}{\partial x_j}, \quad i, j = 1, ..., n,$$

where f_i denotes the i-th component of $\mathcal{F}$ and x_j the j-th component of the state vector x) and $\mathcal{F}_u \in \mathbb{R}^{n\times m}$ the Jacobian of $\mathcal{F}$ with respect to u (analogously). Since $h(t)$ can assumed to be small for small deviations $\tilde{x}$ and $\tilde{u}$ it is omitted from eq. (2.38). Using (2.37) in (2.38) (note that $\mathcal{F}(x(t), u(t))$ cancels since (2.33) holds) with $A = \mathcal{F}_x$ and $B = \mathcal{F}_u$ we obtain the linear system

$$\dot{\tilde{x}}(t) = A\tilde{x}(t) + B\tilde{u}(t), \tag{2.39}$$

with initial condition $\tilde{x}(t_0)$ (using eq (2.36)). The system (2.39) is called *linearized state differential equation.* It can be shown that if the interval $[t_0, t_1]$ is finite, the initial perturbations $\tilde{x}(t_0)$ and $\tilde{u}(t_0)$ are small and the partial derivatives $\mathcal{F}_{x_j}$ and $\mathcal{F}_{u_i}$ are close to the values of x and u from the original system (2.33) solutions of the linearized state differential equations can be made arbitrarily good approximations to solutions of (2.33) (see [18, Sec. 1.2.2]). Therefore we will from now on focus on linear systems.

2.2.3.2 Linear state differential systems

We consider a linear state differential system

$$\begin{cases} \dot{x}(t) = A(t)x(t) + B(t)u(t), & \text{a.e. on } \Omega, \\ x(t_0) = x^0, \end{cases} \tag{2.40}$$

with $\Omega = [t_0, t_1]$ ($-\infty < t_0 < t \leq t_1 < \infty$, t_0 and t_1 fixed) and relaxed smoothness-assumptions on A and B, namely $A \in L^2(\Omega, \mathbb{R}^{n\times n})$ and $B \in L^2(\Omega, \mathbb{R}^{n\times m})$. It can be shown that for a given control $u \in L^2(\Omega, \mathbb{R}^m)$ the state equation (2.40) has a unique solution $x(\cdot)$ in the sense of Caratheodory. This means $x(t_0) = x^0 \in \mathbb{R}^n$ and $x(\cdot)$ is absolutely continuous, thus it has a derivative almost everywhere (a.e.) on Ω which is in $L^2(\Omega, \mathbb{R}^n)$ and $x(\cdot)$ satisfies (2.40) a.e on Ω (see [14, Sec. 2]). We collect the absolutely continuous functions mapping from Ω to $\mathbb{R}^n$ in the set $AC(\Omega, \mathbb{R}^n)$, thus $x \in AC(\Omega, \mathbb{R}^n)$. We summarize some basic facts on the solution of linear state differential systems which will be needed later (see for instance [18, Sec. 1.3][1]).

Theorem 1. *Let $x \in AC(\Omega, \mathbb{R}^n)$, $x^0 \in \mathbb{R}^n$ and $A \in L^2(\Omega, \mathbb{R}^{n\times n})$. Then the solution of the homogeneous system*

$$\begin{cases} \dot{x}(t) = A(t)x(t), & \text{a.e on } \Omega, \\ x(t_0) = x^0, \end{cases} \tag{2.41}$$

can be written as

$$x(t) = \Phi(t, t_0)x^0, \tag{2.42}$$

where $\Phi \in AC(\Omega\times\Omega, \mathbb{R}^{n\times n})$ is the fundamental matrix solution of the homogeneous system (2.41)*, i.e. Φ is the solution of the matrix differential equation*

$$\begin{cases} \dfrac{d}{dt}\Phi(t, t_0) = A(t)\Phi(t, t_0), & \text{a.e on } \Omega, \\ \Phi(t_0, t_0) = I. \end{cases}$$

[1] Though the results given there are stated for continuous right-hand sides the extension to L^2-functions is straightforward.

The fundamental matrix solution has the following properties which will be useful later.

Lemma 2. *Let Φ be the fundamental matrix solution of the homogeneous system* (2.41). *Then Φ satisfies*

1) $\Phi(\cdot, t_0)$ *is non singular a.e. on* Ω.

2) $\Phi(\cdot, t_0)^{-1} = \Phi(t_0, \cdot)$ *a.e on* Ω.

3) $\dfrac{d}{dt}\Phi(t_0, t)^\top = -A(t)^\top \Phi(t_0, t)^\top$ *a.e. on* Ω.

Though the solution to any homogeneous system (2.41) satisfying the assumptions given in Theorem 1 is given by (2.42) the fundamental matrix solution is of limited practical value since it can very seldom be obtained directly in terms of standard functions (see [18, Sec. 1.3]). However, the fundamental matrix solution has great theoretical benefits of which will be made use of later. If the fundamental matrix solution of the homogeneous system is known it is straightforward to give a representation of the solution to the state differential system (2.40) (compare [18, Sec. 1.3]).

Theorem 3. *Let $x \in AC(\Omega, \mathbb{R}^n)$, $x^0 \in \mathbb{R}^n$, $A \in L^2(\Omega, \mathbb{R}^{n\times n})$, $B \in L^2(\Omega, \mathbb{R}^{n\times m})$ and $u \in L^2(\Omega, \mathbb{R}^m)$. Then the solution of* (2.40) *is given by*

$$x(t) = \Phi(t, t_0)x(t_0) + \int_{t_0}^{t} \Phi(t, \tau)B(\tau)u(\tau)\, d\tau.$$

2.2.3.3 The finite-time horizon LQR-problem

The finite-time linear-quadratic optimal regulator problem is the task of finding a control $u(\cdot)$ that drives the linear system (2.40) from any given initial condition x^0 to the zero state, i.e. $x = 0$, as fast as possible. We formulate this problem using an optimization approach: we want to minimize some criterion such that $x(t_1) = 0$. There are many ways to get suitable criteria for this problem. Since we deal with L^2-functions a natural criterion for x is to minimize some weighted L^2-norm:

$$\int_{t_0}^{t_1} x(t)^\top Q(t)x(t)\, dt, \tag{2.43}$$

where $Q(t) \in \mathbb{R}^{n\times n}$ is a weighting matrix. This criterion penalizes overall aberrations of x from the zero state on the interval Ω. The matrix $Q(\cdot)$ determines whether deviations in some components of x are respected more or less (if all components are considered to be equally important then for all $t \in \Omega : Q(t) = I$). However, minimizing (2.43) can lead to indefinitely large control responses $u(t)$ (see [18, Sec. 3.3.1]), thus this has to be compensated by including u in the criterion as well:

$$\int_{t_0}^{t_1} x(t)^\top Q(t)x(t) + u(t)^\top R(t)u(t)\, dt, \tag{2.44}$$

where $R(t) \in \mathbb{R}^{m\times m}$ is a weighting matrix too. It may occur that the time interval $[t_0, t_1]$ is too short to get $x(t_1) = 0$, thus a natural claim is that the system should be as close as possible to the zero state at the final time $t = t_1$. Therefore (2.44) is finally expanded to

$$\int_{t_0}^{t_1} \Big(x(t)^\top Q(t)x(t) + u(t)^\top R(t)u(t) \Big)\, dt + x(t_1)^\top S x(t_1),$$

with $S \in \mathbb{R}^{n\times n}$. Before we sum up these considerations in a definition we make some assumptions on $Q(\cdot)$, $R(\cdot)$ and S which will be needed in the course of deriving the solution to the depicted problem (taken from [14, Sec. 7]).

Assumption 4.

1) The matrix $Q \in L^2(\Omega, \mathbb{R}^{n\times n})$ is symmetric and positive semi-definite a.e. on Ω.

2) $S \in \mathbb{R}^{n\times n}$ is symmetric and positive semi-definite.

3) $R \in L^2(\Omega, \mathbb{R}^{m\times m})$ is symmetric a.e. on Ω and there exists $\alpha \in L^2(\Omega, \mathbb{R})$ with $\alpha(t) \geq 0$ a.e. on Ω and $1/\alpha \in L^2(\Omega, \mathbb{R})$. Furthermore for all $v \in \mathbb{R}^m$ the following estimate holds a.e. on Ω

$$v^\top R(t)v \geq \alpha(t) \|v\|_2^2 .$$

Note that Assumption 4.3) implies the following: Since $\alpha(t) \geq 0$ a.e. on Ω and $1/\alpha \in L^2(\Omega, \mathbb{R})$ it follows that $\alpha(t) > 0$ a.e. on Ω (this can be proved by contradiction: assume that $\alpha(t) = 0$ a.e. on Ω, then the assumption $1/\alpha \in L^2(\Omega, \mathbb{R})$ is violated). Furthermore

$$v^\top R(t)v \geq \alpha(t) \|v\|_2^2 , \quad \text{a.e. on } \Omega,$$

implies that (using $\alpha(t) > 0$ a.e. on Ω)

$$\|R(t)v\|_2 \geq \alpha(t) \|v\|_2 > 0, \quad \text{a.e. on } \Omega, \text{ for } v \in \mathbb{R}^m \backslash \{0\},$$

which means that $R(t)^{-1}$ exists a.e. on Ω satisfying

$$\left\|R(t)^{-1}v\right\|_2 \leq \frac{1}{\alpha(t)} \|v\|_2 , \quad \text{a.e. on } \Omega, \text{ with } v \in \mathbb{R}^m.$$

Now everything is set up to define the regulator problem.

Definition 5. Consider $x \in AC(\Omega, \mathbb{R}^n)$ and $u \in L^2(\Omega, \mathbb{R}^m)$ obeying (2.40) with $A \in L^2(\Omega, \mathbb{R}^{n\times n})$, $B \in L^2(\Omega, \mathbb{R}^{n\times m})$ and $Q(\cdot)$, $R(\cdot)$ and S satisfying Assumption 4. *The linear-quadratic (optimal) regulator problem (LQR-problem)* is the task of solving the minimization problem

$$\inf_{u\in L^2(\Omega,\mathbb{R}^m)} J(u, x^0),$$

with

$$J(u, x^0) = \int_{t_0}^{t_1} \Big(x(t)^\top Q(t)x(t) + u(t)^\top R(t)u(t) \Big)\, dt + x(t_1)^\top S x(t_1). \tag{2.45}$$

The cost functional J is also called *performance index* depending on the initial state x^0 and the control $u(\cdot)$.

We will show that the infimum in Definition 5 is achieved: the minimizer is the so-called *optimal control* $\hat{u}(\cdot)$, the value of the cost functional at the minimizer $J(\hat{u}, x^0)$ is called *optimum performance index*. The next result shows that $\hat{u}(\cdot)$ is the unique solution to the regulator problem: it is given by a linear feedback law with a feedback matrix determined by the solution of a matrix Riccati differential equation.

Theorem 6. *The LQR-problem as stated in Definition 5 has a unique solution* $\hat{u}(\cdot)$ *called* optimal control. *This solution is determined by a* linear feedback law

$$\hat{u}(t) = K(t)\hat{x}(t), \quad t \in \Omega,$$

with $K(t) = -R(t)^{-1}B(t)^\top P(t)$. $P(\cdot)$ *is the unique positive semi-definite solution of the* matrix Riccati differential equation

$$\begin{cases} -\dot{P}(t) = P(t)A(t) + A(t)^\top P(t) - P(t)B(t)R(t)^{-1}B(t)^\top P(t) + Q(t), & , t_0 \le t < t_1, \\ P(t_1) = S, \end{cases}$$

and $\hat{x}(\cdot)$ *being the solution to the* closed loop system

$$\begin{cases} \dot{\hat{x}}(t) = (A(t) + B(t)K(t))\,\hat{x}(t), & t_0 < t \le t_1, \\ \hat{x}(t_0) = x^0. \end{cases}$$

Finally the optimal performance index is given by

$$J(\hat{u}, x^0) = (x^0)^\top P(t_0) x^0.$$

Proof. The proof given here is mainly taken from [14, Sec. 7] with some extensions adopted from [18, Sec. 3.3.2], [23, Sec. 8.2] and [1, Sec. 2.3]. We divide it into the following steps:

1. Derivation of a necessary and sufficient condition for $\hat{u}$ being a minimizer of J.
2. If $\hat{u}$ exists then it is given by a linear feedback law.
3. The computation of the feedback matrix $K(t)$ involves the solution of a matrix Riccati differential equation.
4. The optimal performance index is given by a quadratic form.

1. A criterion for optimality of a control We will make use of some techniques from the calculus of variations. Assume that an optimal $\hat{u} \in L^2(\Omega, \mathbb{R}^m)$ exists for a given $x^0 \in \mathbb{R}^n$ and let $\hat{x} \in AC(\Omega, \mathbb{R}^n)$ be the associated solution of (2.40). For $\varepsilon > 0$ and $v \in L^2(\Omega, \mathbb{R}^m)$ a *variation* $u(\cdot)$ of $\hat{u}(\cdot)$ is given by

$$u(\cdot) = \hat{u}(\cdot) + \varepsilon v(\cdot).$$

Now let $x(\cdot)$ be the solution of (2.40) corresponding to the variation $u(\cdot)$. Due to the linearity of (2.40) we can assume that

$$x(\cdot) = \hat{x}(\cdot) + \varepsilon \tilde{x}(\cdot),$$

with some $\tilde{x}(\cdot)$, which has to be specified. Plugging x into (2.40) we get

$$\dot{\hat{x}}(t) + \varepsilon \dot{\tilde{x}}(t) = A(t)\hat{x}(t) + \varepsilon A(t)\tilde{x}(t) + B(t)\hat{u}(t) + \varepsilon B(t)v(t). \tag{2.46}$$

Looking at the optimal state $\hat{x}$ alone yields

$$\dot{\hat{x}}(t) = A(t)\hat{x}(t) + B(t)\hat{u}(t). \tag{2.47}$$

By subtracting (2.47) from (2.46) we see that

$$\dot{\tilde{x}}(t) = A(t)\tilde{x}(t) + B(t)v(t),$$

thus $\tilde{x}$ is the state associated to v. However, since the initial state is not affected by variations of $\hat{u}$ we have $x(t_0) = \hat{x}(t_0) + \varepsilon\tilde{x}(t_0) = x^0$, thus $\tilde{x}(t_0) = 0$. Evaluating the performance index J at the variation $u = \hat{u} + \varepsilon v$ yields (using the symmetry of $Q(\cdot)$, $R(\cdot)$, and S guaranteed by Assumption 4)

$$\begin{aligned}
J(\hat{u}+\varepsilon v, x^0) = &\int_{t_0}^{t_1} \Big((\hat{x}(t)+\varepsilon\tilde{x}(t))^\top Q(t)(\hat{x}(t)+\varepsilon\tilde{x}(t)) + \\
&\qquad (\hat{x}(t)+\varepsilon\tilde{x}(t))^\top R(t)(\hat{x}(t)+\varepsilon\tilde{x}(t))\, dt \Big) + \\
&(\hat{x}(t_1)+\varepsilon\tilde{x}(t_1))^\top S(\hat{x}(t_1)+\varepsilon\tilde{x}(t_1)) \\
= &\int_{t_0}^{t_1} \hat{x}(t)^\top Q(t)\hat{x}(t) + \hat{u}(t)^\top R(t)\hat{u}(t)\, dt + \hat{x}(t_1)^\top S\hat{x}(t_1) + \\
&2\varepsilon \left(\int_{t_0}^{t_1} \tilde{x}(t)^\top Q(t)\hat{x}(t) + v(t)^\top R(t)\hat{u}(t)\, dt + \tilde{x}(t_1)^\top S\hat{x}(t_1) \right) + \\
&\varepsilon^2 \left(\int_{t_0}^{t_1} \tilde{x}(t)^\top Q(t)\tilde{x}(t) + v(t)^\top R(t)v(t)\, dt + \tilde{x}(t_1)^\top S\hat{x}(t_1) \right) \\
= &J(\hat{u}, x^0) + \\
&2\varepsilon \left(\int_{t_0}^{t_1} \tilde{x}(t)^\top Q(t)\hat{x}(t) + v(t)^\top R(t)\hat{u}(t)\, dt + \tilde{x}(t_1)^\top S\hat{x}(t_1) \right) + \\
&\varepsilon^2 J(v, 0).
\end{aligned} \tag{2.48}$$

Now let $g(\varepsilon) = J(\hat{u} + \varepsilon v)$. We assumed that $\hat{u}$ is the optimal control, thus the variation $u = \hat{u} + \varepsilon v$ will necessarily increase the value of the performance index J. Therefore g attains its minimum at $\varepsilon = 0$. Since g is quadratic it has to hold that

$$\frac{d}{d\varepsilon} g(\varepsilon)\Big|_{\varepsilon=0} = 0,$$

or equivalently

$$\int_{t_0}^{t_1} \tilde{x}(t)^\top Q(t)\hat{x}(t) + v(t)^\top R(t)\hat{u}(t)\, dt + \tilde{x}(t_1)^\top S\hat{x}(t_1) = 0, \tag{2.49}$$

which is a necessary condition for $\hat{u}$ to be optimal. It is left to show that (2.49) is sufficient as well. Conversely let $\varepsilon = 1$ and $v \neq 0$. Using (2.49) in (2.48) yields

$$J(\hat{u} + v, x^0) = J(\hat{u}, x^0) + J(v, 0). \tag{2.50}$$

According to Assumption 4, $Q(\cdot)$ is positive semi-definite a.e. on Ω and S is positive semi-definite. Thus we can estimate

$$\int_{t_0}^{t_1} \tilde{x}(t)^\top Q(t)\tilde{x}(t)\, dt + \tilde{x}(t_1)^\top S\hat{x}(t_1) \geq 0.$$

This together with Assumption 4.3) (and its consequence $\alpha(t)>0$ a.e. on Ω) yields further (remember that we assumed $v \neq 0$)

$$J(v,0) \geq \int_{t_0}^{t_1} v(t)^\top R(t)v(t)\,dt \geq \int_{t_0}^{t_1} \alpha(t)\,\|v\|_2^2\,dt > 0. \tag{2.51}$$

Now let $u \in L^2(\Omega,\mathbb{R}^m)$ be arbitrary. With $v = u - \hat{u} \in L^2(\Omega,\mathbb{R}^m)$ we finally obtain using (2.51) and (2.50)

$$J(u,x^0) = J(\hat{u}+v,x^0) = J(\hat{u},x^0) + J(v,0) > J(\hat{u},x^0).$$

This shows that (2.49) is not only necessary but also sufficient for $\hat{u}$ to be optimal.

2. The optimal control is given by a linear feedback law We make again use of the variations introduced in Step 1. According to Theorem 3 the solution $\tilde{x}$ of (2.40) with control v and initial condition $\tilde{x}(t_0) = 0$ can be written in terms of the fundamental matrix solution

$$\begin{aligned}\tilde{x}(t) =& \Phi(t,t_0)\tilde{x}(t_0) + \int_{t_0}^{t} \Phi(t,\tau)B(\tau)v(\tau)\,d\tau \\ =& \int_{t_0}^{t} \Phi(t,\tau)B(\tau)v(\tau)\,d\tau.\end{aligned}$$

Using this representation of $\tilde{x}$ in (2.49) yields (using Fubini's theorem and factorizing $v^\top$ and $B^\top$)

$$\begin{aligned}0 =& \int_{t_0}^{t_1} \left(\int_{t_0}^{t} \Phi(t,\tau)B(\tau)v(\tau)\,d\tau\right)^\top Q(t)\hat{x}(t) + v(t)^\top R(t)\hat{u}(t)\,dt \\ &+ \left(\int_{t_0}^{t_1} \Phi(t_1,\tau)B(\tau)v(\tau)\,d\tau\right)^\top S\hat{x}(t_1) \\ =& \int_{t_0}^{t_1} v(t)^\top \left(B(t)^\top \left(\int_t^{t_1} \Phi(\tau,t)^\top Q(\tau)\hat{x}(\tau)\,d\tau + \Phi(t_1,t)^\top S\hat{x}(t_1)\right) + R(t)\hat{u}(t)\right) dt.\end{aligned}$$

Introducing the abbreviation

$$p(t) = \int_t^{t_1} \Phi(\tau,t)^\top Q(\tau)\hat{x}(\tau)\,d\tau + \Phi(t_1,t)^\top S\hat{x}(t_1), \tag{2.52}$$

we conclude

$$\int_{t_0}^{t_1} v(t)^\top \Big(B(t)^\top p(t) + R(t)\hat{u}(t)\Big)\,dt = 0. \tag{2.53}$$

According to Step 1 (2.49) is sufficient for $\hat{u}$ to be optimal. Thus (2.53) has to hold for all $v \in L^2(\Omega,\mathbb{R}^m)$ which means

$$B(t)^\top p(t) + R(t)\hat{u}(t) = 0 \quad \text{a.e. on } \Omega,$$

and therefore we obtain the feedback law (note that Assumption 4 3 implies that $R(t)^{-1}$ exists a.e. on Ω)

$$\hat{u}(t) = -R(t)^{-1}B(t)^\top p(t) \quad \text{a.e. on } \Omega. \tag{2.54}$$

As soon as $p(t)$ is determined (2.54) gives the optimal control at time t. Hence we transform the representation (2.52) into a differential equation for $p(t)$:

$$\begin{aligned}\dot{p}(t) =& \frac{d}{dt}\left(-\int_{t_1}^{t}\Phi(\tau,t)^\top Q(\tau)\hat{x}(\tau)\,d\tau + \Phi(t_1,t)^\top S\hat{x}(t_1)\right)\\ =& -\Phi(t,t)^\top Q(t)\hat{x}(t) + \frac{\partial}{\partial t}\Phi(t_1,t)^\top S\hat{x}(t_1) + \int_t^{t_1}\frac{\partial}{\partial t}\Phi(\tau,t)^\top Q(\tau)\hat{x}(\tau)\,d\tau.\end{aligned}$$

Since Φ is the fundamental matrix solution of (2.40) with control v and initial condition $\tilde{x}(t_0) = 0$ we can make use of its properties pointed out in Lemma 2.3)

$$\begin{aligned}\dot{p}(t) =& -Q(t)\hat{x}(t) - A(t)^\top\Phi(t_1,t)^\top S\hat{x}(t_1) - A(t)^\top\int_t^{t_1}\Phi(\tau,t)^\top Q(\tau)\hat{x}(\tau)\,d\tau\\ =& -Q(t)\hat{x}(t) - A(t)^\top\left(\int_t^{t_1}\Phi(\tau,t)^\top Q(\tau)\hat{x}(\tau)\,d\tau + \Phi(t_1,t)^\top S\hat{x}(t_1)\right)\\ =& -Q(t)\hat{x}(t) - A(t)^\top p(t),\end{aligned} \tag{2.55}$$

where we employed again relation (2.52) for $p(t)$. Furthermore using the feedback law (2.54) for the optimal control $\hat{u}$ in the state differential equations (2.40) results in

$$\dot{\hat{x}}(t) = A(t)\hat{x}(t) - B(t)R(t)^{-1}B(t)^\top p(t). \tag{2.56}$$

Equations (2.55) and (2.56) form a set of $2n$ simultaneous linear differential equations in the two n-dimensional unknowns $\hat{x}(t)$ and $p(t)$. Using the initial condition for $\hat{x}$ and evaluating relation (2.52) for $p(t)$ at $t = t_0$ gives the boundary conditions

$$\begin{aligned}\hat{x}(t_0) =& x^0,\\ p(t_1) =& \Phi(t_1,t_1)^\top S\hat{x}(t_1) = S\hat{x}(t_1).\end{aligned} \tag{2.57}$$

This can be written compactly as

$$\begin{cases}\begin{pmatrix}\dot{\hat{x}}(t)\\ \dot{p}(t)\end{pmatrix} = \begin{pmatrix}A(t) & -B(t)R(t)^{-1}B(t)^\top\\ -Q(t) & -A(t)^\top\end{pmatrix}\begin{pmatrix}\hat{x}(t)\\ p(t)\end{pmatrix},\\ \hat{x}(t_0) = x^0,\\ p(t_1) = S\hat{x}(t_1),\end{cases} \tag{2.58}$$

thus we are faced with a two-point boundary value problem. The system (2.58) is called *variational equations* and $p(t)$ is the *adjoint variable*. For solving problem (2.58) we will use its fundamental matrix solution which we denote by $\Theta(t,t_0) \in \mathbb{R}^{2n\times 2n}$ and partition it into four $n \times n$-blocks

$$\Theta(t,t_0) = \begin{pmatrix}\Theta_{11}(t,t_0) & \Theta_{12}(t,t_0)\\ \Theta_{21}(t,t_0) & \Theta_{22}(t,t_0)\end{pmatrix}.$$

According to Theorem 1 we can express the unknowns $(\hat{x}(t), p(t))^\top$ in terms of $\Theta(\cdot,t_1)$ and the terminal values $(\hat{x}(t_1), p(t_1))^\top$

$$\begin{pmatrix}\hat{x}(t)\\ p(t)\end{pmatrix} = \begin{pmatrix}\Theta_{11}(t,t_1) & \Theta_{12}(t,t_1)\\ \Theta_{21}(t,t_1) & \Theta_{22}(t,t_1)\end{pmatrix}\begin{pmatrix}\hat{x}(t_1)\\ p(t_1)\end{pmatrix}.$$

Using the terminal condition (2.57) yields

$$\begin{aligned}\hat{x}(t) =&\Theta_{11}(t,t_1)\hat{x}(t_1) + \Theta_{12}(t,t_1)S\hat{x}(t_1)\\ =&\left(\Theta_{11}(t,t_1) + \Theta_{12}(t,t_1)S\right)\hat{x}(t_1),\end{aligned}$$

and analogously

$$p(t) = \left(\Theta_{21}(t,t_1) + \Theta_{22}(t,t_1)S\right)\hat{x}(t_1). \tag{2.59}$$

We use the abbreviation

$$\tilde{\Theta}(\cdot,t_1) = \left(\Theta_{11}(\cdot,t_1) + \Theta_{12}(\cdot,t_1)S\right). \tag{2.60}$$

We see that (note, according to Assumption 4.2) S is positive semi-definite)

$$\tilde{\Theta}_1(t,t_1)\Big|_{t=t_1} = \left(\Theta_{11}(t,t_1) + \Theta_{12}(t,t_1)S\right)|_{t=t_1} = (I + I\cdot S),$$

is invertible. Since the fundamental matrix solution is (absolutely) continuous there exists $s_0 < t_1$ such that $\tilde{\Theta}_1(\cdot,t_1)$ is invertible at least on $(s_0,t_1]$. Hence we can express $\hat{x}(t_1)$ on $(s_0,t_1]$ as

$$\hat{x}(t_1) = \tilde{\Theta}_1(t,t_1)^{-1}\hat{x}(t).$$

Plugging this into (2.70) gives

$$p(t) = \left(\Theta_{21}(t,t_1) + \Theta_{22}(t,t_1)S\right)\tilde{\Theta}_1(t,t_1)^{-1}\hat{x}(t), \quad t\in(s_0,t_1].$$

Introducing the $n\times n$-matrix

$$P(t) = \left(\Theta_{21}(t,t_1) + \Theta_{22}(t,t_1)S\right)\tilde{\Theta}_1(t,t_1)^{-1}, \quad t\in(s_0,t_1], \tag{2.61}$$

we can write $p(t)$ as

$$p(t) = P(t)\hat{x}(t), \quad t\in(s_0,t_1].$$

Employing this relation in the expression (2.54) and setting

$$K(t) = -R(t)^{-1}B(t)P(t), \quad t\in(s_0,t_1],$$

finally gives the promised linear feedback law for the optimal control at least on the interval $(s_0,t_1]$:

$$\hat{u}(t) = K(t)\hat{x}(t), \quad t\in(s_0,t_1]. \tag{2.62}$$

3. The linear feedback law leads to a Riccati equation The feedback matrix $K(t)$ appearing in the linear feedback law (2.62) derived in Step 2 involves some matrix $P(t)$ which is given in terms of the fundamental matrix solution of the variational equations (2.58) on some interval $(s_0,t_1]$. The goal in this part of the proof is to give a more applicable representation of $P(t)$ on the whole interval Ω.
We start by collecting some information about the time-derivative of an inverted matrix function: let $M(t)\in\mathbb{R}^{n\times n}$ be invertible. By differentiating the identity $M(t)M(t)^{-1} = I$ we get

$$\begin{aligned}\dot{M}(t)M(t)^{-1} + M(t)\dot{M}(t)^{-1} =&0\\ \dot{M}(t)^{-1} =& -M(t)^{-1}\dot{M}(t)M(t)^{-1}.\end{aligned} \tag{2.63}$$

Applying (2.63) on $\tilde{\Theta}_1(\cdot, t_1)$ in the course of differentiating (2.61) we obtain for $t \in (s_0, t_1]$

$$\begin{aligned}\dot{P}(t) =& \frac{d}{dt}\left((\Theta_{21}(t,t_1) + \Theta_{22}(t,t_1)S)\,\tilde{\Theta}_1(t,t_1)^{-1}\right)\\ =& \left(\dot{\Theta}_{21}(t,t_1) + \dot{\Theta}_{22}(t,t_1)S\right)\tilde{\Theta}_1(t,t_1)^{-1}\\ &+ (\Theta_{21}(t,t_1) + \Theta_{22}(t,t_1)S)\,\dot{\tilde{\Theta}}_1(t,t_1)^{-1}\\ =& \left(\dot{\Theta}_{21}(t,t_1) + \dot{\Theta}_{22}(t,t_1)S\right)\tilde{\Theta}_1(t,t_1)^{-1}\\ &- (\Theta_{21}(t,t_1) + \Theta_{22}(t,t_1)S)\,\tilde{\Theta}_1(t,t_1)^{-1}\dot{\tilde{\Theta}}_1(t,t_1)\tilde{\Theta}_1(t,t_1)^{-1},\end{aligned} \tag{2.64}$$

and by using relation (2.60)

$$\dot{\tilde{\Theta}}_1(t,t_1) = \left(\dot{\Theta}_{11}(t,t_1) + \dot{\Theta}_{12}(t,t_1)S\right) \tag{2.65}$$

According to Theorem 1 $\Theta(\cdot, t_1)$ as the fundamental matrix solution of the variational equations (2.58) satisfies the matrix differential equation

$$\dot{\Theta}(t,t_1) = \begin{pmatrix} A(t) & -B(t)R(t)^{-1}B(t)^\top \\ -Q(t) & -A(t)^\top \end{pmatrix}\Theta(t,t_1),$$

which can be written as (using the introduced partitioning of Θ)

$$\begin{aligned}\dot{\Theta}_{11}(t,t_1) =& A(t)\Theta_{11}(t,t_1) - B(t)R(t)^{-1}B(t)^\top\Theta_{21}(t,t_1),\\ \dot{\Theta}_{12}(t,t_1) =& A(t)\Theta_{12}(t,t_1) - B(t)R(t)^{-1}B(t)^\top\Theta_{22}(t,t_1),\\ \dot{\Theta}_{21}(t,t_1) =& -Q(t)\Theta_{11}(t,t_1) - A(t)^\top\Theta_{21}(t,t_1),\\ \dot{\Theta}_{22}(t,t_1) =& -Q(t)\Theta_{12}(t,t_1) - A(t)^\top\Theta_{22}(t,t_1).\end{aligned}$$

Using this in (2.64) and (2.65) and setting $t = t_1$ in (2.61) we obtain the following Cauchy problem

$$\begin{cases}\dot{P}(t) + Q(t) + A(t)^\top P(t) + P(t)A(t)\\ \qquad\qquad -P(t)B(t)R(t)^{-1}B(t)^\top P(t) = 0, \quad t \in (s_0, t_1),\\ \qquad\qquad P(t_1) = S,\end{cases} \tag{2.66}$$

which is the so-called *Riccati matrix differential equation*. The basic existence theorem for the Riccati matrix differential equation (see for instance [23, Theorem 42]) guarantees the existence of a unique symmetric positive semi-definite solution $P(t)$ of (2.66) not only on $(s_0 t_1]$ but on the whole interval Ω provided that Assumption 4 is satisfied.
Using the solution $P(t)$ of (2.66) in the feedback matrix

$$K(t) = -R(t)^{-1}B(t)^\top P(t), \tag{2.67}$$

and setting

$$\hat{u}(t) = K(t)\hat{x}(t), \quad t \in \Omega, \tag{2.68}$$

where $\hat{x}$ is the solution to

$$\begin{cases}\dot{\hat{x}}(t) = (A(t) + B(t)K(t))\,\hat{x}(t), \quad t_0 < t \le t_1,\\ \hat{x}(t_0) = x^0,\end{cases} \tag{2.69}$$

we will show that criterion (2.49) derived in Step 1 is satisfied, hence $\hat{u}$ is the unique solution of the LQR-problem. Let

$$p(t) = P(t)\hat{x}(t), \quad t \in \Omega, \tag{2.70}$$

then by differentiating (2.66) and using (2.69) we obtain for $t \in \Omega$

$$\begin{aligned}\dot{p}(t) =& \dot{P}(t)\hat{x}(t) + P(t)\dot{\hat{x}}(t)\\ =& \left(-Q(t) - A(t)^\top P(t) - P(t)A(t) + P(t)B(t)R(t)^{-1}B(t)^\top P(t)\right)\hat{x}(t)\\ &+ P(t)\left(A(t) - B(t)R(t)^{-1}B(t)^\top P(t)\right)\hat{x}(t)\\ =& -Q(t)\hat{x}(t) - A(t)^\top P(t)\hat{x}(t)\\ =& -Q(t)\hat{x}(t) - p(t)\hat{x}(t),\end{aligned} \tag{2.71}$$

and by setting $t = t_1$ in (2.70)

$$p(t_1) = S\hat{x}(t_1). \tag{2.72}$$

As in the beginning of Step 2 we use again the solution $\tilde{x}$ of (2.40) with control v and initial condition $\tilde{x}(t_0) = 0$ which using the fundamental matrix solution can be written as

$$\tilde{x}(t) = \int_{t_0}^{t} \Phi(t,\tau)B(\tau)v(\tau)\,d\tau, \quad t \in \Omega. \tag{2.73}$$

According to Lemma 2 the fundamental matrix solution of $\dot{p}(t) = -A(t)^\top p(t)$ is given by $\Phi(t_1,\cdot)^\top$. Thus using Theorem 3 for (2.71) together with (2.72) yields

$$\begin{aligned}p(t) =& \Phi(t_1,t)^\top p(t_1) + \int_t^{t_1} \Phi(\tau,t)^\top Q(\tau)\hat{x}(\tau)\,d\tau\\ =& \Phi(t_1,t)^\top S\hat{x}(t_1) + \int_t^{t_1} \Phi(\tau,t)^\top Q(\tau)\hat{x}(\tau)\,d\tau, \quad t \in \Omega.\end{aligned} \tag{2.74}$$

From the fact that (2.68) is equivalent to (using (2.70))

$$R(t)\hat{u}(t) + B(t)^\top p(t) = 0, \quad t \in \Omega,$$

follows

$$\int_{t_0}^{t_1} v(t)^\top \left(R(t)\hat{u}(t) + B(t)^\top p(t)\right)\,dt = 0.$$

Substituting the derived representation (2.74) for p and using Fubini's theorem yields

$$\begin{aligned}0 =& \int_{t_0}^{t_1} v(t)^\top \left(R(t)\hat{u}(t) + B(t)^\top \left(\Phi(t_1,t)^\top S\hat{x}(t_1) + \int_t^{t_1} \Phi(\tau,t)^\top Q(\tau)\hat{x}(\tau)\,d\tau\right)\right)\,dt\\ =& \int_{t_0}^{t_1} v(t)^\top R(t)\hat{u}(t)\,dt + \left(\int_{t_0}^{t_1} \Phi(t_1,t)B(t)v(t)\,dt\right)^\top S\hat{x}(t_1)\\ &+ \int_{t_0}^{t_1} \left(\int_{t_0}^{t} \Phi(t,\tau)B(\tau)v(\tau)\,d\tau\right)^\top Q(t)\hat{x}(t)\,dt.\end{aligned}$$

Finally employing relation (2.73) for $\tilde{x}$ shows that criterion (2.49) is satisfied

$$0 = \int_{t_0}^{t_1} v(t)^\top R(t)\hat{u}(t)\,dt + \tilde{x}(t_1)^\top S\hat{x}(t_1) + \int_{t_0}^{t_1} \tilde{x}(t)Q(t)\hat{x}(t)\,dt,$$

meaning that $\hat{u}$ as given by (2.68) depending on the solution of the Riccati matrix differential equation (2.66) is the unique solution of the LQR-problem.

4. The quadratic form of the optimal performance index We define a function $\mathcal{H}(t)$ depending on the lower bound of the performance index J:

$$\mathcal{H}(t) = \int_t^{t_1} \Big(x(\tau)^\top Q(\tau) x(\tau) + u(\tau)^\top R(\tau) u(\tau) \Big)\, d\tau + x(t_1)^\top S x(t_1).$$

Let $x^0 \in \mathbb{R}^n$ and $t \in \mathbb{R}$ be fixed. Furthermore let $K \in L^2(\Omega, \mathbb{R}^{m\times n})$ and $u(t) = K(t)x(t)$, $t \in \Omega$. Then h is of the form

$$\mathcal{H}(t) = \int_t^{t_1} x(\tau)^\top \Big(Q(\tau) + K(\tau)^\top R(\tau) K(\tau) \Big)\, x(\tau)\, d\tau + x(t_1)^\top S x(t_1),$$

thus we assume that

$$\mathcal{H}(t) = x(t)^\top W(t) x(t), \quad t \in \Omega, \tag{2.75}$$

for some symmetric positive semi-definite matrix $W(\cdot) \in \mathbb{R}^{n\times n}$ (note that according to Assumption 4, $Q(\cdot)$, $R(\cdot)$ and S are symmetric and at least positive semi-definite). Hence

$$x(t)^\top W(t) x(t) = \int_t^{t_1} x(\tau)^\top \Big(Q(\tau) + K(\tau)^\top R(\tau) K(\tau) \Big)\, x(\tau)\, d\tau + x(t_1)^\top S x(t_1). \tag{2.76}$$

Differentiating gives (where we use (2.40), $u(\cdot) = K(\cdot)x(\cdot)$ and the symmetry of $W(\cdot)$)

$$\begin{aligned}
x(t)^\top \dot W(t) x(t) =& -2x(t)^\top W(t)\dot x(t) - x(t)^\top \Big(Q(t) + K(t)^\top R(t) K(t) \Big)\, x(t) \\
=& -2x(t)^\top \left(W(t)A(t) + W(t)B(t)K(t) \right) x(t) \\
& - x(t)^\top \Big(Q(t) + K(t)^\top R(t) K(t) \Big)\, x(t) \\
=& -\left(W(t)x(t) \right)^\top A(t)x(t) - x(t)^\top W(t) A(t) x(t) - \\
& x(t)^\top \Big(2W(t)B(t)K(t) + Q(t) + K(t)^\top R(t) K(t) \Big)\, x(t) \\
=& x(t)^\top \Big(-A(t)^\top W(t) - W(t)A(t) \\
& -2W(t)B(t)K(t) - Q(t) - K(t)^\top R(t) K(t) \Big)\, x(t).
\end{aligned}$$

Since this is valid for any x and both sides are symmetric we get

$$\dot W(t) = -A(t)^\top W(t) - W(t)A(t) - 2W(t)B(t)K(t) - Q(t) - K(t)^\top R(t) K(t).$$

Let $K(\cdot)$ be the feedback matrix (2.67) then (note that $P(\cdot)$ is symmetric)

$$\begin{aligned}
\dot W(t) =& -A(t)^\top W(t) - W(t)A(t) + 2W(t)B(t)R(t)^{-1}B(t)^\top P(t) - Q(t) \\
& - P(t)B(t)R(t)^{-1}B(t)^\top P(t).
\end{aligned} \tag{2.77}$$

Setting $t = t_1$ in (2.76) gives

$$x(t_1)^\top W(t_1) x(t_1) = x(t_1)^\top S x(t_1) \quad \Rightarrow \quad W(t_1) = S. \tag{2.78}$$

Writing the matrix Riccati differential equation (2.80) as

$$\begin{aligned}
\dot P(t) =& -A(t)^\top P(t) - P(t)A(t) + 2P(t)B(t)R(t)^{-1}B(t)^\top P(t) - Q(t) \\
& - P(t)B(t)R(t)^{-1}B(t)^\top P(t),
\end{aligned}$$

together with (2.77) and $W(t_1) = S = P(t_1)$ yields $W(\cdot) = P(\cdot)$. Thus using (2.75) follows

$$J(\hat{u}, x^0) = h(t_0)|_{u=\hat{u}} = x(t_0)^\top P(t_0) x(t_0) = (x^0)^\top P(t_0) x^0,$$

which ends the proof. □

Having deduced a solution to the LQR-problem for bounded $\Omega = [t_0, t_1]$ with $-\infty < t_0 < t_1 < \infty$ we will now investigate the case $t_1 \to \infty$.

2.2.3.4 The infinite-time horizon LQR-problem

In many applications it is very difficult or even impossible to steer a system to the zero-state in finite time: if the deviation of the initial condition x^0 from the zero-state is large then t_1 has to be chosen sufficiently large as well (see for instance [18, Sec. 3.4]). This motivates the extension of Theorem 6 to infinite end-times t_1. We will focus now on *linear time-invariant state differential systems*, i.e. $A(\cdot) \equiv A \in \mathbb{R}^{n\times n}$ and $B(\cdot) \equiv B \in \mathbb{R}^{n\times m}$, with a so-called *output* $y(\cdot)$, thus we consider systems of the form

$$\begin{cases} \dot{x}(t) = Ax(t) + Bu(t), & t > t_0, \\ y(t) = Cx(t), & t \geq t_0, \\ x(t_0) = x^0, \end{cases} \tag{2.79}$$

where $C \in \mathbb{R}^{k\times n}$ with $k \leq n$. It is often not possible to retrieve information about the complete state vector $x(\cdot)$ of a system. Instead one only has access to some function of k components of $x(\cdot)$ which are given by the output $y(\cdot)$. Consider for instance the human CVS: except for arterial blood pressure (P_{as}), heart rate (H) and (via invasive measurement) central venous pressure (P_{vc} or P_{avc}) it is very difficult to measure other state variables such as resistances or organic blood pressures.
Since we are concerned with time-invariant systems we furthermore set $Q(\cdot) \equiv Q_0 \in \mathbb{R}^{n\times n}$ and $R(\cdot) \equiv R_0 \in \mathbb{R}^{m\times m}$, where Q_0 is symmetric and positive semi-definite and R_0 is symmetric and positive definite. Let $S \in \mathbb{R}^{n\times n}$ be positive semi-definite then for Q_0, R_0 and S Assumption 4 is satisfied and according to Theorem 6 there exists an optimal control $u(\cdot) = K(\cdot)x(\cdot)$ for system (2.79) minimizing the cost functional

$$J(u, x^0) = \int_{t_0}^{t_1} \left(x(t)^\top Q_0 x(t) + u(t)^\top R_0 u(t) \right) dt + x(t_1)^\top S x(t_1).$$

The Riccati matrix differential equation for this problem is is given by

$$\begin{cases} \dot{P}(t) + Q_0 + A^\top P(t) + P(t)A - P(t)BR_0^{-1}B^\top P(t) = 0, & t \in [t_0, t_1), \\ P(t_1) = S, \end{cases} \tag{2.80}$$

which means its solution $P(t)$ and hence the feedback matrix $K(t) = -R_0^{-1}B^\top P(t)$, $t \in [t_0, t_1]$ of the optimal control is still time dependent, although we started from a time-invariant system and weighting matrices Q_0, R_0 and S. So let us assume that there exists some constant matrix $\bar{P}$ which solves the Riccati matrix differential equation (2.80), i.e. $\bar{P}$ is an equilibrium solution of (2.80) which implies that $\bar{P}$ is positive semi-definite. If additionally $\bar{P} = S$ then the feedback matrix is constant, i.e. $K = -R_0^{-1}B^\top \bar{P}$, and determines the optimal control for any given end-time $t_1 > t_0$ (see

for instance [18, Sec. 3.4]). These considerations naturally lead to investigation of the case $t_1 \to \infty$ both in the cost functional and in the Riccati matrix differential equation (2.80). Let from now on be $t_0 = 0$. As we did in the finite-time horizon case we formulate an assumption on the matrices appearing in the cost functional.

Assumption 7. *Let the matrix $Q_0 \in \mathbb{R}^{n\times n}$ be symmetric and positive semi-definite and $R_0 \in \mathbb{R}^{m\times m}$ be symmetric and positive definite*

We define the following problem.

Definition 8. Consider system (2.79) with $x \in AC([0,\infty),\mathbb{R}^n)$, $u \in L^2([0,\infty),\mathbb{R}^m)$ and Q_0 and R_0 satisfying Assumption 7. The *infinite-time horizon linear-quadratic (optimal) regulator problem (ILQR-problem)* is the task of solving the minimization problem

$$\inf_{u\in L^2([0,\infty),\mathbb{R}^m)} J_\infty(u,x^0),$$

with

$$J_\infty(u,x^0) = \int_0^\infty x(t)^\top Q_0 x(t) + u(t)^\top R_0 u(t)\,dt. \tag{2.81}$$

Note that since we consider the asymptotic behavior $t_1 \to \infty$ it is no longer necessary to impose a penalty term on $x(t_1)$ in (2.81) as was the issue in (2.45). In contrast to the case $t_1 < \infty$ the existence of the performance index (2.81) is not automatically guaranteed: Since $u \in L^2([0,\infty),\mathbb{R}^m)$ the second term in the integral is bounded but the first term involving the state $x(\cdot)$ may not exist. For guaranteeing existence of (2.81) system (2.79) has to meet additional requirements which leads to the following concepts (see for instance [18, Definition 1.11]).

Definition 9. Let $x^0, x^1 \in \mathbb{R}^n$ and $t_0 \in \mathbb{R}$ be arbitrary. The system (2.79) is called *completely controllable* if for any initial state x^0 at any time t_0, i.e. $x(t_0) = x^0$, there exists $\infty > t_1 > t_0$ and $u \in L^2([t_0,t_1],\mathbb{R}^m)$ such that the system can be transferred to any terminal state x^1 with $x(t_1) = x^1$.

In the case of completely controllable time invariant systems the following result can be established (taken from [14, Corollary 14]).

Lemma 10. *Let the system (2.79) be completely controllable. Then there exists a feedback law $u(t) = Kx(t)$ such that solution of the closed loop system*

$$\begin{cases} \dot{x}(t) = (A+BK)x(t), & t > 0, \\ x(0) = x^0, \end{cases}$$

obeys

$$\|x(t)\| \le Me^{\omega t},$$

with some constants $M \ge 1$ and $\omega < 0$.

Proof. A similar result is proven in [23, Proposition 5.5.6]. □

Now we can conclude that if system (2.79) is completely controllable then according to Lemma 10 $x(\cdot)$ is exponentially bounded thus the cost functional (2.81) exists. However, we still have to determine under which condition a steady state solution $\bar{P}$ of (2.80) exists and if this solution is identical to the limit (if existent) of the solution $P(t)$ of(2.80) as $t_1 \to \infty$. We will use the following property (see [18, Sec. 1.7]).

Definition 11. Let $x^0, \bar{x}^0 \in \mathbb{R}^n$ and $t_0 \in \mathbb{R}$ be arbitrary. The system (2.79) is called *completely observable* if for all t_0 there exists $\infty > t_1 > t_0$ such that the output $y(\cdot)$ of system (2.79) with initial condition x^0 and output $\bar{y}(\cdot)$ of system (2.79) with initial condition x^1 equalize, i.e.

$$y(t) = \bar{y}(t), \quad t_0 \leq t \leq t_1,$$

for all $u \in L^2([t_0, t_1], \mathbb{R}^m)$ implies $x^0 = \bar{x}^0$.

The following result finally guarantees the solvability of the ILQR-problem provided that system (2.79) is completely controllable and completely observable.

Theorem 12. *Let system* (2.79) *be completely controllable and completely observable. Then the so-called* algebraic Riccati matrix equation

$$A^\top \bar{P} + \bar{P}A - \bar{P}BR_0^{-1}B^\top \bar{P} + Q_0 = 0,$$

has exactly one positive semi-definite solution $\bar{P}$ *and*

$$\hat{u}(t) = K\hat{x}(t), \quad t \geq 0,$$

with $K = -R_0^{-1}B^\top \bar{P}$ *and* $\hat{x}(\cdot)$ *being the solution of the closed loop system*

$$\begin{cases} \dot{\hat{x}}(t) = (A + BK)\hat{x}(t), & t > 0, \\ \hat{x}(0) = x^0, \end{cases}$$

is the unique solution of the ILQR-problem as stated in Definition 8. Finally the optimal performance index is given by

$$J_\infty(\hat{u}, x^0) = (x^0)^\top \bar{P} x^0.$$

Proof. Note that this result can be established with weaker assumptions on the system (2.79), namely *stabilizability* and *detectability*, see for instance [23, Theorem 41]. □

Having all needed theoretical results at hand we will now apply the ILQR-formulation to the introduced model (2.24).

2.2.3.5 The ILQR-setup of the model

We want to apply an optimal control approach to model (2.24) which we write in the form (2.27). Assume that the model is in an initial resting equilibrium x^{rest} (the necessary computations are depicted in Appendix A.2) when orthostatic stress is applied . We want to find a control $\hat{u}$ that steers the system from the initial state x^{rest} at time $t_0 = 0$ to a new equilibrium x^{stress} corresponding to the imposed orthostatic stress. As was stated in Sec. 2.2.3.3 the optimal control is designed to bring a system from any given initial state x^0 to the zero-state $x = 0$. Thus for using the previously deduced results we have to introduce the state transformation

$$\xi(t) = x(t) - x^{\text{stress}} \in \mathbb{R}^{16}.$$

Since unstressed volume V_{u}, heart rate H and the net change in vasoconstriction R_{aux} shall be controlled simultaneously it is a priori not clear how to choose a reasonable end-time t_1 at which the zero state $\xi(t_1) = x(t_1) - x^{\text{stress}} = 0$ has to be reached for any level of

orthostatic stress. Hence we will treat the given task as ILQR-problem. As stated above we consider the baroreflex to be the only global short term control mechanism counteracting orthostatic stress. Hence we assume that $\hat{u}$ is generated based on measurements of arterial blood pressure by high pressure sensors in the aortic arch and information of low pressure sensors monitoring central venous pressure. Thus we consider P_{as} and a composite of P_{vc} and P_{avc} as inputs for $\hat{u}$. This implies the output equation

$$y(t) = Cx(t),$$

with

$$C = \begin{pmatrix} q_{\text{as}} \cdot e_1^\top \\ q_{\text{vc}} \cdot e_7^\top \\ q_{\text{avc}} \cdot e_9^\top \end{pmatrix} \in \mathbb{R}^{3\times 16}, \tag{2.82}$$

where e_i denotes the i-th canonical basis vector in $\mathbb{R}^{16}$ and the scalars q_{as}, q_{vc} and q_{avc} are positive weights corresponding to P_{as}, P_{vc} and P_{avc}. Since system (2.27) is non linear we linearize the model around the final steady state x^{stress} (as explained in Sec. 2.2.3.1), i.e. we linearize (2.27) at $\xi = 0$ and obtain the linearized state differential equation

$$\begin{cases} \dot{\xi}(t) = A\xi(t) + Bu(t), & t > 0, \\ \xi(0) = x(0) - x^{\text{stress}} = x^{\text{rest}} - x^{\text{stress}}, \end{cases} \tag{2.83}$$

where $A = \mathcal{F}_x \in \mathbb{R}^{16\times 16}$ and $B = \mathcal{F}_u \in \mathbb{R}^{16\times 3}$. Let further

$$Q_0 = C^\top C \in \mathbb{R}^{16\times 16}, \tag{2.84}$$

and

$$R_0 = \operatorname{diag}(r_1, r_2, r_3) \in \mathbb{R}^{3\times 3}, \tag{2.85}$$

be a diagonal matrix with $r_i > 0$ for $i = 1, 2, 3$. Then Assumption 7 is satisfied and hence the performance index (2.81) exists. Let us further assume that system (2.83) is completely controllable and completely observable. Then according to Theorem 12 there exists a unique optimal control

$$\hat{u}(t) = K\hat{\xi}(t), \quad t \geq 0,$$

that drives the linear system (2.83) from its initial state $\xi(0)$ to the zero state $\xi = 0$ where $\hat{\xi}$ is the solution of the closed loop system

$$\begin{cases} \dot{\hat{\xi}}(t) = (A + BK)\hat{\xi}(t), & t > 0, \\ \hat{\xi}(0) = x^{\text{rest}} - x^{\text{stress}}. \end{cases}$$

The question is whether this control is practicable for the non linear system (2.27) as well. Take

$$\hat{u}(t) = K(\hat{x}(t) - x^{\text{stress}}), \tag{2.86}$$

for $t \geq 0$ where $\hat{x}$ is now the solution to the non linear closed loop system

$$\begin{cases} \dot{\hat{x}}(t) = \mathcal{F}(\hat{x}(t), K(\hat{x}(t) - x^{\text{stress}}, t), & t > 0, \\ \hat{x}(0) = x^{\text{rest}}, \end{cases}$$

with $\mathcal{F}$ given by (2.27). Then (2.86) is a suboptimal but still stabilizing control for the non linear system (2.27) provided that $\left\|\hat{x}(t) - x^{\text{stress}}\right\|$ and $|\hat{u}(t)|$ are small enough (see [6, p. 25]). This together with the fact that linearization is only meaningful in small neighborhoods of the original non linear system leads to the following concept: since for instance the transmural pressure of the lower compartments of the model changes as LBNP is simulated the state of the model may change noticeably and the control response (2.86) must be updated. Hence the above depicted concept of linearizing system (2.27), computing a control (2.86) and applying it to the original system is done iteratively (a similar concept was used in [4]). Starting at an initial resting steady state $x(0) = x^{\text{rest}}$ we compute a steady state x^{trans} at time Δt corresponding to the currently applied level of orthostatic stress. We linearize the model (2.27) around x^{trans} and compute the optimal control that drives the linearized system from x^{rest} to x^{trans} and apply it to the non linear system (2.27). The end-state of the non linear system at time Δt is then used as initial condition for the next step. This procedure is summarized in Algorithm 2.1. Note that in the context of this thesis this algorithm is only reliable if the computed linearized systems are always completely controllable and completely observable[2].

[2] As mentioned in the proof of Theorem 12, the assumptions on the linearized systems can be weakened: it is sufficient if the arising systems are stabilizable and detectable.

Algorithm 2.1 Iterative ILQR

Consider the matrices C, Q_0 and R_0 defined by (2.82), (2.84) and (2.85) respectively and choose $\Delta t > 0$ and $N \in \mathbb{N}$. Compute a resting equilibrium x^{rest} of the model (2.27) according to Appendix A.2 and set $x(0) = x^{\text{rest}}$.

for $i = 0$ to N

1. Compute the steady state x^{trans} corresponding to the current level of orthostatic stress and set $\xi(\cdot) = x(\cdot) - x^{\text{trans}}$.

2. Linearize the model (2.27) around $\xi = 0$ which gives the following system

$$\begin{cases} \dot{\xi}(t) = A\xi(t) + Bu(t), & t > i \cdot \Delta t, \\ \xi(i \cdot \Delta t) = x(i \cdot \Delta t) - x^{\text{trans}}, \end{cases} \tag{2.87}$$

   where $A = \mathcal{F}_x \in \mathbb{R}^{16\times 16}$ and $B = \mathcal{F}_u \in \mathbb{R}^{16\times 3}$.

3. Compute the control $\hat{u}(t) = K\hat{\xi}(t)$ for the linearized system (2.87) where $K = -R_0^{-1}B^\top \bar{P}$ with $\bar{P}$ being the solution to the algebraic Riccati matrix equation

$$A^\top \bar{P} + \bar{P}A - \bar{P}BR_0^{-1}B^\top \bar{P} + Q_0 = 0, \tag{2.88}$$

   and $\hat{\xi}$ solving the closed loop system

$$\begin{cases} \dot{\hat{\xi}}(t) = (A + BK)\hat{\xi}(t), & t > i \cdot \Delta t, \\ \hat{\xi}(i \cdot \Delta t) = x(i \cdot \Delta t) - x^{\text{trans}}. \end{cases}$$

4. Set $\hat{u}(t) = K(\hat{x}(t) - x^{\text{trans}})$ with $\hat{x}$ being the solution of the closed loop system

$$\begin{cases} \dot{\hat{x}}(t) = \mathcal{F}(\hat{x}(t), K(\hat{x}(t) - x^{\text{trans}}, t), & t > i \cdot \Delta t, \\ \hat{x}(i \cdot \Delta t) = x(i \cdot \Delta t), \end{cases}$$

   and apply the computed control to the non linear system

$$\dot{x}(t) = \mathcal{F}(x(t), K(\hat{x}(t) - x^{\text{trans}}), t),$$

   for $t > i \cdot \Delta t$ to compute $x\left((i+1) \cdot \Delta t\right)$.

end for

3 Simulation Results

All simulations were carried out in MATLAB^{TM} 7 (R14) using the inbuilt ODE-solver `ode15s` which is a numerical solver for stiff differential equations based on multistep methods of variable order. The stiffness of model (2.24) made it necessary to decrease maximum and relative error tolerances from 10^{-3} and 10^{-6} down to 10^{-6} and 10^{-9} respectively. Algorithm 2.1 was implemented by iteratively employing the MATLAB function `lqr` (found in the control system toolbox; we used standard options) which numerically computes the feedback gain matrix K (for details about both routines see [20]). The jacobian matrices $A = \mathcal{F}_x \in \mathbb{R}^{16\times 16}$ and $B = \mathcal{F}_u \in \mathbb{R}^{16\times 3}$ appearing in the linearized systems (2.87) were computed numerically using central finite differences with step length $h = 10^{-9}$. The used operating system was openSUSE 11.1 (32 bit, Kernel 2.6.27) running on a HP subnotebook with 2,0 GHz Intel Core 2 Duo P7350 CPU and 3GB RAM.
Since we consider only the short term behavior of the human CVS, the simulation interval was chosen to be 25 minutes starting at $t_0 = 0$ min. For better comparison the procedure of the simulations was identical for all controls: first a resting steady state was computed (as explained in Appendix A.2) which was used as initial condition for the ODE-model (2.24). After two minutes of unperturbed simulation the LBNP procedure was started: an external lower body negative pressure was smoothly increased from 0 to P_{LBNP} [mmHg] within one minute and maintained until the end of the simulation at $t_1 = 25$ min.

3.1 LBNP Setup

The 'hips'-case (explained in Sec. 1.3) of LBNP is the usual LBNP setup (compare for instance [15]) and is simulated here. Let t_{on} denote the time of onset of LBNP (i.e. $t_{\text{on}} = 2$ min). The following sigmoidal function climbing from zero to one on the interval $[t_{\text{on}}, t_{\text{on}} + 1]$ was chosen to simulate the smooth increase in external pressure

$$\alpha(t) = \frac{1}{1 + e^{-15(t-t_{\text{on}}-1/2)}}. \tag{3.1}$$

As suggested in [12] the compartments affected by LBNP were chosen to be the lower limbs ('leg'-compartment) and for simulation of blood shifts in larger veins the vena cava and abdominal vena cava ('avc' and 'vc') were picked. However, at the latter ones only a reduced external pressure P_{LBNP} is applied (otherwise venous return to the heart would drop significantly even for low values of P_{LBNP} which is physiologically not meaningful as explained below). We assume zero atmospheric pressure thus all external pressures applied to the compartments are zero except for $P^{\text{bias}}_{\text{leg}}$, $P^{\text{bias}}_{\text{avc}}$ and $P^{\text{bias}}_{\text{vc}}$ which are given by

$$P^{\text{bias}}_{\text{comp}}(t) = \begin{cases} 0, & t < t_{\text{on}}, \\ k^{\text{LBNP}}_{\text{comp}} \cdot \alpha(t) \cdot P_{\text{LBNP}}, & t_{\text{on}} \le t_{\text{on}} + 1, \\ P_{\text{LBNP}}, & t > t_{\text{on}} + 1, \end{cases} \tag{3.2}$$

where 'comp' stands for 'leg', 'avc' and 'vc' with $k_{\text{leg}}^{\text{LBNP}} = 1$ and $k_{\text{avc}}^{\text{LBNP}} = k_{\text{vc}}^{\text{LBNP}} = 0.3$ (as listed in Appendix A.3) and $\alpha(t)$ given by (3.1). According to literature (see for instance [12, 7, 19, 3]) low levels of LBNP were chosen to be at $P_{\text{LBNP}} = -10$ mmHg whereas high levels were simulated by values of P_{LBNP} less than or equals -40 mmHg.

3.2 Parameter Assignments

The compliances of the compartments and initial values of compartmental pressures (as well as most other model parameters) were chosen according to [12, 16, 6, 15, 13]. Thus we obtain by employing relation (2.25) a typical total blood volume of 5.5 liters. For better comparison maximal and minimal values of V_{u}, R_{aux}, and H were chosen to be identical for arctan and set point controls (if possible). Thus we assumed maximal and minimal heart rates $H^{\max}$ and $H^{\min}$ of 120 bpm and 40 bpm respectively. In the case of the set point control for R_{aux} we chose sigmoidal parameters to reflect sympathetic net activation such that R_{aux} provokes realistic changes in local resistances as given by eq. (2.19). As explained in Sec. 2.2.1, when employing the arctan controls a maximal value for R_{aux} is not needed thus we provide only a guesstimate for $R_{\text{aux}}^{\min}$. For making it possible to compare the simulations to results from literature we plot the total peripheral resistance R_{s} given by relation (A.3) (its computation is explained in Appendix A.1) instead of R_{aux}. We assume the initial amount of total unstressed volume to be 60% of the total blood volume (see for instance [12, 15]). Since we consider recruitable unstressed volume to be located only in the abdominal region (namely the compartments 'ren' and 'spl', see Sec. 2.1.3) we compute the blood volumes V_{ren} and V_{spl} of these compartments and set $V_{\text{u}}^{\min} = V_{\text{u}}(0) - 0.6 \cdot (V_{\text{ren}} + V_{\text{spl}})$. We assume heart rate control to be the most rapid followed by changes in resistance and finally unstressed volume recruitment (compare [25]). Thus we assume the time constants for H and R_{aux} in the set point controls (2.32) to be $\tau_3 = 1$ and $\tau_2 = 2$ respectively and set $\tau_1 = 30$ for V_{u}. As mentioned in Sec. 2.2.1 the constants appearing in the arctan controls (2.29) were adopted from [12]. The weights for the optimal control as well as a list summarizing all used parameters and assigned values are given in Appendix A.3.
The initial steady state was computed by picking P_{as} and P_{vc} and calculating all other states using equilibrium relations (as explained in Appendix A.2). We assumed a resting arterial blood pressure $P_{\text{as}}(0)$ of 87.7 mmHg and initial venous pressure $P_{\text{vc}}(0)$ of 7.5 mmHg. Thus for the set point controls we fixed $\hat{P}_{\text{as}}$ to be 87.7 mmHg and $\hat{P}_{\text{vc}}$ to be 7.5 mmHg. Initial values and units of all state variables are depicted in Appendix A.2.

3.3 Low-level LBNP

We want to examine whether the three different controls presented here are able to mimic typically seen reactions to LBNP. Note that variations in these reactions can be huge between individuals since short term regulation mechanisms in the human body act simultaneously leading to similar effects: an increase in local resistance is equivalent to a decrease in compliance in the same region. Thus we focus on a list of prototype reactions which is not intended to be exhaustive. Consulting literature we summarize the following: according to Lucini et al. [19] low-level LBNP (induced in healthy male adults) leads to a decrease in central venous pressure but has almost no effect on arterial blood pressure (which is supported by Brown et al. [7]). Additionally Heldt et al. [12] report of only

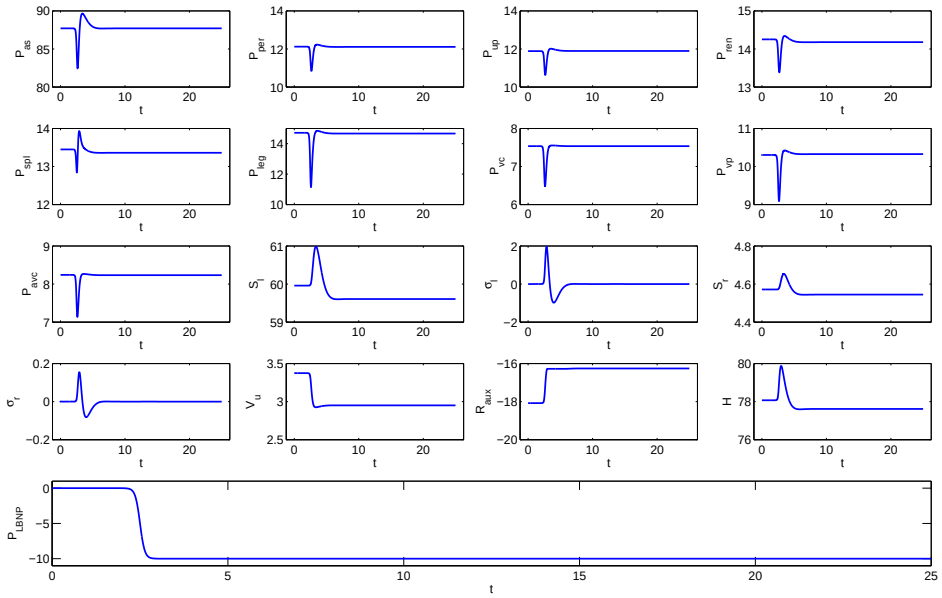

Figure 3.1: State variables of the model using the arctan controls with $P_{\mathrm{LBNP}} = -10$ mmHg.

negligible changes in heart rate but an increase in total peripheral resistance. The role of unstressed volume is still not completely clear but in accordance to Kappel et al. [15] it is assumed to be decreasing during LBNP.

3.3.1 The arctan-controls

Considering the case of $P_{\mathrm{LBNP}} = -10$ mmHg an exemplary complete (i.e. all 16 state variables are shown) model output using the arctan controls (2.29) is depicted in Fig. 3.1, Fig. 3.2 shows the most informative auxiliary variables. As discussed in Sec. 2.2.1 the arctan controls are designed to maintain initial values of arterial and venous blood pressures P_{as}^0 and P_{vc}^0 respectively. We see an initial decrease in P_{as} of about 6% and a drop in P_{vc} which is more pronounced (-14%). However, heart rate H shows no significant response (a temporary increase of ca. 2% followed by an even lower value than at the start of the simulation). So far the behavior of the model is consistent with physiology. But looking at R_{s} (Fig. 3.2) we see that the increase in systemic resistance is negligible as well (the visible growth is less than 1%). The only control which shows a significant response is V_{u} due to the larger decrease of P_{vc} compared to P_{as}. We see an immediate drop in unstressed volume of about 13%. Since we assume the only resorts of recruitable unstressed volume to be the compartments 'ren' and 'spl' a similar rebound in P_{spl} and (less pronounced) in P_{ren} as in P_{as} can be observed. Thus the model is stabilized mainly via very fast volume shifts in the abdominal compartments. Though the exact mode of operation of unstressed volume recruitment is not fully investigated yet (see for instance [15]) this reaction is unrealistic mainly for two reasons: firstly, volume recruitments of this magnitude (under the assumption made on unstressed volume distribution stated in Sec. 3.2 13% of total unstressed volume represent about 7% of the

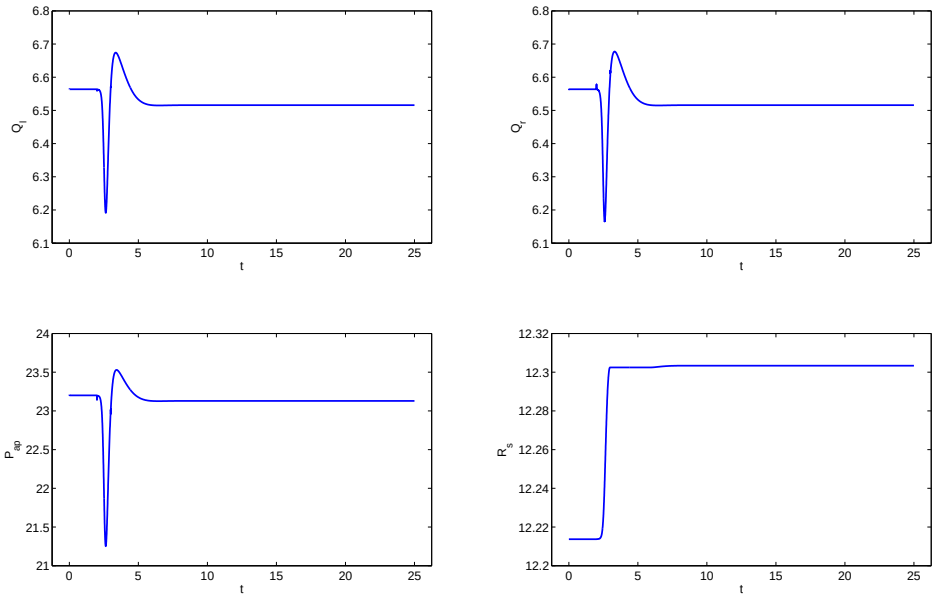

Figure 3.2: Auxiliary variables of the model using the arctan controls with $P_{\mathrm{LBNP}} = -10$ mmHg.

total blood volume) take much longer in the human body (see [24]). Secondly, it is questionable if LBNP of this level provokes such volume shifts (compare the findings by Ursino et al. about the relation of carotid sinus pressure and blood volume changes [25], Kappel et al. [15] come to a similar result when simulating LBNP). Thus the arctan controls need some extensions: one way would be to include a dependency on P_{vc} into the equations for H and R_{aux} so that not only V_{u} is sensitive to changes in P_{vc}. Another approach would include a decay in V_{u} to prevent this control from being too dominant. The latter is to some extent realized in the set point controls.

3.3.2 The set point controls

Figure 3.3 shows the most interesting model variables using the set point controls (2.32) under a LBNP of -10 mmHg. The most obvious difference compared to the arctan controls is the significant response not only of V_{u} but H and R_{s} as well. Since the time constant of V_{u} was chosen to be $\tau_3 = 30$, unstressed volume recruitment takes much longer than with the arctan controls. This forces heart rate H and resistance R_{s} to react to the imposed LBNP as well. The time course of total unstressed volume V_{u} looks more plausible and we observe a noticeable (about 10% at minute 3) increase in systemic resistance R_{s} which was not seen with the arctan controls. The heart rate reacts with an initial increase of ca. 6% which declines slowly so that H remains slightly elevated until the end of the simulation. Arterial blood pressure P_{as} shows a comparable decrease as it was the case with the arctan controls though it is not immediately recovered. The drop of the venous pressures P_{vc} and P_{avc} is more pronounced and cannot be stabilized immediately so that both pressures stay below their initial values for the rest of the simulation. This is mainly due to the fact that unstressed volume recruitment is much slower and both R_{aux} and H are only

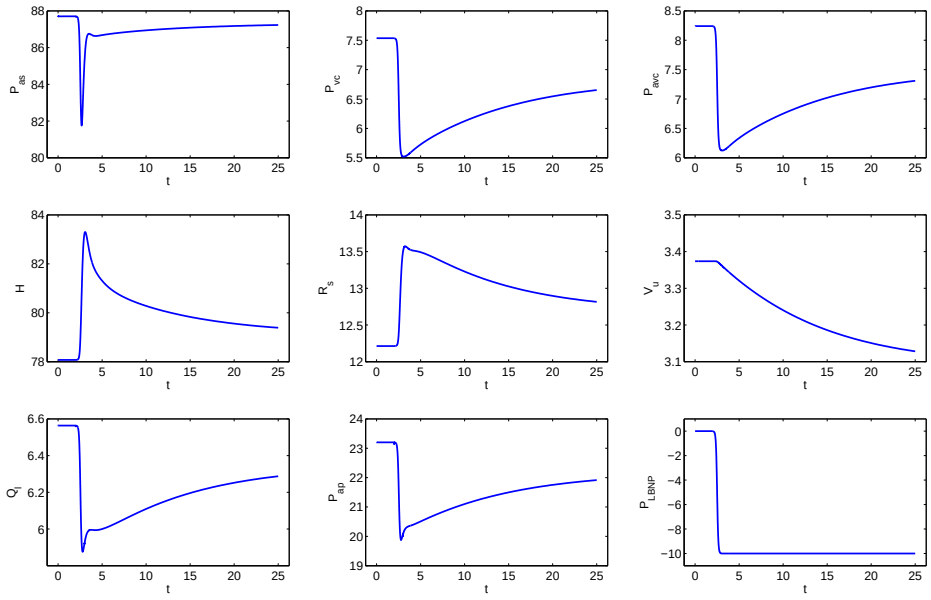

Figure 3.3: Model output using the set point controls with $P_{\mathrm{LBNP}} = -10$ mmHg.

depending on P_{as} which is not substantially altered by the decreased venous return to the heart. Nevertheless arterial pulmonary pressure P_{ap} and therefore cardiac output of the left heart Q_ℓ reflect the lower value of P_{vc}. However, this is compensated by the increased inflow resistances to the systemic compartments as well as by the slightly increased heart rate such that P_{as} is not affected too heavily. This may not be an exact copy of the typical reactions to low-level LBNP summarized in the beginning but nevertheless no striking contradictions to general physiological knowledge can be observed. Thus the set point controls provide a much more realistic response than the arctan controls.

3.3.3 The optimal control

Employing Algorithm 2.1 with $P_{\mathrm{LBNP}} = -10$ mmHg gives the results depicted in Fig. 3.4. The red lines show the computed steady state values over time. It should be noted that `lqr` finished the simulation without any errors in the occurring algebraic Riccati matrix equations (2.88) but due to numerical instabilities in the steady state computation (as explained in Appendix A.2) we see oscillations in P_{as} as well as Q_ℓ and P_{ap} at the onset of LBNP ($t_{\mathrm{on}} = 2$) which leads to a drop in R_{s} in the beginning. Though the amount of the initial decrease in P_{as} is similar to previous simulations using arctan or set point controls it takes much longer to steer P_{as} back to its initial value. However, what immediately leaps out is that heart rate is not increased nor held constant but decreased by about 36% until minute 5 and stabilizes at a level 16% lower than in the beginning. This has to be compensated by a temporary 25%-increase in resistance. Unstressed volume recruitment is faster than in the set point control case but by far not as rapid as with the arctan controls and stabilizes at approximately the same level. All this provokes P_{vc} and P_{avc} to be even higher at the end of the simulation than in the beginning. Because of the

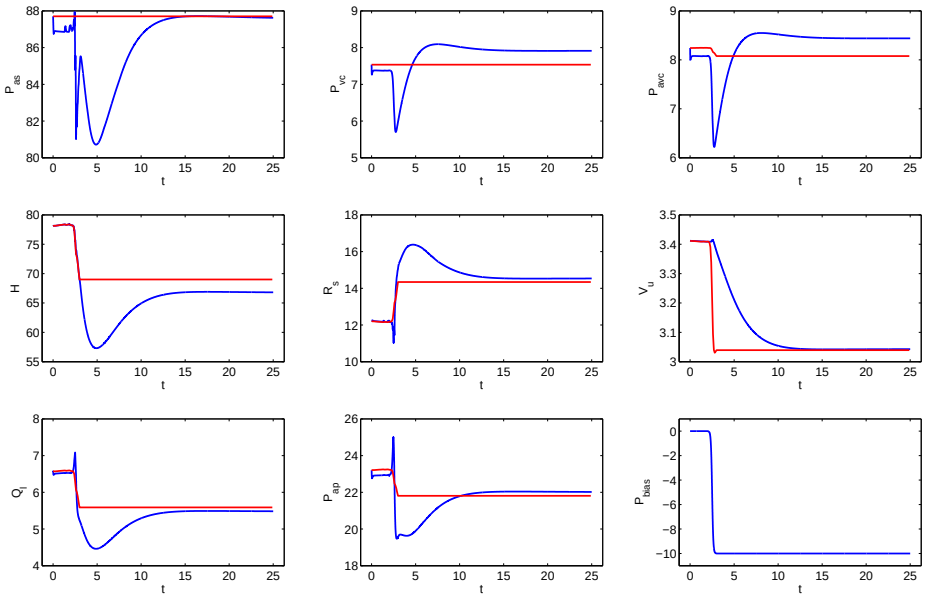

Figure 3.4: Model output (blue) using the optimal control approach with $P_{\mathrm{LBNP}} = -10$ mmHg. Red lines are computed steady state values.

decreased heart rate after imposing LBNP cardiac output stabilizes at a lower level as well. Overall these reactions are definitely not typical but at least all variables stay within physiologically meaningful regions and exhibit changes on a plausible time scale. Thus the optimal control response can be interpreted to mimic an 'outlier'-reaction to LBNP.

3.4 High-level LBNP

We only consider a LBNP of -40 mmHg here since more severe LBNP stresses have a significant effect on compliances in the venous system (see for instance [7]). External LBNP deforms compliant vessel walls so that the nonlinear nature of the pressure-compliance relationship (as discussed at the beginning of Sec. 2.1.1) becomes important. This means that compliances are not assumed to be constant parameters but functions of transmural pressure, i.e. $c = c(P - P_{\mathrm{bias}})$. However, we assume that at $P_{\mathrm{LBNP}} = -40$ mmHg the effect of LBNP on compliant vessel walls can be neglected since increasing resistance and decreasing unstressed volume leads to similar results in this situation (compare [15]). The typical net reaction to high-level LBNP is comparable to the effects seen under low-level LBNP but mainly differs in magnitude: central venous pressure drops substantially, arterial blood pressure slightly decreases, heart rate and resistance increase noticeably and larger volume shifts occur in the abdomen (compare [19, 7, 12]).

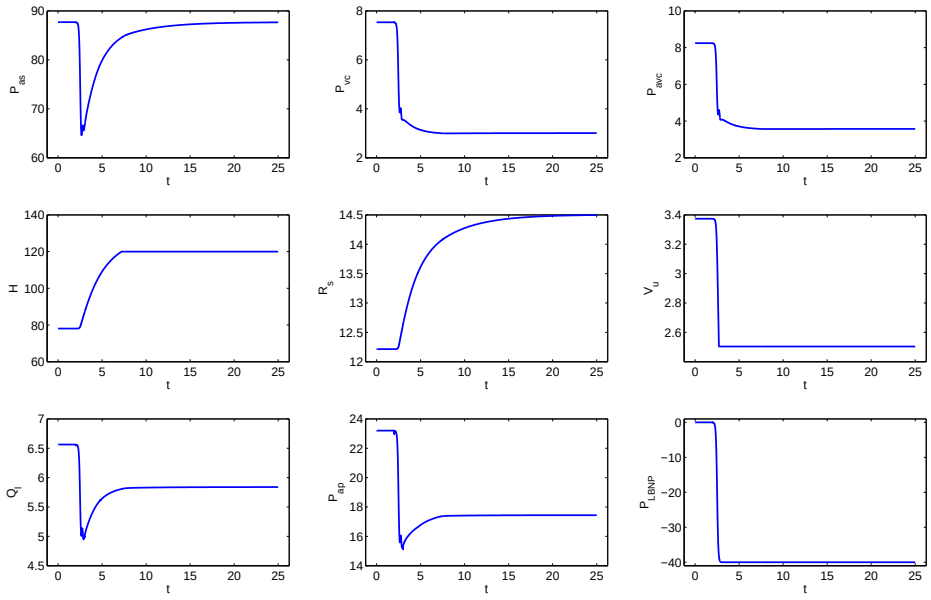

Figure 3.5: Model output using the arctan controls with $P_{\mathrm{LBNP}} = -40$ mmHg.

3.4.1 The arctan-controls

The simulation of the model using the arctan controls (2.29) under a LBNP of -40 mmHg is depicted in Fig. 3.5. In contrast to the low-level LBNP case, the swift decrease in unstressed volume alone is not enough to stabilize the model. Looking at the controls we immediately see that this level of stress is much more challenging: heart rate and unstressed volume reach their imposed extremal values $H^{\max}$ and $V_{\mathrm{u}}^{\min}$, respectively. Unsurprisingly the drop in V_{u} is again very fast due to the rapid decrease of P_{vc}. Note that systemic resistance grows only slightly. This is due to the fact that the responses of H and V_{u} are much faster so that both controls reach their imposed bounds and stabilize the model before an increase in R_{s} becomes relevant. Thus the control reaction mainly involves heart rate and unstressed volume. The vena cava pressure P_{vc} drops by about 40% and remains lowered for the rest of the simulation. This explains the decrease in P_{ap} and Q_ℓ which is, however, at least partly compensated by the responses of V_{u} and H. Despite the fact that P_{as} shows a significant 35%-drop at the onset of LBNP as well it can be stabilized so that it rises to its initial value again. This takes longer than in the low-level LBNP case and does not show a comparable overshoot after the rebound. Thus the arctan controls provide a more realistic response to high-level LBNP than for the low-level LBNP case before. However, there are still some points which need to be remedied: firstly, the rapid unstressed volume recruitment is still unrealistic; secondly, the increase in resistance is too modest; thirdly the amount of the initial drop in P_{as} is questionable.

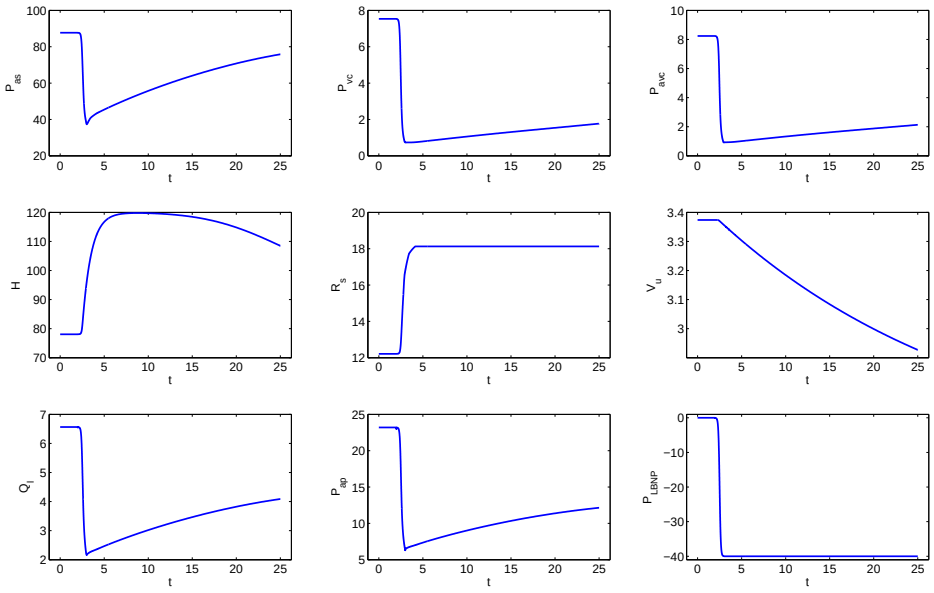

Figure 3.6: Model output using the set point controls with $P_{\mathrm{LBNP}} = -40$ mmHg.

3.4.2 The set point controls

Looking at Fig. 3.6 we see that the set point controls can hardly stabilize the model under this level of LBNP. The vena cava pressure P_{vc} drops severely (by 90%) in the beginning and recovers very slowly. Arterial blood pressure decreases dramatically as well at the onset of LBNP but at least almost reaches its initial value at the end of the simulation. The counteract to the stress is mainly determined by a rapid increase in systemic resistance which immediately reaches its overall maximal value (which depends on local upper bounds on compartmental inflow resistances as determined by eq. (2.19)). Though not as fast, heart rate grows rapidly to its imposed maximal value as well. However, after about 15 minutes H decreases again since P_{as} has sufficiently recovered by that time. Nevertheless R_{s} remains at its maximum level due to the steeper shape of the underlying sigmoidal function $R_{\mathrm{aux}}^{\mathrm{ctrl}}$ (see Fig. 2.3) but starts decreasing just before the end of the simulation when P_{as} has almost completely recovered. Unstressed volume recruitment is again the slowest control mechanism and shows a larger decrease than in the low-level LBNP case (as it should be). Pulmonary arterial pressure P_{ap} and hence cardiac output Q_ℓ exhibit (as expected) severe drops as well since venous return to the heart falls dramatically after the onset of LBNP. The slow recovering of P_{vc} provokes a slight increase in P_{ap} which makes Q_ℓ growing as well but cardiac output profits especially from the increased heart rate. Summarizing, the control responses to $P_{\mathrm{LBNP}} = -40$ mmHg are consistent with physiology. However, the decrease in vena cava pressure is too severe and the drop in P_{as} is rarely seen in healthy people and would rather indicate some pathology.

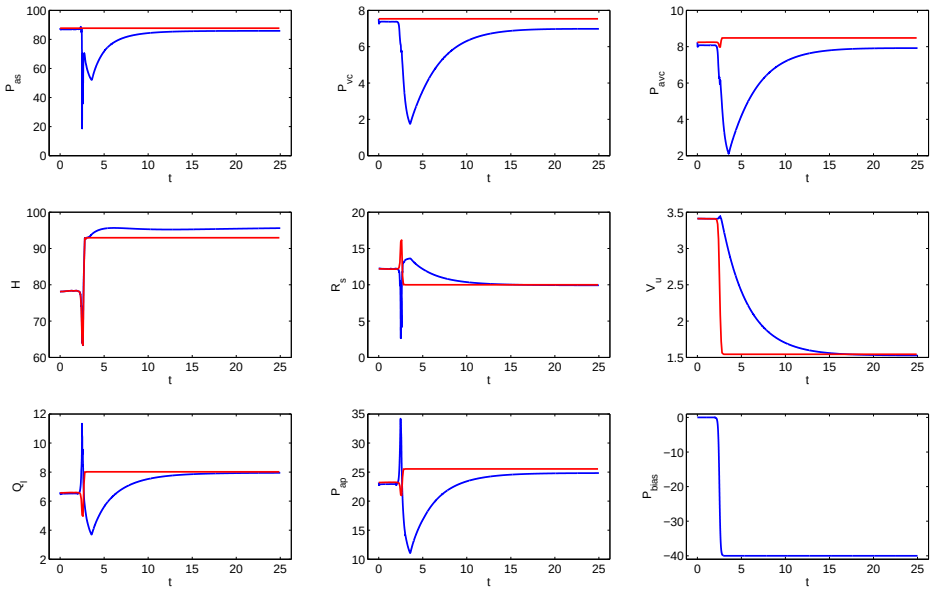

Figure 3.7: Model output (blue) using the optimal control approach with $P_{\mathrm{LBNP}} = -40$ mmHg. Red lines are computed steady state values.

3.4.3 The optimal control

The reaction of the optimal control strategy exhibits large differences under the two presented LBNP levels. In the case of low-level LBNP we saw an though not impossible but at least atypical reaction. This time (see Fig. 3.7) the controls mimic a rather expected response: we see a spontaneous increase in heart rate and a pronounced drop in unstressed volume. Though H does not climb to values comparable to set point or arctan controls we recall that with $P_{\mathrm{LBNP}} = -10$ mmHg heart rate was even decreasing. Note that except for the weighting matrices $Q_0 = C^\top C$ and R_0 appearing in Algorithm 2.1 we did not impose any constraints on V_{u}, R_{aux} or H. As explained in Sec. 3.2 in case of arctan and set point controls we imposed a lower bound for unstressed volume depending on the blood volume of the compartments 'ren' and 'spl'. Thus when using the arctan or set point controls, V_{u} can drop at maximum by 34%. Here we see that unstressed volume is lowered by about 44% which is unrealistic: under the assumption that V_{u} is recruited only from the splanchnic region a decrease in unstressed volume of this magnitude would empty abdominal blood reservoirs. Moreover, this large volume shift has the side effect that systemic resistance shows no significant response: we see an intial drop (again caused by numerical problems) then a slight increase which declines promptly so that by the end of the simulation R_{s} is lower than in the beginning. However, the optimal control accomplishes its task. We see that P_{as} and even the venous pressures P_{vc} and P_{avc} drop at the onset of LBNP but can be recovered so that all three pressures almost attain their initial values. The recovery of P_{vc} and P_{avc} affects Q_ℓ and P_{ap} which do not show a similar decrease as with arctan or set point controls. In summary, the optimal control approach is indeed able to stabilize the system (note that all depicted quantities are close to their equilibrium values at the end of the simulation) which was a priori not clear due to the iterative linearization of the model

(see the discussion at the end of Sec. 2.2.3.5). However, the results are again atypical compared to physiological expectations: though heart rate shows the expected increase resistance exhibits almost no reaction (even a decrease) and unstressed volume drops dramatically. The latter response is physiologically questionable. However, considering the time course of P_{as}, P_{vc} and P_{avc} and their corresponding steady state values this obviously represents an extremely good compensation of the imposed stress.

3.5 Discussion

We want to emphasize that the purpose of the numerical simulations was to give a qualitative overview of the three presented controls under orthostatic stress. The choice of controls investigated here was not random but represents popular techniques currently used in physiological modeling (see for instance [12, 22, 15, 6]). The model was not validated using experimental data nor a parameter identification was carried out since this would have gone beyond the scope of this thesis. Thus we want to investigate benefits and drawbacks when employing these (or similar) controls in comparable lumped compartmental models.
Clearly the optimal control approach is computationally the most costly whereas arctan or set point controls are mere ODEs which are solved simultaneously together with the model. If the controls have to be fit to data the arctan controls (as mentioned in the beginning of Sec. 2.2) are of limited flexibility since neither slope nor asymptotic values of the arc tangent can be altered as easily as with the set point controls. On the other hand the sigmoidal functions (2.30) appearing in the set point controls require detailed knowledge about the underlying control loops which can be problematic especially if mechanisms are modeled whose exact mode of operation is not fully understood. These difficulties can be avoided by formulating given feedback loops as an optimal control problem. However, the troubles of designing an explicit control gain are then to some extent shifted to choosing proper weighting matrices for the cost functional.
We have seen that all introduced controls are able to stabilize the CVS model (2.24) under both low- and high-level LBNP. The simplest control formulation, namely the arctan controls, have proven to be very robust in both simulations. However, the responses (especially the unstressed volume recruitment) were in both cases unrealistic. The set point controls representing a more elaborate but still rather easy-to-handle approach provided the physiologically most realistic control for low-level LBNP. For $P_{\text{LBNP}} = -40$ mmHg the response was still physiologically meaningful but the initial drops in P_{as} and P_{vc} were atypically pronounced. The optimal control approach based on Algorithm 2.1, being the theoretically most complex formulation, showed an atypical but still possible reaction in the first case. The high-level LBNP simulation using the optimal control was physiologically unrealistic but mathematically satisfactory: the components of the state vector which were observed, i.e. P_{as}, P_{vc} and P_{avc} (see eq. (2.82)), were steered to their corresponding steady state values.
Figure 3.8 provides an overview of the reactions we have seen under low-level LBNP. A popular though not undisputed hypothesis is that during mild levels of LBNP mainly veno-atrial baroreceptors are stimulated (compare [6, p. 109]) which hence provokes the reactions depicted at the beginning of Sec. 3.3. As stated above we see that the set point controls capture this typical behavior by far at best. However, this should not be interpreted as evidence of correctness of this hypothesis. We assumed in the case of the explicit controls,

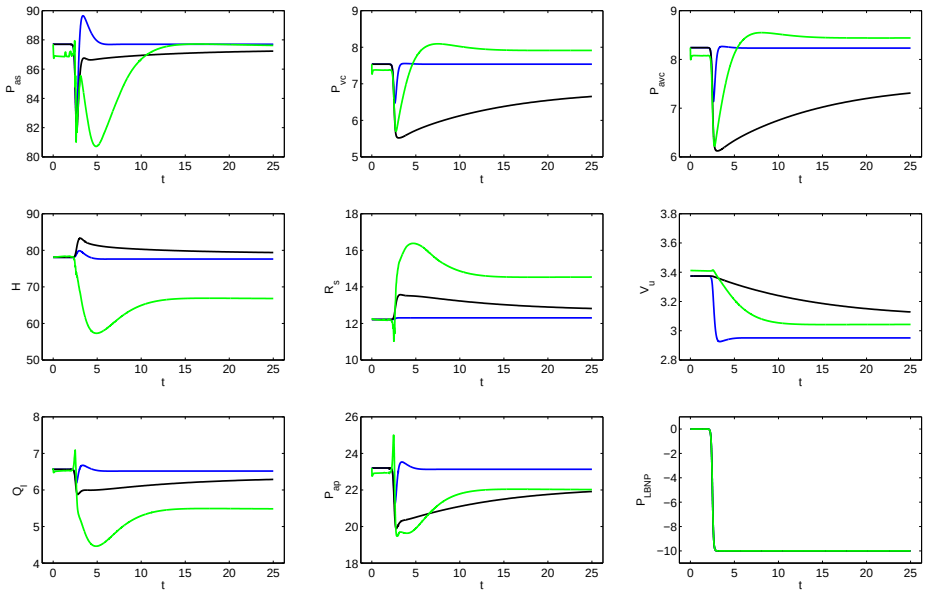

Figure 3.8: Model output using the arctan controls (blue), the set point controls (black) and the optimal control (green) with $P_{\mathrm{LBNP}} = -10$ mmHg.

i.e. arctan and set point controls, that heart rate H and sympathetic net activation R_{aux} depended on arterial blood pressure P_{as}, whereas unstressed volume recruitment was assumed to be solely influenced by vena cava pressure P_{vc}. This is a very rough simplification of reality based on experimental observations. Such assumptions cannot be derived from a-priori considerations as was the case in the use of physical principles in the derivation of relation (2.5), the general mass balance equation of a compartment. Thus these results cannot give detailed information about physiological facts but they do provide an indication of plausible correlations.

However, one advantage of using explicit controls is the predictability of results. In Fig. 3.9 the output of each control for V_{u}, R_{s} and H under both levels of LBNP is depicted. Note that responses of both explicit controls differ mainly in magnitude whereas the optimal control shows a completely distinct behavior under low- and high-level LBNP. This emphasizes that the optimal control is from a modeling point of view a 'black box' meaning the solution of the involved minimization problem, i.e. the control response, is a priori unknown. In contrast to explicit controls, it is even uncertain if a solution and thus a control exists. Thus designing an optimal control formulation that produces physiologically reasonable responses is a very complex and time consuming endeavor.

A compact overview of the reactions of all three controls under high-level LBNP is given in Fig. 3.10. As mentioned in Sec. 3.4.3 we see that the optimal control decreases V_{u} dramatically as compared to arctan or set point controls whereas heart rate and resistance show only mild responses. It should be noted that we tested various values for the weights q_{as}, q_{vc}, q_{avc} and r_1, r_2, r_3 appearing in the output matrix C as defined in (2.82) and the weighting matrix R_0 as given by (2.85), respectively. However, the qualitative behavior of the optimal control approach did not change and in some cases even deteriorated.

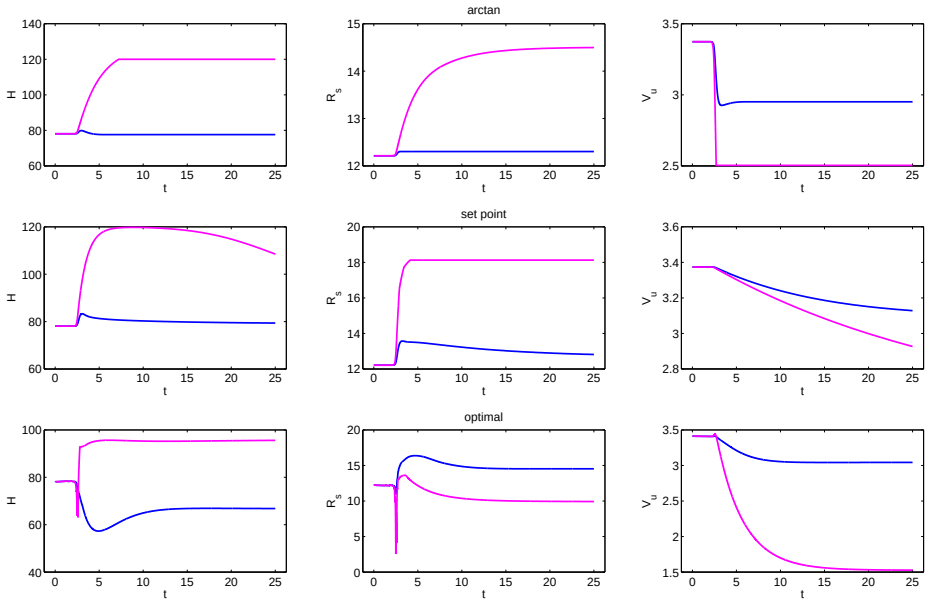

Figure 3.9: Output of the arctan controls (top row), the set point controls (middle row) and the optimal control (bottom row) under low- (blue) and high-level LBNP (magenta).

The response of the optimal control is admittedly physiologically questionable, however, the three plotted pressures P_{as}, P_{vc} and P_{avc} show a very credible reaction when using the optimal control as compared to arctan and set point controls. On the other hand the explicit controls designed based on physiological considerations provide more plausible responses of V_{u}, R_{s} and H but worse results concerning P_{as}, P_{vc} and P_{avc}. Thus there are obviously some mechanisms lacking which help counteracting orthostatic stress. A possible remedy may provide the following considerations. At very high stress levels it becomes important that many controls are to some extent coupled: for instance a decrease in compliance changes vasculature dimensions leading to a changed stressed/unstressed volume relationship and influences local resistance which in turn has again some effect on compliant vessel walls (see for instance [11]). Hence the responses of the controls cannot be seen completely separated from each other. Moreover it is doubtful if the human body tries to maintain resting values of arterial and venous blood pressures under very challenging stresses (compare [15]). However, this is implicitly assumed when using the arctan or set point controls under very high LBNP levels since both are designed to steer P_{as} and P_{vc} back to P_{as}^0 and P_{vc}^0 or $\hat{P}_{\text{as}}$ and $\hat{P}_{\text{vc}}$ respectively. Moreover, the steady state targets for the optimal control were computed using initial values of P_{as} and P_{vc} as well (see Appendix A.2). This fact and the assumption of constant compliances (as discussed at the beginning of Sec. 3.4) make results obtained by using these or comparable controls under very high levels of orthostatic stress questionable. Incorporating the complex interdependencies and changing steady state targets of the controls explicitly is very difficult due to the lack of detailed physiological knowledge in this area (compare the discussion in [15]). However, it should be possible to compute an equilibrium of the model without a-priori assumptions on P_{as} and P_{vc}: in accordance to the notation introduced in Appendix A.2 let

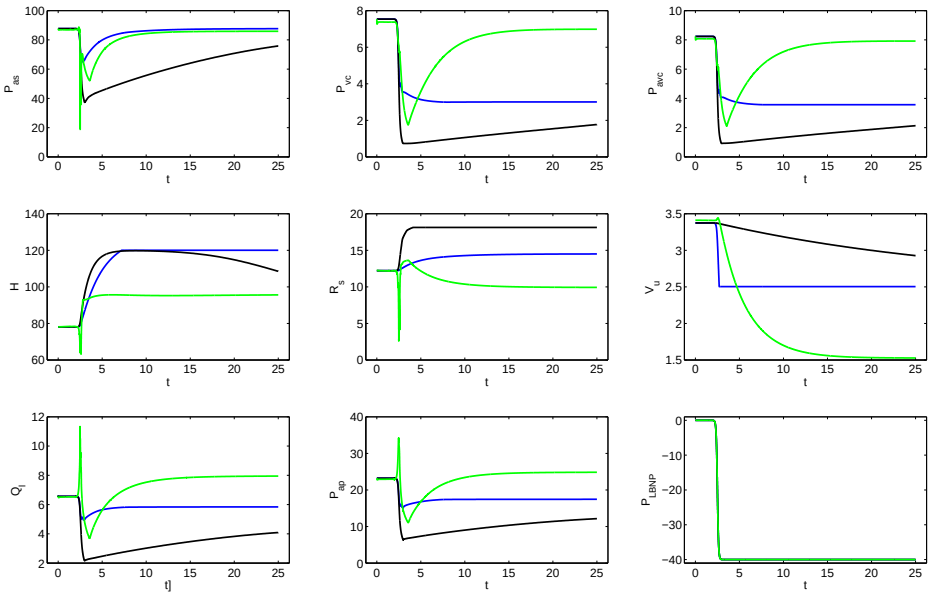

Figure 3.10: Model output using the arctan controls (blue), the set point controls (black) and the optimal control (green) with $P_{\mathrm{LBNP}} = -40$ mmHg.

$\bar{t}$ denote the actual time step. We treat $R^0_{\mathrm{aux}} = 0$ and $\bar{V}_{\mathrm{u}} = V_{\mathrm{u}}(\bar{t})$ as parameters and take the current values of arterial pressure $\bar{P}_{\mathrm{as}} = P_{\mathrm{as}}(\bar{t})$, vena cava pressure $\bar{P}_{\mathrm{vc}} = P_{\mathrm{vc}}(\bar{t})$ and $\bar{H} = H(\bar{t})$ to do the calculations depicted in Appendix A.2. Finally we define $\tilde{F} : \mathbb{R}^2 \to \mathbb{R}^2$ to be $\tilde{F}(\bar{P}_{\mathrm{as}}, \bar{P}_{\mathrm{vc}}) = F(\bar{V}_{\mathrm{u}}, \bar{R}_{\mathrm{aux}})$. Thus we compute the steady state x^{trans} by varying P_{as} and P_{vc} instead of V_{u} and R_{aux}. This approach was tested in the course of implementing Algorithm 2.1, however, it was numerically extremely unstable and thus did not provide reasonable results. Finding a possible remedy will most probably require detailed analysis of the steady state properties of the system and comprehensive testing with various optimization methods. Nevertheless, when extreme stresses have to be simulated it may be more convenient (though by far not unproblematic) to use an extended and adapted optimal control approach.

A Appendix

A.1 Auxiliary Equations for the CVS model

The systemic compartments 'per', 'up', 'ren', 'spl' and 'leg' are connected in parallel to the arterial systemic compartment (see Fig. 2.1). The inflow resistances (the outflow resistances are assumed to be constant) of these compartments are subject to sympathetic vasoconstriction and thus changed dynamically by R_{aux} according to eq. (2.19) which gives

$$\begin{aligned} R^{\text{in}}_{\text{per}} &= \min(R^0_{\text{per}} + \kappa_{\text{per}} R_{\text{aux}},\, K_{\text{per}} R^0_{\text{per}}), & R^{\text{in}}_{\text{spl}} &= \min(R^0_{\text{spl}} + \kappa_{\text{spl}} R_{\text{aux}},\, K_{\text{spl}} R^0_{\text{spl}}), \\ R^{\text{in}}_{\text{up}} &= \min(R^0_{\text{up}} + \kappa_{\text{up}} R_{\text{aux}},\, K_{\text{up}} R^0_{\text{up}}), & R^{\text{in}}_{\text{leg}} &= \min(R^0_{\text{leg}} + \kappa_{\text{leg}} R_{\text{aux}},\, K_{\text{leg}} R^0_{\text{leg}}). \\ R^{\text{in}}_{\text{ren}} &= \min(R^0_{\text{ren}} + \kappa_{\text{ren}} R_{\text{aux}},\, K_{\text{ren}} R^0_{\text{ren}}), \end{aligned} \tag{A.1}$$

Thus we obtain the following inflows by using relation (2.20)

$$F^{\text{in}}_{\text{per}} = \frac{P_{\text{as}} - P_{\text{per}}}{R^{\text{in}}_{\text{per}}}, \qquad F^{\text{in}}_{\text{spl}} = \frac{P_{\text{as}} - P_{\text{spl}}}{R^{\text{in}}_{\text{spl}}}, \qquad F^{\text{in}}_{\text{ren}} = \frac{P_{\text{as}} - P_{\text{ren}}}{R^{\text{in}}_{\text{ren}}},$$
$$F^{\text{in}}_{\text{up}} = \frac{P_{\text{as}} - P_{\text{up}}}{R^{\text{in}}_{\text{up}}}, \qquad F^{\text{in}}_{\text{leg}} = \frac{P_{\text{as}} - P_{\text{leg}}}{R^{\text{in}}_{\text{leg}}}.$$

The compartments 'per' and 'up' are connected to the vena cava. We assumed that flows in the venous part of the systemic circuit are subject to the action of venous valves. Thus by using relation (2.21) we obtain

$$F^{\text{out}}_{\text{per}} = \max(0, \frac{P_{\text{per}} - P_{\text{vc}}}{R^{\text{out}}_{\text{per}}}), \qquad F^{\text{out}}_{\text{up}} = \max(0, \frac{P_{\text{up}} - P_{\text{vc}}}{R^{\text{out}}_{\text{up}}}).$$

For renal, splanchnic and legs compartments which are connected to the abdominal vena cava follows analogously

$$F^{\text{out}}_{\text{ren}} = \max(0, \frac{P_{\text{ren}} - P_{\text{avc}}}{R^{\text{out}}_{\text{ren}}}), \quad F^{\text{out}}_{\text{spl}} = \max(0, \frac{P_{\text{spl}} - P_{\text{avc}}}{R^{\text{out}}_{\text{spl}}}), \quad F^{\text{out}}_{\text{leg}} = \max(0, \frac{P_{\text{leg}} - P_{\text{avc}}}{R^{\text{out}}_{\text{leg}}}).$$

Finally the flow from abdominal vena cava to vena cava is given by

$$F^{\text{out}}_{\text{avc}} = \max(0, \frac{P_{\text{avc}} - P_{\text{vc}}}{R^{\text{out}}_{\text{avc}}}).$$

These equations together with relation (2.22) and the cardiac outputs of the left and right heart (2.17) represent all flows appearing in the CVS model (2.24). As mentioned in Sec. 3.2, we want to visualize the effects of vasoconstriction using the total peripheral resistance R_{s} rather than R_{aux}. In case of model (2.24) we consider the systemic resistance to be the total resistance the blood flow has to overcome between arterial systemic and vena cava compartments (compare Fig. 2.1). Thus we first compute the resistance the

compartments 'ren', 'spl' and 'leg' exhibit to blood flow using the laws for parallel and serial resistances

$$R_{\text{lower}} = \frac{1}{\frac{1}{R^{\text{in}}_{\text{ren}}+R^{\text{out}}_{\text{ren}}} + \frac{1}{R^{\text{in}}_{\text{spl}}+R^{\text{out}}_{\text{spl}}} + \frac{1}{R^{\text{in}}_{\text{leg}}+R^{\text{out}}_{\text{leg}}}}. \tag{A.2}$$

The total resistance of the compartments 'per', 'up', 'ren', 'spl', 'leg' and 'avc' and thus the systemic resistance is hence given by

$$R_{\text{s}} = \frac{1}{\frac{1}{R_{\text{lower}}+R^{\text{out}}_{\text{avc}}} + \frac{1}{R^{\text{in}}_{\text{per}}+R^{\text{out}}_{\text{per}}} + \frac{1}{R^{\text{in}}_{\text{up}}+R^{\text{out}}_{\text{up}}}}. \tag{A.3}$$

A.2 Equilibrium Computation

A dynamical system is said to be in steady state if it is not changing over time, or equivalently, if the time derivatives of its state variables are zero. However, setting the right hand side of (2.24) to zero and treating it as a non linear equation system for the first 13 state variables (the controls would add three trivial equations $0 = 0$) is numerically extremely unstable and computationally costly. Thus we follow a different approach. We will not analyze existence or stability of equilibria of the CVS model (2.24) but only provide a way for computing its stationary points (assuming that they exist). We choose initial values of arterial and vena cava blood pressures P^0_{as} and P^0_{vc}, respectively, as parameters for the calculation. By using P^0_{as} and P^0_{vc} and taking the current values of the controlled quantities V_{u}, R_{aux} and H we use steady state relations to get the remaining state variables which we denote by the superscript 'SS'. These values are used in a numerical computation of an equilibrium which we denote by x^{trans}.
Let $\bar{t}$ be the actual timestep of the simulation and $\bar{V}_{\text{u}} = V_{\text{u}}(\bar{t})$, $\bar{R}_{\text{aux}} = R_{\text{aux}}(\bar{t})$ and $\bar{H} = H(\bar{t})$ (as mentioned above we have $u = 0$ thus V_{u}, R_{aux} and H are constant). In steady state we have $\ddot{S}_\ell = \ddot{S}_{\text{r}} = \dot{S}_\ell = \dot{S}_{\text{r}} = 0$ which yields using (2.23)

$$\sigma^{\text{SS}}_\ell = 0, \qquad \sigma^{\text{SS}}_{\text{r}} = 0, \qquad S^{\text{SS}}_\ell = \frac{\beta_\ell}{\alpha_\ell}\bar{H}, \qquad S^{\text{SS}}_{\text{r}} = \frac{\beta_{\text{r}}}{\alpha_{\text{r}}}\bar{H}.$$

In a stationary situation inflows and outflows to all compartments equalize (otherwise compartmental pressures would change, i.e. their time derivatives would not be zero). Thus we compute the total blood flow through the peripheral compartment 'per' by using P^0_{as} and P^0_{vc} (compare Fig. 2.1)

$$F_{\text{per}} = \frac{P^0_{\text{as}} - P^0_{\text{vc}}}{\bar{R}^{\text{in}}_{\text{per}} + R^{\text{out}}_{\text{per}}},$$

where we employed $\bar{R}_{\text{aux}}$ in relation (A.1) to compute $\bar{R}^{\text{in}}_{\text{per}}$ (note that the outflow resistances are constant parameters). Since in steady state total blood flow through a compartment equals the inflow to the compartment, F_{per} obeys the following relation as well

$$F_{\text{per}} = \frac{P^0_{\text{as}} - P^{\text{SS}}_{\text{per}}}{\bar{R}^{\text{in}}_{\text{per}}},$$

and thus we get $P^{\text{SS}}_{\text{per}}$ by rearranging terms

$$P^{\text{SS}}_{\text{per}} = P^0_{\text{as}} - F_{\text{per}}\bar{R}^{\text{in}}_{\text{per}}.$$

Analogously we compute

$$F_{\text{up}} = \frac{P^0_{\text{as}} - P^0_{\text{vc}}}{\bar{R}^{\text{in}}_{\text{up}} + R^{\text{out}}_{\text{up}}},$$

which yields

$$P^{\text{SS}}_{\text{up}} = P^0_{\text{as}} - F_{\text{up}}\bar{R}^{\text{in}}_{\text{up}}.$$

By employing $\bar{R}_{\text{aux}}$ in eq. (A.1) we obtain the current inflow resistances to the compartments 'ren', 'spl' and 'leg' which we use to compute their total resistance to blood flow

$$\bar{R}_{\text{lower}} = \frac{1}{\frac{1}{\bar{R}^{\text{in}}_{\text{ren}}+R^{\text{out}}_{\text{ren}}} + \frac{1}{\bar{R}^{\text{in}}_{\text{spl}}+R^{\text{out}}_{\text{spl}}} + \frac{1}{\bar{R}^{\text{in}}_{\text{leg}}+R^{\text{out}}_{\text{leg}}}},$$

using relation (A.2). Now we can compute the total blood flow through the abdominal vena cava compartment

$$F_{\text{avc}} = \frac{P^0_{\text{as}} - P^0_{\text{vc}}}{\bar{R}_{\text{lower}} + R^{\text{out}}_{\text{avc}}},$$

which we use in the outflow-relation of compartment 'avc' to get

$$P^{\text{SS}}_{\text{avc}} = F_{\text{avc}}R^{\text{out}}_{\text{avc}} + P^0_{\text{vc}}.$$

Having computed the pressure in compartment 'avc' we are able to compute

$$F_{\text{ren}} = \frac{P^0_{\text{as}} - P^{\text{SS}}_{\text{avc}}}{\bar{R}^{\text{in}}_{\text{ren}} + R^{\text{out}}_{\text{ren}}}, \qquad F_{\text{spl}} = \frac{P^0_{\text{as}} - P^{\text{SS}}_{\text{avc}}}{\bar{R}^{\text{in}}_{\text{spl}} + R^{\text{out}}_{\text{spl}}}, \qquad F_{\text{leg}} = \frac{P^0_{\text{as}} - P^{\text{SS}}_{\text{avc}}}{\bar{R}^{\text{in}}_{\text{leg}} + R^{\text{out}}_{\text{leg}}},$$

which used in the corresponding inflow relations yields

$$P^{\text{SS}}_{\text{ren}} = P^0_{\text{as}} - F_{\text{ren}}\bar{R}^{\text{in}}_{\text{ren}}, \qquad P^{\text{SS}}_{\text{spl}} = P^0_{\text{as}} - F_{\text{spl}}\bar{R}^{\text{in}}_{\text{spl}}, \qquad P^{\text{SS}}_{\text{leg}} = P^0_{\text{as}} - F_{\text{leg}}\bar{R}^{\text{in}}_{\text{leg}}.$$

The total flow in the systemic circuit of the model is

$$\bar{F}_{\text{s}} = \frac{P^0_{\text{as}} - P^0_{\text{vc}}}{\bar{R}_{\text{s}}},$$

where the stationary systemic resistance is given by (using relation (A.3))

$$\bar{R}_{\text{s}} = \frac{1}{\frac{1}{\bar{R}_{\text{lower}}+R^{\text{out}}_{\text{avc}}} + \frac{1}{\bar{R}^{\text{in}}_{\text{per}}+R^{\text{out}}_{\text{per}}} + \frac{1}{\bar{R}^{\text{in}}_{\text{up}}+R^{\text{out}}_{\text{up}}}}.$$

With the same argument as before we conclude that in a stationary situation the following relation has to hold

$$\bar{Q}_\ell = \bar{F}_{\text{s}} = \bar{Q}_{\text{r}} = \bar{F}_{\text{p}}. \tag{A.4}$$

We will use this fact to compute the venous pulmonary pressure. From (A.4) we get the trivial equation

$$P^{\text{SS}}_{\text{vp}}\bar{Q}_\ell = \bar{F}_{\text{s}}P^{\text{SS}}_{\text{vp}}.$$

We rearrange terms and obtain

$$\begin{aligned} P^{\text{SS}}_{\text{vp}} =& \bar{F}_{\text{s}}\frac{P^{\text{SS}}_{\text{vp}}}{\bar{Q}_\ell} \\ =& \frac{P^0_{\text{as}} - P^0_{\text{vc}}}{\bar{R}_{\text{s}}} \cdot \frac{a_\ell(\bar{H})P^0_{\text{as}} + k_\ell(\bar{H})\min(S^{\text{SS}}_\ell, P^0_{\text{as}})}{\bar{H}c_\ell a_\ell(\bar{H})\min(S^{\text{SS}}_\ell, P^0_{\text{as}})}, \end{aligned}$$

Variable	Value	Unit
$V_{\mathrm{u}}(0)$	3.3	ℓ
$R_{\mathrm{aux}}(0)$	0	1
$H(0)$	78	1/min
P_{as}^0	87.7	mmHg
P_{vc}^0	7.5	mmHg

Table A.1: Initial guesses for the controlled quantities and values of P_{as}^0 and P_{vc}^0.

where we made use of (2.17). Finally we compute the arterial pulmonary pressure by using all calculated pressures and the currently applied external pressures $\bar{P}_{\mathrm{ren}}^{\mathrm{bias}} = P_{\mathrm{ren}}^{\mathrm{bias}}(\bar{t})$, $\bar{P}_{\mathrm{spl}}^{\mathrm{bias}} = P_{\mathrm{spl}}^{\mathrm{bias}}(\bar{t})$ and $\bar{P}_{\mathrm{leg}}^{\mathrm{bias}} = P_{\mathrm{leg}}^{\mathrm{bias}}(\bar{t})$ (note that as mentioned in Sec. 3.1 only the compartments 'ren', 'spl' and 'leg' are subject to external pressure) in relation (2.26) which yields

$$\begin{aligned} P_{\mathrm{ap}}^{\mathrm{SS}} =& \frac{1}{c_{\mathrm{up}}} \big(V_{\mathrm{tot}} - \bar{V}_{\mathrm{u}} - c_{\mathrm{as}} P_{\mathrm{as}}^0 - c_{\mathrm{per}} P_{\mathrm{per}}^{\mathrm{SS}} - c_{\mathrm{up}} P_{\mathrm{up}}^{\mathrm{SS}} \\ & - c_{\mathrm{ren}} (P_{\mathrm{ren}}^{\mathrm{SS}} - \bar{P}_{\mathrm{ren}}^{\mathrm{bias}}) - c_{\mathrm{spl}} (P_{\mathrm{spl}}^{\mathrm{SS}} - \bar{P}_{\mathrm{spl}}^{\mathrm{bias}}) - c_{\mathrm{leg}} (P_{\mathrm{leg}}^{\mathrm{SS}} - \bar{P}_{\mathrm{leg}}^{\mathrm{bias}}) \\ & - c_{\mathrm{vc}} P_{\mathrm{vc}}^{\mathrm{SS}} - c_{\mathrm{vp}} P_{\mathrm{vp}}^{\mathrm{SS}} - c_{\mathrm{avc}} P_{\mathrm{avc}}^{\mathrm{SS}} \big) . \end{aligned}$$

Computing the stationary cardiac output by using (2.17)

$$\bar{Q}_{\mathrm{r}} = \bar{H} \frac{c_{\mathrm{r}} P_{\mathrm{vc}}^0 a_{\mathrm{r}}(\bar{H}) \min(S_{\mathrm{r}}^{\mathrm{SS}}, P_{\mathrm{ap}}^{\mathrm{SS}})}{a_{\mathrm{r}}(\bar{H}) P_{\mathrm{ap}}^{\mathrm{SS}} + k_{\mathrm{r}}(\bar{H}) \min(S_{\mathrm{r}}^{\mathrm{SS}}, P_{\mathrm{ap}}^{\mathrm{SS}})},$$

and the stationary pulmonary flow by applying (2.22)

$$\bar{F}_{\mathrm{p}} = \frac{P_{\mathrm{ap}}^{\mathrm{SS}} - P_{\mathrm{vp}}^{\mathrm{SS}}}{R_{\mathrm{p}}},$$

we are eventually able to compute x^{trans} by solving a homogeneous two-dimensional non linear equation system. Let $F : \mathbb{R}^2 \to \mathbb{R}^2$ be given by

$$F(\bar{V}_{\mathrm{u}}, \bar{R}_{\mathrm{aux}}) = \begin{pmatrix} \left| \bar{F}_{\mathrm{s}} - \bar{Q}_{\ell} \right|^2 \\ \left| \bar{F}_{\mathrm{p}} - \bar{Q}_{\mathrm{r}} \right|^2 \end{pmatrix}.$$

As stated above in steady state relation (A.4) has to hold. Thus a root of F is a stationary point of the model (2.24). We assume that F has a root which we denote by $(V_{\mathrm{u}}^{\mathrm{trans}}, R_{\mathrm{aux}}^{\mathrm{trans}})$. By repeating the computations depicted above with $V_{\mathrm{u}}^{\mathrm{trans}}$ and $R_{\mathrm{aux}}^{\mathrm{trans}}$ instead of $\bar{V}_{\mathrm{u}}$ and $\bar{R}_{\mathrm{aux}}$ respectively we get the steady state vector x^{trans} given by

$$\begin{aligned} x^{\mathrm{trans}} =& (P_{\mathrm{as}}^0, P_{\mathrm{per}}^{\mathrm{trans}}, P_{\mathrm{up}}^{\mathrm{trans}}, P_{\mathrm{ren}}^{\mathrm{trans}}, P_{\mathrm{spl}}^{\mathrm{trans}}, P_{\mathrm{leg}}^{\mathrm{trans}}, P_{\mathrm{vc}}^0, \\ & P_{\mathrm{vp}}^{\mathrm{trans}}, P_{\mathrm{avc}}^{\mathrm{trans}}, S_{\ell}^{\mathrm{trans}}, \sigma_{\ell}^{\mathrm{trans}}, S_{\mathrm{r}}^{\mathrm{trans}}, \sigma_{\mathrm{r}}^{\mathrm{trans}}, V_{\mathrm{u}}^{\mathrm{trans}}, R_{\mathrm{aux}}^{\mathrm{trans}}, \bar{H})^{\top}. \end{aligned}$$

The initial guess for the resting steady state x^{rest} corresponding to $P_{\mathrm{LBNP}} = 0$ mmHg and $\bar{t} = 0$ min (i.e. according to relation (3.2) $\bar{P}_{\mathrm{ren}}^{\mathrm{bias}} = \bar{P}_{\mathrm{spl}}^{\mathrm{bias}} = \bar{P}_{\mathrm{leg}}^{\mathrm{bias}} = 0$ mmHg) is depicted in Table A.1, Table A.2 shows the calculated steady state values.
The MATLAB routine `fsolve` which is by default a trust-region Powell dogleg method (see [20] for details) was used to compute a root of F. We imposed P_{as}^0 and P_{vc}^0 as parameters for the steady state computation throughout the whole simulation. Thus especially

Variable	Value	Unit
P_{as}^{0}	87.7	mmHg
$P_{\text{per}}^{\text{rest}}$	12.1	mmHg
$P_{\text{up}}^{\text{rest}}$	7.8	mmHg
$P_{\text{ren}}^{\text{rest}}$	14.2	mmHg
$P_{\text{spl}}^{\text{rest}}$	13.4	mmHg
$P_{\text{leg}}^{\text{rest}}$	14.7	mmHg
P_{vc}^{0}	7.5	mmHg
$P_{\text{vp}}^{\text{rest}}$	10.3	mmHg

Variable	Value	Unit
$P_{\text{avc}}^{\text{rest}}$	8.2	mmHg
S_{ℓ}^{rest}	59.9	mmHg
$\sigma_{\ell}^{\text{rest}}$	0	$\text{mmHg}/\text{min}^{-2}$
$S_{\text{r}}^{\text{rest}}$	4.5	mmHg
$\sigma_{\text{r}}^{\text{rest}}$	0	$\text{mmHg}/\text{min}^{-2}$
$V_{\text{u}}^{\text{rest}}$	3.4	ℓ
$R_{\text{aux}}^{\text{rest}}$	18	mmHg
$H(0)$	78	$1/\text{min}$

Table A.2: Initial steady state x^{rest}. The euclidean norm of $F(V_{\text{u}}^{\text{trans}}, R_{\text{aux}}^{\text{trans}})$ is of the order 10^{-8}.

in the case of high-level LBNP the starting point for the numerical computation could not be guaranteed to be sufficiently close to the exact solution at all times. Hence the non local convergence properties of the trust-region method were advantageous. However, for the sake of computational efficiency (and due to the fact that we did not know if an exact zero of F existed) we did not change standard error tolerances or maximum number of iterations of `fsolve`. Thus especially in the transition phase between onset and full inset of LBNP the computed steady states are of limited accuracy. However, `fsolve` terminated always successfully in all simulations. It should be noted that the form of F was not chosen accidentally: if F does not have a root it can be seen as cost functional of a non linear least squares minimization problem. If the residual of the computed minimizer is small enough the computed 'steady state' can still be meaningful in the context of Algorithm 2.1.

A.3 Parameters

Parameter	Meaning	Value	Unit
c_{as}	Compliance of the arterial systemic compartment	0.002	ℓ/mmHg
c_{per}	Compliance of the peripheral compartment	0.008	ℓ/mmHg
c_{up}	Compliance of the upper compartment	0.008	ℓ/mmHg
c_{ren}	Compliance of the renal compartment	0.015	ℓ/mmHg
c_{spl}	Compliance of the splanchnic compartment	0.055	ℓ/mmHg
c_{leg}	Compliance of the legs compartment	0.019	ℓ/mmHg
c_{vc}	Compliance of the vena cava compartment	0.017	ℓ/mmHg
c_{vp}	Compliance of the venous pulmonary compartment	0.0084	ℓ/mmHg
c_{avc}	Compliance of the abdominal vena cava compartment	0.025	ℓ/mmHg
c_{ap}	Compliance of the arterial pulmonary compartment	0.0043	ℓ/mmHg
V_{tot}	Total blood volume	5.5	ℓ
c_ℓ	Compliance of the left ventricle	0.0128	ℓ/mmHg
c_{r}	Compliance of the right ventricle	0.0607	ℓ/mmHg
R_ℓ	Inflow resistance of the left ventricle	11.35	mmHg min/ℓ
R_{r}	Inflow resistance of the right ventricle	4.158	mmHg min/ℓ
κ	Coefficient in the eq. for the duration of the diastole (2.9)	0.05	$\mathrm{min}^{1/2}$
α_ℓ	Coefficient of S_ℓ in eq. (2.18)	89.47	min^{-2}
α_{r}	Coefficient of S_{r} in eq. (2.18)	28.46	min^{-2}
β_ℓ	Coefficient of H in eq. (2.18)	68.712	mmHg/min
β_{r}	Coefficient of H in eq. (2.18)	1.66	mmHg/min
γ_ℓ	Coefficient of $\dot{S}_\ell$ in eq. (2.18)	37.33	min^{-1}
γ_{r}	Coefficient of $\dot{S}_{\mathrm{r}}$ in eq. (2.18)	11.88	min^{-1}
$k_{\mathrm{avc}}^{\mathrm{LBNP}}$	Coefficient determining the impact of P_{LBNP} on the abdominal vena cava compartment	0.3	1
$k_{\mathrm{vc}}^{\mathrm{LBNP}}$	Coefficient determining the impact of P_{LBNP} on the vena cava compartment	0.3	1
$k_{\mathrm{leg}}^{\mathrm{LBNP}}$	Coefficient determining the impact of P_{LBNP} on the legs compartment	1	1
k_{ren}	Constant influencing the sequestration of V_{u} in the renal compartment	0.1	1
k_{spl}	Constant influencing the sequestration of V_{u} in the splanchnic compartment	0.9	1

Table A.3: Vascular, cardiac and LBNP parameters

Parameter	Meaning	Value	Unit
R^0_{per}	Initial inflow resistance at the peripheral compartment	64.974	mmHg min/ℓ
R^0_{up}	Initial inflow resistance at the upper compartment	64.974	mmHg min/ℓ
R^0_{ren}	Initial inflow resistance at the renal compartment	68,306	mmHg min/ℓ
R^0_{spl}	Initial inflow resistance at the splanchnic compartment	49,98	mmHg min/ℓ
R^0_{leg}	Initial inflow resistance at the legs compartment	59,976	mmHg min/ℓ
κ_{per}	Parameter influencing the impact of R_{aux} on the peripheral compartment	0.1	mmHg min/ℓ
κ_{up}	Parameter influencing the impact of R_{aux} on the upper compartment	0.1	mmHg min/ℓ
κ_{ren}	Parameter influencing the impact of R_{aux} on the renal compartment	0.4	mmHg min/ℓ
κ_{spl}	Parameter influencing the impact of R_{aux} on the splanchnic compartment	0.4	mmHg min/ℓ
κ_{leg}	Parameter influencing the impact of R_{aux} on the legs compartment	0.2	mmHg min/ℓ
K_{per}	Maximal increase in inflow resistance at the peripheral compartment	1.5	1
K_{up}	Maximal increase in inflow resistance at the upper compartment	1.1	1
K_{ren}	Maximal increase in inflow resistance at the renal compartment	1.5	1
K_{spl}	Maximal increase in inflow resistance at the splanchnic compartment	1.8	1
K_{leg}	Maximal increase in inflow resistance at the legs compartment	1.7	1
$R^{\text{out}}_{\text{per}}$	Outflow resistance at the peripheral compartment	3.831	mmHg min/ℓ
$R^{\text{out}}_{\text{up}}$	Outflow resistance at the upper compartment	3.831	mmHg min/ℓ
$R^{\text{out}}_{\text{ren}}$	Outflow resistance at the renal compartment	4.998	mmHg min/ℓ
$R^{\text{out}}_{\text{spl}}$	Outflow resistance at the splanchnic compartment	2.998	mmHg min/ℓ
$R^{\text{out}}_{\text{leg}}$	Outflow resistance at the legs compartment	4.998	mmHg min/ℓ
$R^{\text{out}}_{\text{avc}}$	Outflow resistance at the abdominal vena cava compartment	0.166	mmHg min/ℓ
R_{p}	Resistance in the pulmonary circuit	1.965	mmHg min/ℓ

Table A.4: Parameters influencing local resistance

Parameter	Meaning	Value	Unit
$V_{\mathrm{u}}^{\max}$	Upper bound for V_{u} in the arctan controls (2.29) and upper asymptote for $V_{\mathrm{u}}^{\mathrm{ctrl}}$ given by eq. (2.30)	4.27	ℓ
$V_{\mathrm{u}}^{\min}$	Lower bound for V_{u} in the arctan controls (2.29) and upper asymptote for $V_{\mathrm{u}}^{\mathrm{ctrl}}$ given by eq. (2.30)	2.53	ℓ
$R_{\mathrm{aux}}^{\max}$	Upper asymptote for for R_{aux} in $R_{\mathrm{aux}}^{\mathrm{ctrl}}$ given by eq. (2.30)	600	1
$R_{\mathrm{aux}}^{\min}$	Lower bound for R_{aux} in the arctan controls (2.29) and upper asymptote for $R_{\mathrm{aux}}^{\mathrm{ctrl}}$ given by eq. (2.30)	-600	1
$H^{\max}$	Upper bound for H in the arctan controls (2.29) and upper asymptote for H^{ctrl} given by eq. (2.30)	120	bpm
$H^{\min}$	Lower bound for H in the arctan controls (2.29) and upper asymptote for H^{ctrl} given by eq. (2.30)	40	bpm
c_1	Constant in $g_1(P_{\mathrm{vc}})$ given by eq. (2.28)	5	mmHg
c_2	Constant in $g_2(P_{\mathrm{as}})$ given by eq. (2.28)	18	mmHg
$\bar{c}_1$	Constant in $g_1(P_{\mathrm{vc}})$ given by eq. (2.28)	5	ℓ/min
$\bar{c}_2$	Constant in $g_2(P_{\mathrm{as}})$ given by eq. (2.28)	18	1/min
P_{vc}^0	Initial guess for P_{vc} in $g_1(P_{\mathrm{vc}})$ given by eq. (2.28)	7.5	mmHg
P_{as}^0	Initial guess for P_{as} in $g_2(P_{\mathrm{as}})$ given by eq. (2.28)	87.7	mmHg
$\hat{P}_{\mathrm{vc}}$	Predefined set point value of P_{vc} in $V_{\mathrm{u}}^{\mathrm{ctrl}}$ given by eq. (2.30)	7.5	mmHg
$\hat{P}_{\mathrm{as}}$	Predefined set point value of P_{as} in H^{ctrl} and $R_{\mathrm{aux}}^{\mathrm{ctrl}}$ given by eq. (2.30)	88.7	mmHg
k_1	Exponent in $V_{\mathrm{u}}^{\mathrm{ctrl}}$ given by eq. (2.30)	7	1
k_2	Exponent in $R_{\mathrm{aux}}^{\mathrm{ctrl}}$ given by eq. (2.30)	7.5	1
k_3	Exponent in H^{ctrl} given by eq. (2.30)	12	1
τ_1	Time constant influencing V_{u} in the set point controls (2.32)	30	min
τ_2	Time constant influencing R_{aux} in the set point controls (2.32)	2	min
τ_3	Time constant influencing H in the set point controls (2.32)	1	min

Table A.5: Parameters of the arctan and set point controls

Parameter	Meaning	Value	Unit
q_{as}	Weight for P_{as} appearing in the observation matrix C given by eq. (2.82)	1	$\mathrm{min}^{-2}\mathrm{mmHg}^{-1}$
q_{vc}	Weight for P_{vc} appearing in the observation matrix C given by eq. (2.82)	0.5	$\mathrm{min}^{-2}\mathrm{mmHg}^{-1}$
q_{avc}	Weight for P_{avc} appearing in the observation matrix C given by eq. (2.82)	0.5	$\mathrm{min}^{-2}\mathrm{mmHg}^{-1}$
r_1	Upper diagonal element of the weighting matrix R_0 given by eq. (2.85)	500	$\mathrm{min}^{-2}\ell^{-1}$
r_2	Middle diagonal element of the weighting matrix R_0 given by eq. (2.85)	0.0001	min^{-2}
r_3	Lower diagonal element of the weighting matrix R_0 given by eq. (2.85)	0.002	$\mathrm{min}^{-2}\mathrm{bpm}^{-1}$

Table A.6: Parameters of the optimal control

Bibliography

[1] B. Anderson and J. Moore. *Optimal Control: Linear Quadratic Methods*. Prentice Hall, 1990.

[2] Allyn & Bacon. Digital image archive for exercise physiology. Currently available at `www.abacon.com/dia/exphys/index.html`.

[3] R. Barbieri, J. K. Triedman, and J. P. Saul. Heart rate control and mechanical cardiopulmonary coupling to assess central volume: a systems analysis. *American Journal of Physiology*, 283(5):R1210–1220, 2002.

[4] J. J. Batzel, M. Fink, and F. Kappel. Hemorrhage and transfusion regimen design: a modelling application. Technical report, Institute for Mathematics and Scientific Computing, Karl Franzens Universität Graz.

[5] J. J. Batzel, S. Fürtinger, F. Kappel, M. Bachar, and M. Fink. Sensitivity analysis of a cardiovascular control system model. *Submitted*.

[6] J. J. Batzel, F. Kappel, D. Schneditz, and H. T. Tran. *Cardiovascular & Respiratory Systems: Modeling, Analysis & Control*. SIAM, U.S., 2006.

[7] C. M. Brown, M. J. Hecht, B. Neundörfer, and M. J. Hilz. Effects of lower body negative pressure on cardiac and vascular responses to carotid baroreflex stimulation. *Physiological Research*, 52(5):637–645, 2003.

[8] The New York Medical Center. Orthostatic stress testing & instrumentation. Currently available at `https://www.nymc.edu/fhp/centers/syncope/Orthostatic Stress Testing & instrumentation.htm`.

[9] M. Fink, J.J. Batzel, and F.Kappel. An optimal control approach to modeling the cardiovascular-respiratory system: An application to orthostatic stress. *Cardiovascular Engineering: An International Journal*, 4:27–38, March 2004.

[10] M. Fink, S. Fürtinger, and J. Batzel. Predicting changes in pulse pressure due to the baroreceptor-reflex. *Submitted*.

[11] S. Fürtinger, J. J. Batzel, and M. Fink. Investigating physiological controls of the cardiovascular system. Technical report, Institute for Mathematics and Scientific Computing, Karl Franzens Universität Graz, December 2007.

[12] T. Heldt, E. B. Shim, R. D. Kamm, and R. G. Mark. Computational modeling of cardiovascular response to orthostatic stress. *Journal of Applied Physiology*, 92(3):1239–1254, Mar 2002.

[13] F. C. Hoppensteadt and C. S. Peskin. *Mathematics in Medicine and the Life Sciences*. Springer Verlag New York, 2nd edition, 2001.

[14] F. Kappel. Course 1 on control theory. Unpublished Lecture Notes on the Summerschool on Biomathematics, Schloss Seggau, July 25 - August 5, 2005.

[15] F. Kappel, M. Fink, and J. J. Batzel. Aspects of control of the cardiovascular-respiratory system during orthostatic stress induced by lower body negative pressure. *Mathematical Biosciences*, 206(2):273–308, Apr 2007.

[16] F. Kappel and R. O. Peer. A mathematical model for fundamental regulation processes in the cardiovascular system. *Journal of Mathematical Biology*, 31(6):611–631, 1993.

[17] R. Klabunde. *Cardiovascular Physiology Concepts*. Lippincott Williams & Wilkins, 2005.

[18] H. Kwakernaak and R. Sivan. *Linear Optimal Control Systems*. Wiley-Interscience, New York, 1972.

[19] D. Lucini, R. Furlan, P. Villa, R. Mosqueda-Garcia, A. Diedrich, D. Robertson, A. Malliani, A. Porta, and M. Pagani. Altered profile of baroreflex and autonomic responses to lower body negative pressure in chronic orthostatic intolerance. *Journal of Hypertension*, 22(8):1535–1542, 2004.

[20] The MathWorks. MATLAB help desk. Currently available at `http://www.mathworks.com/access/helpdesk/help/techdoc/`.

[21] Mosby, editor. *Mosby's Medical Dictionary*. Mosby, 8th edition, Dec. 2008.

[22] Mette S Olufsen, Johnny T Ottesen, Hien T Tran, Laura M Ellwein, Lewis A Lipsitz, and Vera Novak. Blood pressure and blood flow variation during postural change from sitting to standing: model development and validation. *Journal of Applied Physiology*, 99(4):1523–1537, Oct 2005.

[23] E. Sontag. *Mathematical Control Theory: Deterministic Finite Dimensional Systems*. Springer Verlag New York, 2nd edition, 1998.

[24] M. Ursino. Interaction between carotid baroregulation and the pulsating heart: a mathematical model. *American Journal of Physiology*, 275(5 Pt 2):H1733–H1747, Nov 1998.

[25] M. Ursino, M. Antonucci, and E. Belardinelli. Role of active changes in venous capacity by the carotid baroreflex: analysis with a mathematical model. *American Journal of Physiology*, 267(6 Pt 2):H2531–H2546, Dec 1994.

[26] C. Zalpour, editor. *Für die Physiotherapie: Anatomie und Physiologie*. Urban & Fischer bei Elsevier, 2nd edition, 2006.